

Wolff-Type Embedding Algorithms for General Nonlinear σ -Models*

Sergio Caracciolo

*Scuola Normale Superiore and INFN – Sezione di Pisa
Piazza dei Cavalieri
Pisa 56100, ITALIA*

Internet: CARACCIO@UX1SNS.SNS.IT
Bitnet: CARACCIO@IPISNSVA.BITNET
Hepnet/Decnet: 39198::CARACCILO

Robert G. Edwards

*Supercomputer Computations Research Institute
Florida State University
Tallahassee, FL 32306 USA*

Internet: EDWARDS@MAILER.SCRI.FSU.EDU

Andrea Pelissetto

*Dipartimento di Fisica
Università degli Studi di Pisa
Pisa 56100, ITALIA*

Internet: PELISSET@SUNTHPI1.DIFI.UNIPI.IT
Bitnet: PELISSET@IPISNSVA.BITNET
Hepnet/Decnet: 39198::PELISSETTO

Alan D. Sokal

*Department of Physics
New York University
4 Washington Place
New York, NY 10003 USA*

Internet: SOKAL@ACF3.NYU.EDU

October 31, 2018

Abstract

We study a class of Monte Carlo algorithms for the nonlinear σ -model, based on a Wolff-type embedding of Ising spins into the target manifold M . We argue heuristically that, at least for an asymptotically free model, such an algorithm can have dynamic critical exponent $z \ll 2$ only if the embedding is based on an (involutive) isometry of M whose fixed-point manifold has codimension 1. Such an isometry exists only if the manifold is a discrete quotient of a product of spheres. Numerical simulations of the idealized codimension-2 algorithm for the two-dimensional $O(4)$ -symmetric σ -model yield $z_{int, \mathcal{M}^2} = 1.5 \pm 0.5$ (subjective 68% confidence interval), in agreement with our heuristic argument.

*Submitted to Nuclear Physics B.

1 Introduction

Wolff [1, 2, 3] has recently proposed an extraordinarily efficient collective-mode Monte Carlo algorithm for simulating the nonlinear σ -model taking values in the sphere S^{N-1} and having symmetry group $O(N)$ [also called the N -vector model]. Numerical tests of the dynamic critical behavior of this algorithm show the complete or almost complete absence of critical slowing-down ($z \lesssim 0.1$) for two-dimensional models with $N = 2, 3, 4$ [1, 2, 3, 4, 5], and a small but apparently nonzero critical slowing-down ($z \approx 0.25 - 0.5$) for the three-dimensional XY model [6, 7].¹

In this paper²

we consider generalizations of Wolff's algorithm to σ -models taking values in manifolds other than spheres. (We see this as a first step toward generalizing the Wolff algorithm to lattice gauge theories.) Our conclusion is somewhat surprising: we argue that the generalized Wolff algorithm can work well (i.e. have $z \ll 2$) *only* if the manifold is a discrete quotient of a product of spheres (e.g. real projective space). This conclusion is based on a combination of a heuristic argument and a rigorous mathematical theorem; it is supported by a numerical test in one prototypical case.

Wolff's algorithm for the N -vector model is based on an embedding of Ising spins $\{\varepsilon\}$ into N -component continuous spins $\{\boldsymbol{\sigma}\}$ according to

$$\boldsymbol{\sigma}_x = \boldsymbol{\sigma}_x^\perp + \varepsilon_x |\boldsymbol{\sigma}_x^\parallel| \mathbf{r}, \quad (1.1)$$

where \mathbf{r} is a unit vector chosen randomly on S^{N-1} , $\boldsymbol{\sigma}_x^\perp \equiv \boldsymbol{\sigma}_x - (\boldsymbol{\sigma}_x \cdot \mathbf{r})\mathbf{r}$ and $\boldsymbol{\sigma}_x^\parallel \equiv (\boldsymbol{\sigma}_x \cdot \mathbf{r})\mathbf{r}$ are the components of $\boldsymbol{\sigma}_x$ perpendicular and parallel to \mathbf{r} , and $\varepsilon_x \equiv \text{sgn}(\boldsymbol{\sigma}_x \cdot \mathbf{r}) = \pm 1$. Flipping the Ising spin ε_x corresponds to a reflection of $\boldsymbol{\sigma}_x$ in the hyperplane perpendicular to \mathbf{r} . With $\{\boldsymbol{\sigma}^\perp\}$ and $\{|\boldsymbol{\sigma}^\parallel|\}$ held fixed, the σ -model Hamiltonian

$$H(\{\boldsymbol{\sigma}\}) = -\beta \sum_{\langle xy \rangle} \boldsymbol{\sigma}_x \cdot \boldsymbol{\sigma}_y \quad (1.2)$$

reduces to the ferromagnetic random-bond Ising model (in zero magnetic field) defined by

$$H(\{\varepsilon\}) = -\sum_{\langle xy \rangle} J_{xy} \varepsilon_x \varepsilon_y + \text{const}, \quad (1.3)$$

where $J_{xy} = \beta |\boldsymbol{\sigma}_x \cdot \mathbf{r}| |\boldsymbol{\sigma}_y \cdot \mathbf{r}|$. The Ising model (1.3) can then be simulated by any legitimate Monte Carlo algorithm, such as the Swendsen-Wang (SW) algorithm [9, 10] or its single-cluster variant [1, 11, 12, 13].

The dynamic critical behavior of Wolff-type algorithms is determined by the combined effect of two *completely distinct* issues:

- i) How well the embedding (1.1) succeeds in "encoding" the important large-scale collective modes of the σ -model into the Ising variables $\{\varepsilon\}$.

¹But, regarding [6, 7], see our discussion in Section 5 below.

²A preliminary version of this work was reported at the Lattice '90 conference [8].

- ii) How well any given algorithm for Ising models (e.g. standard SW or single-cluster SW) succeeds in updating the spins $\{\varepsilon\}$ governed by the (random) Hamiltonian (1.3).

We wish to emphasize the importance of studying these questions *separately*. If the physically relevant large-scale collective motions of the σ -model cannot be obtained by varying the $\{\varepsilon\}$ at fixed $\{\sigma^\perp, |\sigma^\parallel|\}$, then the Wolff algorithm will have severe critical slowing-down *no matter what* method is used to update the Ising variables $\{\varepsilon\}$. On the other hand, if the Wolff algorithm with a *particular* choice of Ising-updating method shows severe critical slowing-down, this does *not* necessarily mean that the embedding (1.1) works badly: the poor performance might be due to slow decorrelation in the Ising-updating subroutine, and could possibly be remedied by switching to a better Ising algorithm.

In this paper our goal is to study the *embedding* defined by (1.1) or its generalizations, independently of the question of how the induced Ising model is to be updated. To address this question, it is conceptually useful to consider the *idealized Wolff algorithm*, which for the N -vector model goes as follows: a vector \mathbf{r} is chosen randomly from the unit sphere S^{N-1} ; and a new configuration of Ising spins $\{\varepsilon\}$, *independent of the old configuration*, is generated with probabilities given by the Hamiltonian (1.3). Of course, such an algorithm is not practical, but that is not its role. Rather, it serves as a standard of comparison (and presumed lower bound on the autocorrelation time) for *all* algorithms based on the embedding (1.1). If the idealized Wolff algorithm performs badly, then so must any algorithm based on the given embedding. On the other hand, if the idealized Wolff algorithm performs well, then it is clearly worthwhile to seek (if necessary) new Ising-model algorithms capable of simulating efficiently the induced Ising Hamiltonian.

To approximate in practice the idealized Wolff algorithm, we update the $\{\varepsilon\}$ configuration by N_{hit} hits of some chosen Ising-model algorithm (e.g. standard SW) and extrapolate to $N_{hit} = \infty$.³ To be sure, this test procedure can be very time-consuming. But it is essential if we wish to obtain *physical insight* into the embedding.

The extraordinary performance of the Wolff algorithm for N -vector models has spurred attempts (so far unsuccessful) to generalize it to lattice gauge theories. Gauge theories differ from N -vector models in two ways:

- a) The field takes values in a *group* rather than a sphere. [$U(1)$ and $SU(2)$ are spheres, but higher Lie groups are not.]
- b) The field is a 1-form rather than a 0-form, i.e. it lives on *links* rather than sites. Correspondingly, the energy is the *curl* of the field rather than its gradient, and it lives on *plaquettes* rather than links. As a result, the theory has a *local gauge invariance* rather than just a global symmetry.

The deep physical difference between gauge and spin models is, of course, item (b). The fact of gauge invariance, and the transverseness of physical excitations in a gauge

³Preferably we would perform simulations for successively increasing values of N_{hit} until the autocorrelation time is constant within error bars. However, this may not always be feasible.

theory, will impose severe constraints, we believe, on the as-yet-unknown analogue of the embedding (1.1) [if indeed such an analogue exists].⁴ At present we have little to say in this direction (though some insight might possibly be gleaned from the Swendsen-Wang algorithm for Potts lattice gauge theories [15, 16]). In this paper we address the less profound, but still highly nontrivial, problem (a). To do this, we ask whether the embedding (1.1) can be generalized to nonlinear σ -models with values in *manifolds other than spheres* — such as $SU(N)$ for $N \geq 3$ — and, if so, what is the dynamic critical behavior of the corresponding idealized Wolff algorithm.

Our approach is as follows: First we ask what are the fundamental properties of the embedding (1.1) that cause the Wolff algorithm to work so well. Then we ask whether embeddings having these properties exist also in other Riemannian manifolds M ; this is a question in differential geometry to which we are able to give a fairly complete answer. Finally, we perform a numerical study to test (in one case) whether our theoretical reasoning is correct. The conclusion of this analysis is quite surprising: roughly speaking, we find that a generalized Wolff algorithm can work well (i.e. have $z \ll 2$) *only* if the manifold M is either a sphere, a product of spheres, or the quotient of such a space by a discrete group (for example, real projective space RP^{N-1}). If correct, this conclusion is quite disappointing, and lends renewed impetus to other classes of collective-mode algorithms such as multi-grid Monte Carlo [17, 14, 18, 19] and Fourier acceleration [20, 21, 22, 23].

The plan of this paper is as follows: In Section 2 we define generalized Wolff-type embedding algorithms for σ -models taking values in a Riemannian manifold M . We argue heuristically that such an algorithm will work well — at least for asymptotically free σ -models — only if the embedding is based on an (involutive) isometry of M whose fixed-point manifold has codimension 1. This argument is the key physical idea of this paper. In Section 3 we study the conditions under which such an isometry can exist. In Section 4 we test our heuristic argument with a large-scale numerical study of the codimension-2 idealized embedding algorithm for the two-dimensional N -vector model with $N = 4$. In Section 5 we discuss our results. Appendix A collects some results from topology and differential geometry that are essential to our argument in Sections 2 and 3. Some of these results are difficult to find in the mathematical literature, and at least a few appear to be new. Appendix B contains a complete classification of the involutive isometries for the physically important case of $SU(N)$. Much to our surprise, we have been unable to find this classification anywhere in the mathematical or physical literature.

2 Generalized Embedding Algorithms

2.1 Wolff algorithm for the N -vector model

The single-spin configuration space of the N -vector model is the sphere

$$S^{N-1} = \{\boldsymbol{\sigma} \in \mathbb{R}^N: |\boldsymbol{\sigma}| = 1\}, \quad (2.1)$$

⁴The same issue arises in devising multi-grid algorithms for gauge theories [14, Section V].

and the key object of the Wolff algorithm is the map of *reflection in the equator*:

$$T(\sigma^1, \sigma^2, \dots, \sigma^N) = (-\sigma^1, \sigma^2, \dots, \sigma^N). \quad (2.2)$$

(This corresponds to $\mathbf{r} = (1, 0, \dots, 0)$; obviously the case of arbitrary \mathbf{r} can be obtained by conjugating with a rotation.) The map T has two key properties:

- a) T is an isometry (i.e. it preserves distances).
- b) The fixed-point set $\text{Fix}(T) \equiv \{\boldsymbol{\sigma} \in S^{N-1}: T\boldsymbol{\sigma} = \boldsymbol{\sigma}\}$ — which is of course the equator — has codimension 1.

We argue that these are the crucial properties that make the Wolff algorithm work so well.

Because T is an *isometry*, a global application of T is an exact symmetry (zero change in energy), and the application of T in a large but bounded region costs only a *surface* energy. (If T were not an isometry, then the application of T in a region would cost a *bulk* energy, and the idealized Wolff update would probably be unable to make any significant large-scale change in the $\{\boldsymbol{\sigma}\}$ configuration.)

To see the importance of the *codimension-1 property*, let us review our heuristic understanding [4] of why the Wolff algorithm works so well. Consider a slowly varying spin configuration $\{\boldsymbol{\sigma}\}$. Since $J_{xy} = \beta|\boldsymbol{\sigma}_x \cdot \mathbf{r}||\boldsymbol{\sigma}_y \cdot \mathbf{r}|$, the Hamiltonian (1.3) *almost decouples* along the surfaces where $\boldsymbol{\sigma} \cdot \mathbf{r} \approx 0$, i.e. where $\boldsymbol{\sigma}$ is on or near the equator. These surfaces (= codimension-1 submanifolds) divide x -space into disconnected regions R_i in which $\boldsymbol{\sigma} \cdot \mathbf{r} > 0$ or $\boldsymbol{\sigma} \cdot \mathbf{r} < 0$. Provided that we are working in an *non-magnetized* phase (i.e. there is no preferred orientation for the spins), the largest of the regions R_i will presumably have linear size on the order of the correlation length ξ . In particular, if $1 \ll \xi \lesssim L/2$ (here L is the lattice linear size), then there will be, with high probability, at least two disjoint large regions R_i . Now let us apply an idealized Wolff update: the spins $\{\varepsilon\}$ will be given new values, and these values will be *almost independent* in distinct regions R_i . That is, the choice to reflect or not reflect a spin $\boldsymbol{\sigma}$ will have been made almost independently in distinct regions R_i (but very coherently within each R_i). If the original configuration $\{\boldsymbol{\sigma}\}$ is a long-wavelength spin wave, then these almost-independent reflections correspond roughly to a long-wavelength collective-mode change in $\{\boldsymbol{\sigma}\}$ (Figure 1). We predict, therefore, that the *idealized* Wolff algorithm will have dynamic critical exponent z much less than 2, and quite possibly $z \approx 0$. This prediction has been confirmed numerically in the two-dimensional N -vector models with $N = 2, 3, 4$ [1, 2, 3, 4, 5], and in the three-dimensional model with $N = 2$ [6, 7].⁵

The assumption in this argument that $\{\boldsymbol{\sigma}\}$ is slowly varying requires some clarification.⁶ Consider first the case in which the critical point is at zero temperature ($\beta_c = \infty$); this case corresponds to asymptotically free theories such as the two-dimensional

⁵Regarding [6, 7], see our discussion in Section 5 below.

⁶ We did not fully understand these subtleties when we wrote [4, 8]. (Quite possibly we still don't.)

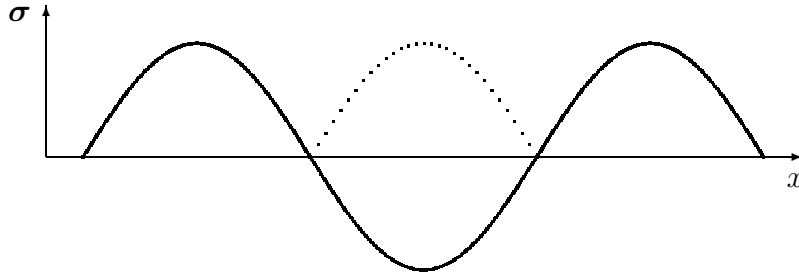


Figure 1: Action of the Wolff algorithm on a long-wavelength spin wave. For simplicity, both spin space (σ) and physical space (x) are depicted as one-dimensional.

N -vector models for $N \geq 3$. For such theories, the typical spin configurations become smooth as $\beta \rightarrow \beta_c = \infty$: more precisely, for a nearest-neighbor pair of sites x, y , we have $\langle \sigma_x \cdot \sigma_y \rangle \approx 1 - c/\beta$ for a (calculable) constant c . That is, the typical angle between nearest-neighbor spins is of order $1/\sqrt{\beta}$; so on bonds $\langle xy \rangle$ where σ_x and σ_y are near the equator, we typically have $J_{xy} \equiv \beta |\sigma_x \cdot \mathbf{r}| |\sigma_y \cdot \mathbf{r}| \sim \beta (1/\sqrt{\beta})^2 \sim 1$. Note that this behavior occurs not only on the bonds $\langle xy \rangle$ where σ crosses the equator [i.e. for which $(\sigma_x \cdot \mathbf{r})(\sigma_y \cdot \mathbf{r}) < 0$], but also on the nearby bonds where σ remains near the equator. On the other hand, on bonds $\langle xy \rangle$ where σ_x and σ_y are far from the equator (i.e. bonds deep inside one of the regions R_i), we typically have $J_{xy} \sim \beta$. Thus, the couplings $\{J_{xy}\}$ of the induced Ising model have typically the following structure: there are regions R_i of linear size $\sim \xi$ within which the couplings are very strong (of order β), surrounded by transition layers (of width probably ~ 1) where the couplings are of moderate strength (of order 1).

Now, from this information alone we cannot determine the phase structure of the induced Ising model. For example, if the couplings $\{J_{xy}\}$ in the transition layers — which are “of order 1” — were typically greater than the critical coupling $J_{c, \text{Ising}}$ for a d -dimensional translation-invariant Ising ferromagnet, then the induced Ising model would surely exhibit long-range order. (The strongly ferromagnetic couplings $J_{xy} \sim \beta$ within the regions R_i would only strengthen this long-range order.) On the other hand, if the transition-layer couplings were sufficiently smaller than $J_{c, \text{Ising}}$, then the induced Ising model could exhibit exponentially-decaying correlations in spite of the large couplings $J_{xy} \sim \beta$ within the regions R_i . The distinction between these two scenarios seems to depend on the precise values of the transition-layer couplings $\{J_{xy}\}$, as well as on the widths of the transition layers — quantities which our order-of-magnitude argument is too crude to predict.

On the other hand, we know that the original N -vector model is in a phase with exponentially decaying correlations; in particular, we expect that

$$\langle \text{sgn}(\sigma_x \cdot \mathbf{r}) \text{sgn}(\sigma_y \cdot \mathbf{r}) \rangle \sim e^{-|x-y|/\xi} \quad (2.3)$$

as $|x - y| \rightarrow \infty$. [This is not the usual correlation function $\langle \sigma_x \cdot \sigma_y \rangle$, but it should exhibit the same correlation length.] On the other hand, the unconditional expecta-

tion (2.3) is equal to the average over $\{\boldsymbol{\sigma}^\perp, |\boldsymbol{\sigma}^\parallel|\}$ (with Boltzmann-Gibbs weight) of the *conditional* expectations

$$\langle \text{sgn}(\boldsymbol{\sigma}_x \cdot \mathbf{r}) \text{sgn}(\boldsymbol{\sigma}_y \cdot \mathbf{r}) | \{\boldsymbol{\sigma}^\perp, |\boldsymbol{\sigma}^\parallel|\} \rangle \equiv \langle \varepsilon_x \varepsilon_y \rangle_{\{J_{xy}\}}. \quad (2.4)$$

Now, the conditional expectations (2.4) are always *nonnegative*, since the induced Ising model is purely ferromagnetic. So there is no possibility of “cancellations” in forming (2.3) from (2.4). We conclude that the induced-Ising-model correlations (2.4) should also exhibit exponential (or faster-than-exponential) decay, on a characteristic scale ξ (or smaller), for “nearly all” configurations $\{\boldsymbol{\sigma}^\perp, |\boldsymbol{\sigma}^\parallel|\}$.

This exponential decay is clearly not due to the large couplings $J_{xy} \sim \beta$ within the regions R_i ; it must be due to the moderate couplings $J_{xy} \sim 1$ in the transition layers. In other words, the transition layers *do* succeed in (almost-)decoupling neighboring (or at least almost-neighboring) regions R_i . This reasoning justifies, in the case of an asymptotically free model, our proposed mechanism for the good dynamic critical behavior ($z \approx 0$) of the *idealized* Wolff algorithm.

Next consider the case of a critical point at finite temperature ($\beta_c < \infty$), as in the two-dimensional XY model or the N -vector models (all N) in dimension $d \geq 3$. Here the spin configurations for $\beta \approx \beta_c$ are *rough* at short distance scales: for a nearest-neighbor pair of sites x, y , we have $\langle \boldsymbol{\sigma}_x \cdot \boldsymbol{\sigma}_y \rangle \leq C < 1$ uniformly in β ($\approx \beta_c$) and L . Thus, the distinction between “regions R_i ” and “transition layers” is no longer so clear. The couplings $\{J_{xy}\}$ will be highly irregular, but we may expect $J_{xy} \sim \beta_c \sim 1$ more or less everywhere. On the other hand, for $\beta < \beta_c$ it remains true that the correlations (2.3) decay exponentially; so we may again conclude that the induced-Ising-model correlations (2.4) decay exponentially on scale ξ for “nearly all” $\{\boldsymbol{\sigma}^\perp, |\boldsymbol{\sigma}^\parallel|\}$. In this case, the *mechanism* of the decay is not the decoupling of regions R_i , but simply the fact that the “average” J_{xy} is less than $J_{c, \text{Ising}}$. Irrespective of the mechanism, however, it remains true that an *independent* resampling of the induced Ising model will produce a significant collective change on scale ξ (and all smaller scales). We may thus continue to expect that $z \approx 0$ for the *idealized* Wolff algorithm.

Remarks. 1. For the two-dimensional XY model near the Kosterlitz-Thouless transition, spin waves are not the only important large-scale collective modes: there are also large-scale collective modes associated with vortices. Therefore, to explain heuristically why $z \ll 2$, it is necessary to show also that the (idealized) Wolff updates are capable of destroying a widely-separated vortex-antivortex pair. This has been done in [4].

2. The foregoing reasoning does not apply to a *magnetized* phase (except in the scaling region near the critical point, where the magnetization is very small): the trouble is that the spins will be aligned in some particular direction⁷, and nearly all the spins will lie in a single cluster R_i unless the direction of alignment happens to be almost perpendicular to \mathbf{r} . Therefore, in order for the Wolff algorithm to work

⁷In finite volume with free or periodic boundary conditions, this direction of alignment is *random*, and will vary from configuration to configuration. Nevertheless, in each individual configuration, the spins will be rather strongly aligned in *some* direction.

well in a magnetized phase, it may be necessary to choose the direction vector \mathbf{r} with a probability distribution that *depends on the current spin configuration* $\{\boldsymbol{\sigma}\}$. For example, one possible algorithm would be to choose at random a site x , and then choose \mathbf{r} to be a random vector orthogonal to $\boldsymbol{\sigma}_x$. Since $\boldsymbol{\sigma}_x$ will be unchanged under the subsequent move, this algorithm is easily seen to satisfy detailed balance.⁸ (If $N = 2$, this choice of \mathbf{r} given $\boldsymbol{\sigma}_x$ is deterministic, and the algorithm is nonergodic: for example, if the spins $\boldsymbol{\sigma}_x$ are all aligned along one axis, they will forever remain so. The ergodicity can be restored by admixing, with a nonzero probability, moves of the usual type with a randomly chosen \mathbf{r} .) The hope here is that \mathbf{r} would most of the time be chosen approximately perpendicular to the current total magnetization $\mathcal{M} = \sum_x \boldsymbol{\sigma}_x$, so that the Goldstone spin waves would be sliced as in Figure 1. (One might inquire about the algorithm in which \mathbf{r} is chosen to be perpendicular to \mathcal{M} itself. Unfortunately, this algorithm fails to satisfy detailed balance, and we strongly suspect that it fails to leave invariant the correct Gibbs measure.)

3. In a preliminary version of this work [8], we emphasized an additional property of T , namely that it is *involutive* (i.e. its square is the identity map). This property ensures that the induced Ising model has zero magnetic field (which is convenient although perhaps not essential). In fact, it turns out that an isometry possessing the codimension-1 property is *automatically* involutive: see Theorem A.9 in Appendix A.

Next we would like to argue that the *practical* Wolff algorithm based on standard SW (or single-cluster SW) updates of the induced Ising model (with $N_{hit} = 1$) should also have $z \ll 2$. We can give two alternative lines of reasoning:

1) We have already argued that the idealized Wolff algorithm has $z \approx 0$. On the other hand, the induced Ising model is ferromagnetic, and the SW (or 1CSW) algorithm is known to perform well for Ising ferromagnets: the exponential autocorrelation time behaves as $\tau_{exp,SW} \sim \min(\xi, L)^{z_{exp,SW}}$, where the best currently available estimates of $z_{exp,SW}$ (standard SW algorithm) for translation-invariant nearest-neighbor ferromagnets are

$$z_{exp,SW} \approx \begin{cases} 0 - 0.3 & \text{for } d = 2 \text{ [9, 11, 24, 13, 26]} \\ 0.35 - 0.75 & \text{for } d = 3 \text{ [9, 11, 25, 26]} \\ 1 & \text{for } d = 4 \text{ [27, 26]} \end{cases} \quad (2.5)$$

Of course, our induced Ising model is a *non-translation-invariant* ferromagnet, but the performance is likely to be qualitatively similar. Now, N_{hit} hits of the SW algorithm are at least $1 - e^{-N_{hit}/\tau_{exp,SW}}$ times as effective as independent sampling in generating a “new” Ising configuration. Thus, we expect

$$\tau_{Wolff,practical} \lesssim \tau_{Wolff,idealized} / (1 - e^{-N_{hit}/\tau_{exp,SW}}) \quad (2.6a)$$

$$\sim \tau_{Wolff,idealized} \tau_{exp,SW} / N_{hit} \quad \text{if } N_{hit} \lesssim \tau_{exp,SW} \quad (2.6b)$$

— hence $z_{Wolff,practical} \leq z_{Wolff,idealized} + z_{exp,SW} \ll 2$.

⁸The same logic also applies if \mathbf{r} is chosen *parallel* to $\boldsymbol{\sigma}_x$, as $\boldsymbol{\sigma}_x$ will be unchanged up to a sign (and a change of sign of \mathbf{r} is irrelevant). However, we do not know of any useful application for this algorithm.

2) Let us consider the bond configuration that will be generated in the *first* SW (or 1CSW) update. If the nearest-neighbor spins σ_x and σ_y belong to opposite hemispheres — that is, if $(\sigma_x \cdot \mathbf{r})(\sigma_y \cdot \mathbf{r}) \leq 0$ — then the bond $\langle xy \rangle$ is guaranteed to be unoccupied. It follows that if σ_z and $\sigma_{z'}$ are *any* pair of spins belonging to opposite hemispheres, then the sites z and z' are guaranteed to belong to *different* SW clusters. On the other hand, *within* each connected region R_i consisting of spins belonging to the same hemisphere, we expect that the bond occupation probabilities $p_{xy} \equiv 1 - e^{-2J_{xy}}$ will mostly lie beyond the percolation threshold, so that most of the region R_i will belong to the *same* SW cluster. [This is clear in the asymptotically free case, where $J_{xy} \sim \beta$ and $p_{xy} \approx 1$. In the finite- β_c case, however, the J_{xy} are of order 1, and there is a nonzero probability (uniformly in $\beta \approx \beta_c$ and L) for a small cluster of spins to become detached from its surroundings. Thus, each region R_i would have the structure of Swiss cheese: there would be one or a few large SW clusters in which there live a nonzero density of small SW clusters. Nevertheless, it is reasonable to expect that the large clusters will still be of linear size $\sim \xi$, i.e. that the small clusters will not be so numerous as to disconnect the large clusters into pieces of size $\ll \xi$.] Thus, each region R_i will be reflected more or less coherently — but distinct regions R_i will be reflected *independently* — in the first SW update. This corresponds to a long-wavelength collective mode (Figure 1).

2.2 Wolff algorithm for the RP^{N-1} model

Let us now consider a second example of a Wolff-type embedding algorithm, namely the case of the nonlinear σ -model taking values in the real projective space RP^{N-1} , where $N \geq 3$. This example differs from the N -vector model in two principal ways:

1) The equator in S^{N-1} not only has codimension 1, but has the stronger property of dividing the sphere into two *disconnected* regions (the northern and southern hemispheres). That is,

b') The complement of $\text{Fix}(T)$ is disconnected.

This property implies the codimension-1 property, but is strictly stronger (see Theorems A.1 and A.8 in Appendix A). It is not clear, at first glance, whether our heuristic argument in the preceding section was based on (b) or on (b'). Analysis of the RP^{N-1} model, which satisfies (b) but not (b'), will clarify this issue.

2) In the Wolff embedding algorithm for the N -vector model, the induced Ising model is *unfrustrated*. [When written in the form (1.1)/(1.3), it is manifestly ferromagnetic; when written in the alternate form (2.10)–(2.12), it is equivalent via a Z_2 gauge transformation to a ferromagnetic model.] In the embedding algorithm for the RP^{N-1} model, by contrast, the induced Ising model is generically *frustrated*. It is important to know what difference, if any, this makes.

The real projective space RP^{N-1} is, by definition, the sphere S^{N-1} with antipodal points identified, i.e. $RP^{N-1} = S^{N-1}/Z_2$. One could now proceed to pick a parametrization of RP^{N-1} (e.g. by embedding it diffeomorphically as a submanifold of some \mathbb{R}^m [28]); but it is simpler and more convenient to consider instead spins taking values in the sphere S^{N-1} , subject to the condition that the Hamiltonian and

all physical observables must be invariant under the Z_2 local gauge transformation $\boldsymbol{\sigma}_x \rightarrow \eta_x \boldsymbol{\sigma}_x$ ($\eta_x = \pm 1$). The simplest lattice Hamiltonian for this model is therefore

$$H(\{\boldsymbol{\sigma}\}) = -\frac{\beta}{2} \sum_{\langle xy \rangle} (\boldsymbol{\sigma}_x \cdot \boldsymbol{\sigma}_y)^2. \quad (2.7)$$

We use the same embedding as before, namely (1.1), but the coefficients $\{J_{xy}\}$ in the induced Ising Hamiltonian (1.3) are now

$$J_{xy} = \beta(\boldsymbol{\sigma}_x^\perp \cdot \boldsymbol{\sigma}_y^\perp) |\boldsymbol{\sigma}_x \cdot \mathbf{r}| |\boldsymbol{\sigma}_y \cdot \mathbf{r}|. \quad (2.8)$$

(For $N \geq 3$, this is generically a *frustrated* Ising model.) Since the reflection in the equator on S^{N-1} commutes with the map $\boldsymbol{\sigma} \rightarrow -\boldsymbol{\sigma}$, this reflection also induces a well-defined map T on the quotient space RP^{N-1} . Its fixed-point set $\text{Fix}(T)$ is the union of two disjoint components: one component consists of a single point, namely the pole (\equiv the image of the north or south pole in S^{N-1} under the canonical projection $\pi: S^{N-1} \rightarrow RP^{N-1}$); the other component consists of the ‘‘equator’’ in RP^{N-1} (\equiv the image of the equator in S^{N-1} under the canonical projection π), which is isometric to RP^{N-2} . Note that the equator in RP^{N-1} has codimension 1, but (unlike what happens in S^{N-1}) it does *not* disconnect the space RP^{N-1} : this is because in RP^{N-1} there is no distinction between the northern and southern hemispheres. Therefore, the map T on RP^{N-1} satisfies property (b) but *not* (b').

We now wish to analyze the behavior of the idealized Wolff algorithm for the RP^{N-1} model, by heuristic arguments analogous to those used for the N -vector model. Consider, therefore, a slowly varying spin configuration $\{\boldsymbol{\sigma}\}$. For such a configuration, we can imagine the lattice \mathbb{Z}^d to be replaced by a continuous space \mathbb{R}^d , and we can imagine the configuration $\{\boldsymbol{\sigma}\}$ to be a smooth map from \mathbb{R}^d into RP^{N-1} . Then the set of points in x -space where $\boldsymbol{\sigma} \cdot \mathbf{r} = 0$ is again (generically) a codimension-1 submanifold (= hypersurface) of \mathbb{R}^d (see Theorems A.4 and A.5). Since \mathbb{R}^d is simply connected, this hypersurface divides \mathbb{R}^d into at least two disconnected regions R_i (Theorem A.2). [*Alternative argument:* Since \mathbb{R}^d is simply connected, the map $\boldsymbol{\sigma}: \mathbb{R}^d \rightarrow RP^{N-1}$ lifts to a continuous map $\tilde{\boldsymbol{\sigma}}: \mathbb{R}^d \rightarrow S^{N-1}$ satisfying $\boldsymbol{\sigma} = \pi \circ \tilde{\boldsymbol{\sigma}}$. Now make the same argument as for the N -vector model, but using $\tilde{\boldsymbol{\sigma}}$ in place of $\boldsymbol{\sigma}$.] Therefore, by the same arguments as in the N -vector case, the induced Ising Hamiltonian (2.8) almost decouples along the surfaces where $\boldsymbol{\sigma}$ (or equivalently $\tilde{\boldsymbol{\sigma}}$) lies on or near the equator, and under an idealized Wolff update the regions R_i will be updated almost independently. We thus predict that the *idealized* Wolff algorithm for the RP^{N-1} model (in a non-magnetized phase) will have dynamic critical exponent $z \ll 2$, and quite possibly $z \approx 0$.

Remark. If x -space is not simply connected (e.g. X is the torus T^d if periodic boundary conditions are used), then the foregoing argument fails: a single hypersurface need not disconnect X . However, a *few* hypersurfaces suffice to disconnect X (see Theorem A.3); and if $1 \ll \xi \lesssim L/4$, then it is natural to expect that, with reasonable probability, the set where $\boldsymbol{\sigma} \cdot \mathbf{r} = 0$ will have *several* connected components. So we expect the algorithm to have the same dynamic critical exponent irrespective of the boundary conditions used. At worst, the autocorrelation time might be larger

by a *constant factor* for periodic as compared with free boundary conditions, for the same lattice size.

As in the N -vector case, it is necessary to inquire more closely into the assumption that $\{\boldsymbol{\sigma}\}$ is slowly varying. Consider, as before, the two cases:

(a) *The critical point is at zero temperature.* This case corresponds to asymptotically free theories; low-temperature perturbation theory suggests that the two-dimensional RP^{N-1} models for $N \geq 3$ are asymptotically free, but the Monte Carlo evidence is ambiguous (see [29] for references). As $\beta \rightarrow \beta_c = \infty$, the typical spin configurations become smooth modulo a sign: for a nearest-neighbor pair of sites x, y , we have $\langle (\boldsymbol{\sigma}_x \cdot \boldsymbol{\sigma}_y)^2 \rangle \approx 1 - c/\beta$ for a (calculable) constant c . We now claim that the couplings $\{J_{xy}\}$ have the following properties:

- (i) In regions where $\boldsymbol{\sigma}$ is not near the equator or the pole (i.e. deep inside one of the regions R_i), the couplings $\{J_{xy}\}$ are of order β and *globally unfrustrated*.
- (ii) In regions where $\boldsymbol{\sigma}$ is near the equator (i.e. the transition layers between the regions R_i), the couplings $\{J_{xy}\}$ are of order 1 and *locally unfrustrated*, though they may be *globally frustrated*.
- (iii) In regions where $\boldsymbol{\sigma}$ is near the pole (these are isolated patches), the couplings $\{J_{xy}\}$ are of order 1 and may be *frustrated*.

The statements concerning the typical magnitudes of J_{xy} are demonstrated exactly as in the N -vector case, using (2.8). The statements concerning local frustration are proven as follows: Let $x_1, \dots, x_n, x_{n+1} \equiv x_1$ be a (small) closed path of nearest-neighbor sites such that the spins $\boldsymbol{\sigma}_{x_1}, \dots, \boldsymbol{\sigma}_{x_n}$ are *all* close to each other and not near the pole, i.e. there exists $C > \frac{1}{2}$ such that $|\boldsymbol{\sigma}_{x_i} \cdot \boldsymbol{\sigma}_{x_j}| \geq C$ and $|\boldsymbol{\sigma}_{x_i} \cdot \mathbf{r}| \leq \sqrt{C}$ for all $i, j = 1, \dots, n$. Then $J_{cycle} \equiv J_{x_1 x_2} J_{x_2 x_3} \cdots J_{x_{n-1} x_n} J_{x_n x_1} \geq 0$.⁹

To study the global frustration, define $\tilde{J}_{xy} = \beta(\boldsymbol{\sigma}_x^\perp \cdot \boldsymbol{\sigma}_y^\perp)(\boldsymbol{\sigma}_x \cdot \mathbf{r})(\boldsymbol{\sigma}_y \cdot \mathbf{r})$ [these couplings are equivalent to $\{J_{xy}\}$ via a Z_2 gauge transformation]. Now draw a bond between any nearest-neighbor pair of sites $\langle xy \rangle$ for which $\tilde{J}_{xy} > 0$. This will occur, in particular, if $\boldsymbol{\sigma}_x$ and $\boldsymbol{\sigma}_y$ are close to each other and not near the pole or the equator.¹⁰ The connected components formed by the bonds thus drawn correspond roughly to the regions R_i ; it is reasonable to expect that they are of linear size $\sim \xi$, although they

⁹*Proof:* Note first that changing $\boldsymbol{\sigma}_{x_i}$ to $-\boldsymbol{\sigma}_{x_i}$ leaves J_{cycle} unchanged; therefore we may choose the signs of $\boldsymbol{\sigma}_{x_2}, \dots, \boldsymbol{\sigma}_{x_n}$ so that $\boldsymbol{\sigma}_{x_1} \cdot \boldsymbol{\sigma}_{x_i} \geq C > 0$ for $i = 2, \dots, n$. Since $C > \frac{1}{2}$, this means that the angle between $\boldsymbol{\sigma}_{x_1}$ and $\boldsymbol{\sigma}_{x_i}$ is less than 60° ; so the angle between $\boldsymbol{\sigma}_{x_i}$ and $\boldsymbol{\sigma}_{x_j}$ is less than 120° , i.e. $\boldsymbol{\sigma}_{x_i} \cdot \boldsymbol{\sigma}_{x_j} > -\frac{1}{2}$. But $|\boldsymbol{\sigma}_{x_i} \cdot \boldsymbol{\sigma}_{x_j}| \geq C > \frac{1}{2}$ by hypothesis, so $\boldsymbol{\sigma}_{x_i} \cdot \boldsymbol{\sigma}_{x_j} \geq C$. Then $\boldsymbol{\sigma}_{x_i}^\perp \cdot \boldsymbol{\sigma}_{x_j}^\perp = \boldsymbol{\sigma}_{x_i} \cdot \boldsymbol{\sigma}_{x_j} - (\boldsymbol{\sigma}_{x_i} \cdot \mathbf{r})(\boldsymbol{\sigma}_{x_j} \cdot \mathbf{r}) \geq C - (\sqrt{C})^2 = 0$. So each coupling $J_{x_i x_{i+1}}$ is ≥ 0 .

¹⁰More precisely, suppose that there exists $\epsilon \geq 0$ such that $|\boldsymbol{\sigma}_x \cdot \boldsymbol{\sigma}_y| \geq 1 - \epsilon$ and $\sqrt{\epsilon} < |\boldsymbol{\sigma}_x \cdot \mathbf{r}|, |\boldsymbol{\sigma}_y \cdot \mathbf{r}| < \sqrt{1 - \epsilon}$. Then we claim that $\tilde{J}_{xy} > 0$. *Proof:* Since the substitutions $\boldsymbol{\sigma}_x \rightarrow -\boldsymbol{\sigma}_x$ and $\boldsymbol{\sigma}_y \rightarrow -\boldsymbol{\sigma}_y$ leave \tilde{J}_{xy} unchanged, we can assume without loss of generality that $\boldsymbol{\sigma}_x \cdot \mathbf{r}, \boldsymbol{\sigma}_y \cdot \mathbf{r} > 0$. Then $\boldsymbol{\sigma}_x \cdot \boldsymbol{\sigma}_y = \boldsymbol{\sigma}_x^\perp \cdot \boldsymbol{\sigma}_y^\perp + (\boldsymbol{\sigma}_x \cdot \mathbf{r})(\boldsymbol{\sigma}_y \cdot \mathbf{r}) > -1 + (\sqrt{\epsilon})^2 = -(1 - \epsilon)$, so we must have $\boldsymbol{\sigma}_x \cdot \boldsymbol{\sigma}_y \geq 1 - \epsilon$. Then $\boldsymbol{\sigma}_x^\perp \cdot \boldsymbol{\sigma}_y^\perp = \boldsymbol{\sigma}_x \cdot \boldsymbol{\sigma}_y - (\boldsymbol{\sigma}_x \cdot \mathbf{r})(\boldsymbol{\sigma}_y \cdot \mathbf{r}) > (1 - \epsilon) - (\sqrt{1 - \epsilon})^2 = 0$. So $\tilde{J}_{xy} > 0$.

could in principle be larger.¹¹ Within each such connected component, the induced Ising model is *globally unfrustrated*: indeed, for any closed path of nearest-neighbor bonds $(x_1, x_2), (x_2, x_3), \dots, (x_{n-1}, x_n), (x_n, x_{n+1} \equiv x_1)$ such that $\tilde{J}_{x_i x_{i+1}} > 0$ for all i , we trivially have $J_{cycle} \equiv \prod_{i=1}^n J_{x_i x_{i+1}} = \prod_{i=1}^n \tilde{J}_{x_i x_{i+1}} > 0$.

What is the phase structure of this induced Ising model? Here we cannot argue as we did in the N -vector case [cf. (2.3)/(2.4)], because the global frustration of the $\{J_{xy}\}$ in the transition layers could cause “cancellations”. Instead, we can distinguish at least three *a priori* possibilities:

- (i) The induced Ising model exhibits exponentially decaying correlations on a characteristic scale ξ (or smaller).
- (ii) The induced Ising model lies in a spin-glass phase of Parisi-Mézard-Soullas-Toulouse-Virasoro type [30, 31, 32, 33], i.e. there are many “dominant” regions of configuration space which differ on long as well as short length scales (“rough free-energy landscape”).
- (iii) The induced Ising model lies in a spin-glass phase of Fisher-Huse type [34], i.e. there are only two “dominant” regions of configuration space, related to each other by a global spin flip.

In cases (i) and (ii), an *independent* resampling of the induced Ising model will produce a significant collective change on scale ξ (and all smaller scales), so we expect $z \approx 0$ for the *idealized* Wolff algorithm. In case (iii), by contrast, the idealized Wolff updates do essentially nothing (merely a global spin flip), and the performance should be poor.

In dimension $d = 2$, it is believed that there is no spin-glass phase for the ordinary random-bond Ising model [35]. That does not imply anything, of course, for our induced Ising model, in which the structure of the couplings is quite different, but it does *suggest* that scenarios (ii) and (iii) are unlikely, and that scenario (i) is probably the correct one. We therefore expect that $z \approx 0$ for the *idealized* Wolff algorithm. This prediction has been confirmed in a preliminary study [29] of the two-dimensional RP^2 model.

(b) *The critical point is at finite temperature.* This case is expected to hold in the RP^{N-1} models (all N) in dimension $d \geq 3$, whenever the phase transition is continuous (as opposed to first-order). Unfortunately, in this case we have little to say: the typical spin configurations for $\beta \approx \beta_c$ are *rough* at short distance scales, and the induced Ising model will be highly frustrated. Any one of the scenarios (i)–(iii) just discussed — and possibly others as well — could occur. So we are unable to

¹¹There is no *topological* obstacle to these connected components being of size much larger than ξ (e.g. spanning the whole lattice). Indeed, *any* two spin values $\sigma_x, \sigma_{x'}$ not lying on the equator or the pole can potentially be connected by a chain of spins $\sigma_x \equiv \sigma_{x_0}, \sigma_{x_1}, \dots, \sigma_{x_k} \equiv \sigma_{x'}$ such that $\tilde{J}_{x_i x_{i+1}} \equiv (\sigma_{x_i}^\perp \cdot \sigma_{x_{i+1}}^\perp)(\sigma_{x_i} \cdot \mathbf{r})(\sigma_{x_{i+1}} \cdot \mathbf{r}) > 0$ for all i . *Proof:* Assume without loss of generality that σ_x and $\sigma_{x'}$ both lie in the northern hemisphere, with $\text{longitude}(\sigma_x) = 0^\circ$. Then, if $|\text{longitude}(\sigma_{x'})| < 90^\circ$, we can take $k = 1$; if $90^\circ \leq |\text{longitude}(\sigma_{x'})| < 180^\circ$, we can take $k = 2$; and if $|\text{longitude}(\sigma_{x'})| = 180^\circ$, we can take $k = 3$.

predict with confidence whether the idealized Wolff algorithm will exhibit $z \approx 0$ or not.

The behavior of the *practical* Wolff algorithm based on standard SW (or single-cluster SW) updates is even less clear. Although the induced Ising Hamiltonian (2.8) is frustrated, this does not necessarily mean that the SW algorithm will perform poorly for it. To see this, note first that if $\tilde{J}_{xy} \equiv \beta(\boldsymbol{\sigma}_x^\perp \cdot \boldsymbol{\sigma}_y^\perp)(\boldsymbol{\sigma}_x \cdot \mathbf{r})(\boldsymbol{\sigma}_y \cdot \mathbf{r}) \leq 0$, then the bond $\langle xy \rangle$ is guaranteed to be unoccupied. If such bonds are numerous enough to divide the lattice into at least two large clusters R_i of size $\sim \xi$, then the SW algorithm will flip these clusters independently — and thus make a long-wavelength collective-mode change in $\{\boldsymbol{\sigma}\}$ — *irrespective of the frustration within each R_i* . On the other hand, there is no topological guarantee that the lattice will be divided in this way (unlike what happens in the N -vector case); the clusters R_i might have size much larger than ξ , in which case the flips would not be of much use.¹² This whole question deserves further study [29].

2.3 Generalized Wolff-type embedding algorithms

It is now clear how to generalize this reasoning to a nonlinear σ -model taking values in an arbitrary compact Riemannian manifold M . Let us assume that the lattice Hamiltonian is of the form

$$H(\{\boldsymbol{\sigma}\}) = \beta \sum_{\langle xy \rangle} E(\boldsymbol{\sigma}_x, \boldsymbol{\sigma}_y) \quad (2.9)$$

where $E(\boldsymbol{\sigma}, \boldsymbol{\sigma}') = E(\boldsymbol{\sigma}', \boldsymbol{\sigma}) \sim \text{const} + d(\boldsymbol{\sigma}, \boldsymbol{\sigma}')^2$ as $\boldsymbol{\sigma}' \rightarrow \boldsymbol{\sigma}$ (here d is geodesic distance in M).¹³ Now let $T: M \rightarrow M$ be any map satisfying:

- a) T is *energy-preserving*, i.e. $E(T\boldsymbol{\sigma}, T\boldsymbol{\sigma}') = E(\boldsymbol{\sigma}, \boldsymbol{\sigma}')$ for all $\boldsymbol{\sigma}, \boldsymbol{\sigma}' \in M$. [In particular, by taking $\boldsymbol{\sigma}' \rightarrow \boldsymbol{\sigma}$ it follows that T preserves the metric tensor, and is therefore an isometry.]

We can then define an embedding of Ising spins $\{\varepsilon\}$ by the rule

$$\begin{aligned} \varepsilon_x = +1 &\implies \boldsymbol{\sigma}_x^{\text{new}} = \boldsymbol{\sigma}_x^{\text{old}} \\ \varepsilon_x = -1 &\implies \boldsymbol{\sigma}_x^{\text{new}} = T\boldsymbol{\sigma}_x^{\text{old}} \end{aligned} \quad (2.10)$$

¹²In the N -vector model, spins $\boldsymbol{\sigma}_x$ and $\boldsymbol{\sigma}_{x'}$ belonging to different hemispheres [i.e. for which $(\boldsymbol{\sigma}_x \cdot \mathbf{r})(\boldsymbol{\sigma}_{x'} \cdot \mathbf{r}) \leq 0$] are guaranteed to belong to distinct SW clusters. In the RP^{N-1} model, by contrast, *any* two spins $\boldsymbol{\sigma}_x, \boldsymbol{\sigma}_{x'}$ not lying on the equator or the pole can potentially be connected by a chain of spins $\boldsymbol{\sigma}_x \equiv \boldsymbol{\sigma}_{x_0}, \boldsymbol{\sigma}_{x_1}, \dots, \boldsymbol{\sigma}_{x_k} \equiv \boldsymbol{\sigma}_{x'}$ such that $\tilde{J}_{x_i x_{i+1}} \equiv (\boldsymbol{\sigma}_{x_i}^\perp \cdot \boldsymbol{\sigma}_{x_{i+1}}^\perp)(\boldsymbol{\sigma}_{x_i} \cdot \mathbf{r})(\boldsymbol{\sigma}_{x_{i+1}} \cdot \mathbf{r}) > 0$ for all i : see the preceding footnote. Thus, $\boldsymbol{\sigma}_x$ and $\boldsymbol{\sigma}_{x'}$ could belong to the same SW cluster.

¹³More generally, we could sum over *oriented* bonds (x, y) and allow E to be non-symmetric [i.e. $E(\boldsymbol{\sigma}, \boldsymbol{\sigma}') \neq E(\boldsymbol{\sigma}', \boldsymbol{\sigma})$]: this situation arises, for example, in an N -vector model in a fixed external gauge field (in particular, in a frustrated N -vector model). However, only the symmetric part of E contributes to the induced Ising Hamiltonian [see (2.12) below].

so that the induced Ising Hamiltonian is

$$H(\{\varepsilon\}) = - \sum_{\langle xy \rangle} J_{xy} \varepsilon_x \varepsilon_y - \sum_{\langle xy \rangle} h_{xy} (\varepsilon_x - \varepsilon_y) + \text{const} \quad (2.11)$$

where

$$J_{xy} = \frac{\beta}{4} [E(T\boldsymbol{\sigma}_x, \boldsymbol{\sigma}_y) + E(\boldsymbol{\sigma}_x, T\boldsymbol{\sigma}_y) - 2E(\boldsymbol{\sigma}_x, \boldsymbol{\sigma}_y)] \quad (2.12a)$$

$$h_{xy} = \frac{\beta}{4} [E(T\boldsymbol{\sigma}_x, \boldsymbol{\sigma}_y) - E(\boldsymbol{\sigma}_x, T\boldsymbol{\sigma}_y)] \quad (2.12b)$$

(For the original Wolff algorithm, this definition of $\{\varepsilon\}$ differs from (1.1) by a Z_2 gauge transformation.) In particular, if T is involutive, then $E(T\boldsymbol{\sigma}_x, \boldsymbol{\sigma}_y) = E(\boldsymbol{\sigma}_x, T\boldsymbol{\sigma}_y)$, so that the induced Ising Hamiltonian has zero magnetic field:

$$J_{xy} = \frac{\beta}{2} [E(\boldsymbol{\sigma}_x, T\boldsymbol{\sigma}_y) - E(\boldsymbol{\sigma}_x, \boldsymbol{\sigma}_y)] \quad (2.13a)$$

$$h_{xy} = 0 \quad (2.13b)$$

We remark that in general the couplings (2.13a) are frustrated; indeed, in Appendix A we prove that non-frustration occurs essentially *only* in the codimension-1 algorithm for the N -vector model, i.e. the original Wolff algorithm. (See Theorem A.10 and Corollaries A.11 and A.12 for details.)

A *Wolff-type embedding algorithm* is now specified by:

- (i) a collection \mathcal{T} of energy-preserving maps of M ; and
- (ii) a probability distribution ρ on \mathcal{T} .

One step of the algorithm consists of the following operations:

- (i) Choose randomly (with probability distribution ρ) a map $T \in \mathcal{T}$.
- (ii) Initialize $\{\varepsilon\} \equiv +1$.
- (iii) Update the induced Ising model (2.11)/(2.12), using any chosen Monte Carlo algorithm (e.g. standard SW).
- (iv) Update the $\{\boldsymbol{\sigma}\}$ according to (2.10).

If the group generated by \mathcal{T} acts transitively on M , then (under mild conditions on ρ) this algorithm will be ergodic. If not, then the foregoing moves must be supplemented by other types of updates (e.g. a local heat-bath or Metropolis update of the $\{\boldsymbol{\sigma}\}$) so as to make the combined algorithm ergodic.

The *idealized* embedding algorithm is, by definition, the one in which step (iii) consists of obtaining an *independent* sample from the induced Ising model.

Typically \mathcal{T} is obtained from a single map T by conjugating it with isometries of M , and ρ is taken to be an invariant measure; this is the case, for example, in the original Wolff algorithm, with its random choice of the unit vector \mathbf{r} . We shall

henceforth assume \mathcal{T} to be of this form, and shall refer to “the” map T as a shorthand for “any one of the maps $T \in \mathcal{T}$ ”.

In summary, the embedding algorithm can be *defined* for any collection \mathcal{T} of maps which are energy-preserving. But we claim that the algorithm will be *successful* in eliminating or at least radically reducing the critical slowing-down — i.e. have a dynamic critical exponent z significantly smaller than the $z \approx 2$ typical of local algorithms — only if a second property is satisfied:

- b) The fixed-point set $\text{Fix}(T) \equiv \{\boldsymbol{\sigma} \in M: T\boldsymbol{\sigma} = \boldsymbol{\sigma}\}$ has codimension 1.

Let us now set out, in detail, our reasoning supporting this claim:

- 1) In order for an algorithm to do a good job of beating critical slowing-down (i.e. have dynamic critical exponent $z \ll 2$), it is necessary that the algorithm be capable of making quickly (i.e. in one or a very few time steps) a significant change in all of the large-scale collective modes that are relevant for the (static) critical behavior of the given model.
- 2) Among the important large-scale collective modes in the nonlinear σ -models are the long-wavelength spin waves. (There may also be other important modes, such as vortices in the two-dimensional XY model; but there are in any case *at least* spin waves.)
- 3) It follows that for the algorithm to have $z \ll 2$, it is *necessary* that it do a good job of handling long-wavelength spin waves. (This may not be *sufficient*, if other types of collective modes are also important. For example, the multi-grid Monte Carlo algorithm [17, 14] does an excellent job of handling long-wavelength spin waves, but does less well in handling vortices; as a result, it eliminates critical slowing-down in the low-temperature (spin-wave) phase of the two-dimensional XY model, but not on the high-temperature side of criticality [18]. The same appears to be true of Fourier acceleration [22].)
- 4) An idealized Wolff-type embedding algorithm does a good job of handling spin waves *if and only if* it causes x -space to be divided into two or more large disconnected regions R_i which are almost decoupled from each other in the induced Ising Hamiltonian. The same holds true for a practical Wolff-type embedding algorithm, with “if and only if” replaced by “only if”.
- 5) The induced Ising Hamiltonian decouples along the manifold $\{x: \boldsymbol{\sigma}(x) \in \text{Fix}(T)\} = \{x: \boldsymbol{\sigma}(x) \approx T\boldsymbol{\sigma}(x)\}$, *and only there*.¹⁴
- 6) For a manifold to divide x -space into disconnected regions, it is *necessary* that the manifold be of codimension 0 or 1 (see Theorem A.1 in Appendix A).

¹⁴*Proof:* Assume that $E(\boldsymbol{\sigma}, \boldsymbol{\sigma}')$ has a *unique* minimum for fixed $\boldsymbol{\sigma}$ when $\boldsymbol{\sigma}' = \boldsymbol{\sigma}$ (and hence also for fixed $\boldsymbol{\sigma}'$ when $\boldsymbol{\sigma} = \boldsymbol{\sigma}'$). Then consider a bond $\langle xy \rangle$: we have $\boldsymbol{\sigma}_x \approx \boldsymbol{\sigma}_y$, since the original configuration is assumed smooth. Then $J_{xy} \approx 0$ if and only if $E(T\boldsymbol{\sigma}_x, \boldsymbol{\sigma}_y)$ and $E(\boldsymbol{\sigma}_x, T\boldsymbol{\sigma}_y)$ are both $\approx E(\boldsymbol{\sigma}_x, \boldsymbol{\sigma}_y) \approx \min E$. It follows that $T\boldsymbol{\sigma}_x \approx \boldsymbol{\sigma}_x$ (and $T\boldsymbol{\sigma}_y \approx \boldsymbol{\sigma}_y$) by the uniqueness of the minimum of E .

- 7) For a “generic” smooth spin configuration $\sigma: \mathbb{R}^d \rightarrow M$, the codimension of the set $\{x: \sigma(x) \in \text{Fix}(T)\}$ in x -space equals the codimension of $\text{Fix}(T)$ in the target manifold M (see Theorems A.4 and A.5).
- 8) $\text{Fix}(T)$ cannot have codimension 0 except in the trivial case $\text{Fix}(T) = M$ (see Theorem A.8).
- 9) **Conclusion:** For a Wolff-type embedding algorithm to have $z \ll 2$, it is *necessary* (though perhaps not sufficient) that $\text{Fix}(T)$ have codimension 1 in the target manifold M .

In our opinion, the only truly questionable step in this reasoning — at least as regards asymptotically free models — is Step 4. We have explained previously why an idealized Wolff-type embedding algorithm does a good job of handling spin waves *if* it causes x -space to be divided into large disconnected regions which are almost decoupled from each other. It is a substantial — and quite possibly unjustified — leap to assert that this is the *only* mechanism by which an idealized Wolff-type embedding algorithm can do a good job of handling spin waves. For example, suppose that the induced Ising Hamiltonian were to lie in a highly frustrated phase characterized by several “dominant” regions of configuration space which differ on long as well as short length scales. Then the corresponding *idealized* Wolff-type algorithm would, by definition, make frequent transitions between these regions; in particular, it would make frequent *global* changes in the $\{\varepsilon\}$ configuration, and hence presumably also in the $\{\sigma\}$ configuration. These global changes might be sufficient for the algorithm to do a good job of handling spin waves.¹⁵ (Of course, a *practical* Wolff-type algorithm might have great difficulty surmounting the barriers between these dominant regions of configuration space. But that is not our concern at present.)

Since our reasoning is based on considering “smooth” spin configurations, it is also questionable when applied to non-asymptotically-free models, as already discussed in Sections 2.1 and 2.2. Possibly our reasoning *does* become valid when reinterpreted as referring to a suitably coarse-grained spin field; but possibly not. Some insight into this problem could perhaps be obtained by comparing the (idealized) codimension-1 and codimension-2 algorithms [cf. (3.1) for $r = 1, 2$] for the *three*-dimensional N -vector model. However, it will be difficult to disentangle the effects of codimension from those of frustration, as the two phenomena go together (codimension 1 is unfrustrated, while codimension > 1 is frustrated). In this regard the three-dimensional RP^{N-1} model (if its phase transition is indeed continuous) could serve as a valuable comparison, since in this case *both* codimension 1 and codimension > 1 lead to frustrated induced Ising models.

All in all, we consider our Conclusion to be a *plausible conjecture*, which needs to be tested carefully. In Section 4 we test it in one asymptotically free model.

¹⁵We thank Ferenc Niedermayer for pointing out this possibility to us.

3 Classification of (Involutive) Isometries

The reasoning of the preceding section leads us to the following problem in differential geometry: Given a Riemannian manifold M , classify all the isometries of M according to the codimension(s) of their fixed-point manifolds. In particular, if we are interested in fixed-point manifolds of codimension 1, we can restrict attention to *involutive* isometries (see Theorem A.9).

If T is an isometry (resp. involutive isometry) of M , and f is any isometry of M , then $f \circ T \circ f^{-1}$ is also an isometry (resp. involutive isometry) of M ; we say that it is *conjugate to T* via the isometry f . Obviously, conjugacy is an equivalence relation; for any given manifold M , our goal will be to classify the (involutive) isometries of M , modulo conjugacy. Note that if p is a fixed point of T , then $f(p)$ is a fixed point of $f \circ T \circ f^{-1}$. In particular, if $\text{Fix}(T)$ is nonempty and the isometry group $\text{Isom}(M)$ acts transitively on M , then the conjugating map f can be chosen so that $\text{Fix}(f \circ T \circ f^{-1})$ passes through any desired point $q \in M$ (though not necessarily in any desired *direction*). So we can restrict attention, if desired, to (involutive) isometries T that leave fixed some chosen point p .

3.1 Some Examples

Example 1. $M = S^{N-1}$. All involutive isometries of S^{N-1} are conjugate (via an orthogonal transformation) to

$$T(\sigma^1, \dots, \sigma^N) = (-\sigma^1, \dots, -\sigma^r, \sigma^{r+1}, \dots, \sigma^N) \quad (3.1)$$

for some r ($0 \leq r \leq N$).¹⁶ Henceforth we shall write this transformation more compactly as $\sigma \rightarrow I_r \sigma$, where

$$I_r = \text{diag}(\underbrace{-1, \dots, -1}_{r \text{ times}}, \underbrace{+1, \dots, +1}_{N-r \text{ times}}). \quad (3.2)$$

For $0 \leq r \leq N-1$ the fixed-point manifold has codimension r ; for $r = N$ the fixed-point manifold is empty. (More precisely, for $0 \leq r \leq N-2$ the fixed-point manifold is isometric to S^{N-r-1} ; for $r = N-1$ it consists of two points.) The standard Wolff reflection (2.2) corresponds to the case $r = 1$.

Example 2. $M = RP^{N-1}$. Every isometry T of $RP^{N-1} \equiv S^{N-1}/\{\pm I\}$ “lifts” (nonuniquely) to an isometry \tilde{T} of S^{N-1} [hence a matrix $\tilde{T} \in O(N)$]; and conversely,

¹⁶*Proof:* Every isometry of S^{N-1} is induced by an orthogonal matrix $T \in O(N)$. An involutive isometry has $T^2 = I$. It follows that T is symmetric as well as orthogonal, and hence has eigenvalues ± 1 . Any such matrix can be diagonalized by a rotation; and by a further permutation of coordinates (which is also an orthogonal transformation) we can make all the -1 eigenvalues come first. Thus, there exists a matrix $R \in O(N)$ such that $RTR^{-1} = I_r \equiv \text{diag}(\underbrace{-1, \dots, -1}_{r \text{ times}}, \underbrace{+1, \dots, +1}_{N-r \text{ times}})$ for some r

($0 \leq r \leq N$).

every isometry of S^{N-1} commutes with $\pm I$ and hence induces a (unique) isometry on RP^{N-1} . Moreover, T is involutive if and only if $\tilde{T}^2 = \pm I$. We must therefore analyze two cases:

(a) If $\tilde{T}^2 = +I$, then \tilde{T} is conjugate [via an orthogonal transformation $R \in O(N)$] to a transformation of the form (3.1) for some r . Moreover, since R commutes with $\pm I$, this conjugacy acts also on RP^{N-1} , i.e. T is conjugate to the map induced on RP^{N-1} by (3.1).

(b) If $\tilde{T}^2 = -I$, then N must be even [since $\det(\tilde{T}^2) = (\det \tilde{T})^2 = +1$]; and \tilde{T} is easily seen to be conjugate [via some $R \in O(N)$] to the map $\sigma \rightarrow J\sigma$, where

$$J = \begin{pmatrix} 0 & I \\ -I & 0 \end{pmatrix} \quad (3.3)$$

and I is an $(N/2) \times (N/2)$ identity matrix.¹⁷

Thus, T is conjugate to the map induced on RP^{N-1} by one of the following:

(a_r) $\sigma \rightarrow I_r \sigma$. [Note that (a_r) and (a_{N-r}) are the same transformation.] The fixed-point set is the union of two disjoint connected manifolds, one isometric to RP^{N-r-1} and the other isometric to RP^{r-1} ; they have codimensions r and $N-r$, respectively.

(b) [Only for N even] $\sigma \rightarrow J\sigma$. The fixed-point manifold is empty.

Example 3. $M = CP^{N-1}$. The complex projective space CP^{N-1} is, by definition, the set of unit vectors in \mathbb{C}^N modulo the equivalence relation

$$z \simeq z' \iff z = e^{i\theta} z' \text{ for some real number } \theta. \quad (3.4)$$

There is a unique (up to multiples) Riemannian metric on CP^{N-1} that is invariant under the natural action of $U(N)$, namely the Fubini-Study metric [36, vol. II, pp. 159–160, 169]. The geodesic distance associated with this Riemannian metric is¹⁸

$$d(z, w) = 2 \cos^{-1} \left| \sum_{i=1}^N \bar{z}_i w_i \right| \quad (3.5)$$

(where, by abuse of language, we do not distinguish between an equivalence class $z \in CP^{N-1}$ and a representative unit vector $z \in \mathbb{C}^N$). The isometries of CP^{N-1} ($N \geq 2$) are fully classified by *Wigner's theorem*: every such isometry arises from a map $\mathbb{C}^N \rightarrow \mathbb{C}^N$ which is either unitary or antiunitary.¹⁹ Thus, any isometry of CP^{N-1} is of one of the forms

¹⁷*Proof:* Since $\tilde{T}^T \tilde{T} = I$ and $\tilde{T}^2 = -I$, we conclude that \tilde{T} is antisymmetric as well as orthogonal, and hence has eigenvalues $\pm i$. Any such matrix can be brought into 2×2 block-diagonal form by a rotation; and this is equivalent, by a permutation of coordinates, to J . Thus, there exists $R \in O(N)$ such that $R\tilde{T}R^{-1} = J$.

¹⁸This is easily demonstrated by integrating the Fubini-Study metric along the geodesic curves in CP^{N-1} [36, vol. II, p. 277], and appealing to unitary invariance.

¹⁹See e.g. [37] or [38, pp. 305–306].

(a) $z \rightarrow Uz$ with $U \in U(N)$

(b) $z \rightarrow U\bar{z}$ with $U \in U(N)$

A little analysis then shows that every *involutive* isometry of CP^{N-1} is conjugate to one of the following²⁰:

(a_r) $z \rightarrow I_r z$. [Note that (a_r) and (a_{N-r}) are the same transformation.] The fixed-point set is the union of two disjoint connected manifolds, one isometric to CP^{N-r-1} and the other isometric to CP^{r-1} ; they have codimensions $2r$ and $2(N-r)$, respectively.

(b1) $z \rightarrow \bar{z}$. The fixed-point manifold is connected and isometric to RP^{N-1} ; it has codimension $N-1$.

(b2) [Only for N even] $z \rightarrow J\bar{z}$. The fixed-point manifold is empty.

We conclude that *in CP^{N-1} ($N \geq 3$), there do not exist involutive isometries of codimension 1.* (For $N = 2$, CP^1 is isometric to the sphere S^2 , so an involutive isometry of codimension 1 of course does exist, namely $z \rightarrow \bar{z}$.) An even stronger nonexistence result is mentioned in Further Remarks 3 at the end of Appendix A.3.

Example 4. $M = SU(2)$. Since $SU(2)$ is isometric to S^3 via the map

$$\begin{aligned} (\sigma^0, \sigma^1, \sigma^2, \sigma^3) &\mapsto \sigma^0 I + i(\sigma^1 \tau^1 + \sigma^2 \tau^2 + \sigma^3 \tau^3) \\ &= \begin{pmatrix} \sigma^0 + i\sigma^3 & \sigma^2 + i\sigma^1 \\ -\sigma^2 + i\sigma^1 & \sigma^0 - i\sigma^3 \end{pmatrix} \end{aligned} \quad (3.6)$$

where τ^1, τ^2, τ^3 are the usual Pauli matrices, this is a special case of Example 1. But it is useful to translate those results into the $SU(2)$ matrix language, as a hint

²⁰*Proof:* Let T be an involutive isometry of CP^{N-1} . In case (a), we must have $U^2 = e^{i\alpha}I$, and by redefining the phases we can require $U^2 = I$. It follows that the eigenvalues of U are ± 1 , so there exists $V \in SU(N)$ such that $U = VI_r V^\dagger$ for some r ($0 \leq r \leq N$). Thus T is conjugate to the map $z \rightarrow I_r z$. In case (b), we must have $U\bar{U} = e^{i\alpha}I$, hence $U = e^{i\alpha}U^T$. Since $U \neq 0$, the only possibilities are $e^{i\alpha} = \pm 1$; and by taking determinants we see that $e^{i\alpha} = -1$ can occur only for N even. If $U\bar{U} = I$, then $U = XX^T$ for some $X \in U(N)$ [see the proof of case (c1) in Theorem B.4]; but then, taking $f(z) = X^\dagger z$, we have $(f \circ T \circ f^{-1})(z) = \bar{z}$. Similarly, if $U\bar{U} = -I$, then $U = XJX^T$ for some $X \in U(N)$ [see the proof of case (c2) in Theorem B.4]; but then, taking $f(z) = X^\dagger z$, we have $(f \circ T \circ f^{-1})(z) = J\bar{z}$.

Let us now compute the fixed-point manifolds F : *Case (a)*: F consists of points z satisfying $z = e^{i\alpha}I_r z$ for some α . For $\alpha \neq 0, \pi$ there are no $z \neq 0$ which satisfy this equation. Thus F consists of z which satisfy either $z = I_r z$ or $z = -I_r z$. These equations define disjoint connected manifolds isometric to CP^{N-r-1} and CP^{r-1} , respectively. *Case (b1)*: F consists of points z satisfying $z = e^{i\alpha}\bar{z}$ for some α , or equivalently $ze^{-i\alpha/2} = z e^{-i\alpha/2}$. Redefining phases, we can assume that $\alpha = 0$. So F is a connected manifold isometric to RP^{N-1} . *Case (b2)*: F consists of points z satisfying $z = e^{i\alpha}J\bar{z}$ for some α . It follows that $\bar{z} = e^{-i\alpha}Jz = J^2\bar{z} = -\bar{z}$, which is clearly impossible for $z \neq 0$. So the fixed-point manifold is empty.

See also [39, Theorem 7] and [40, Theorem 4.2] (case AIII with $p = N-1, q = 1$) for an alternate derivation of this list, based on a Lie-algebraic analysis.

toward generalizations to $SU(N)$. Recalling the definitions $I_1 = \begin{pmatrix} -1 & 0 \\ 0 & 1 \end{pmatrix}$ and $J = \begin{pmatrix} 0 & 1 \\ -1 & 0 \end{pmatrix}$, here is a (redundant) list of some involutive isometries of $SU(2)$:

Codimension 0:	$A \rightarrow A (= -J\bar{A}J)$	Fixed points:	All $SU(2)$
Codimension 1:	$A \rightarrow -A^\dagger$	Fixed points:	$\sigma^0 = 0$
	$A \rightarrow I_1 A^T I_1$	Fixed points:	$\sigma^1 = 0$
	$A \rightarrow A^T$	Fixed points:	$\sigma^2 = 0$
	$A \rightarrow I_1 A^\dagger I_1$	Fixed points:	$\sigma^3 = 0$
Codimension 2:	$A \rightarrow \bar{A}$	Fixed points:	$\sigma^1 = \sigma^3 = 0$
	$A \rightarrow I_1 A I_1$	Fixed points:	$\sigma^1 = \sigma^2 = 0$
	etc.		
Codimension 3:	$A \rightarrow A^\dagger (= -J A^T J)$	Fixed points:	$\sigma^1 = \sigma^2 = \sigma^3 = 0$
	etc.		

Example 5. $M = SU(N)$. In Appendix B we carry out a complete classification (modulo conjugation by an isometry) of the involutive isometries of $SU(N)$. [Surprisingly, we have been unable to find this classification anywhere in the mathematical or physical literature.] In particular, the involutive isometries of $SU(N)$ having nonempty fixed-point manifold are the following²¹:

(a_{r,r}) $A \rightarrow I_r A I_r$. [Note that (a_{r,r}) and (a_{N-r,N-r}) are the same transformation.] The fixed points are matrices of the form $\begin{pmatrix} B & 0 \\ 0 & C \end{pmatrix}$ with $B \in U(r)$, $C \in U(N-r)$ and $(\det B)(\det C) = 1$. We call this space $S(U(r) \times U(N-r))$; it is a subgroup of $SU(N)$, and has codimension $2r(N-r)$.

(b1) $A \rightarrow A^\dagger$. The fixed-point manifold is

$$\bigcup_{\substack{0 \leq r \leq N \\ r \text{ even}}} F_r,$$

where $F_r \equiv \{U I_r U^\dagger : U \in SU(N)\}$ is the coset space $SU(N)/S(U(r) \times U(N-r))$; it has codimension $r^2 + (N-r)^2 - 1$.

(b2) [Only for N even] $A \rightarrow e^{2\pi i/N} A^\dagger$. The fixed-point manifold is

$$\bigcup_{\substack{0 \leq r \leq N \\ r \text{ odd}}} F_r,$$

²¹See also [40, Theorem 3.3] for an alternate derivation of this list, based on a Lie-algebraic analysis.

where $F_r \equiv \{e^{\pi i/N} U I_r U^\dagger: U \in SU(N)\}$ is isometric to the coset space $SU(N)/S(U(r) \times U(N-r))$; it has codimension $r^2 + (N-r)^2 - 1$.

(c1) $A \rightarrow \bar{A}$. The fixed points are real matrices $A \in SO(N)$. This space is a subgroup of $SU(N)$, and has codimension $\frac{1}{2}(N^2 + N - 2)$.

(c2a) [Only for N even] $A \rightarrow -J\bar{A}J$. The fixed points are matrices A that are symplectic ($A^T J A = J$) as well as unitary. We call this space²² $USp(N/2) \equiv Sp(N/2, \mathbb{C}) \cap U(N)$; it is a subgroup of $SU(N)$, and has codimension $\frac{1}{2}(N^2 - N - 2)$.

(d1) $A \rightarrow A^T$. The fixed points are matrices $A = UU^T$ with $U \in SU(N)$. This is the coset space $SU(N)/SO(N)$; it has codimension $\frac{1}{2}(N^2 - N)$.

(d2) [Only for N even] $A \rightarrow -A^T$. The fixed points are matrices $A = UJU^T$ or $A = e^{2\pi i/N} UJU^T$ with $U \in SU(N)$. These two disjoint manifolds are each isometric to the coset space $SU(N)/USp(N/2)$; they have codimension $\frac{1}{2}(N^2 + N)$.

Therefore, in $SU(3)$ the involutive isometries (other than the identity map) having nonempty fixed-point manifold are:

Codimension 3:	$A \rightarrow A^T$	Fixed points:	$SU(3)/SO(3)$
Codimension 4:	$A \rightarrow I_1 A I_1$	Fixed points:	$S(U(1) \times U(2))$
	$A \rightarrow A^\dagger$	Fixed points:	$SU(3)/S(U(1) \times U(2))$
Codimension 5:	$A \rightarrow \bar{A}$	Fixed points:	$SO(3)$

In $SU(4)$ the non-identity involutive isometries of smallest codimension are

Codimension 5:	$A \rightarrow -J\bar{A}J$	Fixed points:	$USp(2)$
Codimension 6:	$A \rightarrow I_1 A I_1$	Fixed points:	$S(U(1) \times U(3))$
	$A \rightarrow A^T$	Fixed points:	$SU(4)/SO(4)$

In $SU(N)$, $N \geq 5$, the non-identity involutive isometry of smallest codimension is $A \rightarrow I_1 A I_1$, with codimension $2N - 2$.

We conclude that *in $SU(N)$, $N \geq 3$, there do not exist involutive isometries of codimension 1 (or even codimension 2).*

3.2 General Theory

Now let us try to find all Riemannian manifolds (within a certain class to be defined below) admitting an involutive isometry with fixed-point manifold of codimension 1. (Such an involutive isometry is sometimes called a *mirror*.) We need a few definitions and facts from differential geometry [36, 42, 38]:

²²See e.g. [41, pp. 347–349]. In the differential-geometry literature (e.g. [42, p. 340]) this group is often called $Sp(N/2)$.

A Riemannian manifold is called *homogeneous* if it possesses a transitive group of isometries [i.e. if for all $p, q \in M$ there exists an isometry f such that $f(p) = q$]. Every homogeneous Riemannian manifold is complete.

A Riemannian manifold is called *symmetric* (or *globally symmetric*, or a *symmetric space*) if for each $p \in M$ there exists an involutive isometry of M having p as an isolated fixed point. Every Riemannian symmetric space is homogeneous, and the Riemannian symmetric spaces have been completely classified [38, Theorems 8.11.4 and 8.3.12]. Virtually all the target manifolds arising in physical applications are symmetric spaces [43, 44]. (The only exception we know of arises in the σ -model approach to string theory [45, 46], in which general target spaces are needed.)

Let M be a Riemannian manifold with metric tensor g and curvature tensor R . Then, for any point $p \in M$ and any two-dimensional vector subspace S of the tangent space $T_p M$, the *sectional curvature at p along S* is defined to be

$$K(p, S) = \frac{g_p(R_p(v, w)w, v)}{g_p(v, v)g_p(w, w) - g_p(v, w)^2}, \quad (3.7)$$

where v and w are any two linearly independent vectors in S . If $K(p, S) = k$ for all $p \in M$ and all planes $S \subset T_p M$, then M is called a *space of constant curvature k* .^{23,24} Much is known about spaces of constant curvature: see [38], and especially Corollary 2.4.10, Theorem 2.5.1, Theorem 2.7.1 and Corollary 2.7.2. For our purposes, the following results suffice:

Theorem 3.1 *Let M be a connected homogeneous Riemannian manifold of dimension n and constant curvature k . Then either*

(a) $k < 0$ and M is isometric to the hyperbolic space H^n of “radius” $k^{-1/2}$ in \mathbb{R}^{n+1}

or

(b _{m}) [$0 \leq m \leq n$] $k = 0$ and M is isometric to the product $\mathbb{R}^m \times T^{n-m}$ of a Euclidean space with a flat Riemannian torus $T^{n-m} \equiv \mathbb{R}^{n-m}/\Gamma$ (here Γ is a discrete subgroup of the translation group \mathbb{R}^{n-m} , generated by $n - m$ linearly independent vectors)

or else

(c) $k > 0$ and M is isometric to one of the following:

(i) the sphere S^n of radius $k^{-1/2}$ in \mathbb{R}^{n+1}

²³In fact, if $\dim M \geq 3$ it suffices that $K(p, S)$ be independent of S for each $p \in M$; then a theorem of Schur [38, Theorem 2.2.7] ensures that $K(p, S)$ is constant also as a function of p .

²⁴This should not be confused with the constancy of the curvature tensor (or of the sectional curvature) under *parallel translation*. Indeed, these latter conditions provide two alternative definitions of the *Riemannian locally symmetric spaces* [38, pp. Theorem 8.1.1]. At least one book [47] makes the unfortunate decision to use the term “space of constant curvature” for what everyone else calls “Riemannian locally symmetric space”.

- (ii) the real projective space $RP^n \equiv S^n/\{\pm I\}$
- (iii) [only for n odd] the quotient space S^n/Z_m with $m > 2$; here S^n is considered as the unit sphere of $\mathbb{C}^{(n+1)/2}$, and the group $Z_m \subset U(1)$ acts by scalar multiplication
- (iv) [only for $n = 4l + 3$, l integer] one of the quotient spaces S^n/D_m^* with $m > 2$, S^n/T^* , S^n/O^* or S^n/I^* ; here S^n is considered as the unit sphere of $\mathbb{Q}^{(n+1)/4}$ (\mathbb{Q} = quaternions), and D_m^* , T^* , O^* and I^* are the dihedral, tetrahedral, octahedral and icosahedral groups lifted to $SU(2) \simeq U(1, \mathbb{Q})$ and acting by scalar multiplication

In particular, M is compact in cases (b₀) and (c), and only these.

PROOF. This is an immediate consequence of [38, Theorem 2.7.1 and Corollary 2.7.2].

■

Corollary 3.2 *Let M be a connected Riemannian symmetric space of dimension n and constant curvature k . Then either*

(a) $k < 0$ and M is isometric to the hyperbolic space H^n

or

(b _{m}) [$0 \leq m \leq n$] $k = 0$ and M is isometric to a product $\mathbb{R}^m \times T^{n-m}$

or else

(c) $k > 0$ and M is isometric to either the sphere S^n or the real projective space $RP^n \equiv S^n/\{\pm I\}$.

In particular, M is compact in cases (b₀) and (c), and only these.

PROOF. Since every Riemannian symmetric space is homogeneous, it suffices to analyze the cases in Theorem 3.1. By [38, Theorem 8.3.12], the quotient S^n/Γ is a symmetric space if and only if Γ is a discrete subgroup of $\Delta \equiv$ centralizer of $SO(n+1)$ in $O(n+1) = \{\pm I\}$. ■

A connected Riemannian manifold is said to be *irreducible* if it is not locally isometric to a product of lower-dimensional manifolds. Equivalently, M is irreducible if for some (or all) $p \in M$ the linear holonomy group Ψ_p acts irreducibly on the tangent space T_pM .

The irreducible Riemannian symmetric spaces admitting a mirror have been completely classified by Iwahori [48]:

Theorem 3.3 *Let M be an irreducible Riemannian symmetric space of dimension n . Then the following are equivalent:*

- (a) M admits an involutive isometry whose fixed-point manifold has at least one connected component of codimension 1.
- (b) M is a space of constant curvature.
- (c) M is isometric to either the sphere S^n , the real projective space $RP^n \equiv S^n/\{\pm I\}$, or the hyperbolic space H^n .

[Here (b) \iff (c) follows from Corollary 3.2, and (c) \implies (a) is easy. The hard part of the proof is (a) \implies (b).]

Thus, the only irreducible compact Riemannian symmetric spaces admitting a mirror are the examples we already know: the sphere S^n and the real projective space RP^n .

Remarks. 1. It is, as far as we know, an open question whether (a) \implies (b) in Theorem 3.3 holds also for irreducible homogeneous Riemannian manifolds that are not symmetric spaces.

2. Some relevant related work can be found in [49, 50]; unfortunately, we have not yet been able to obtain a copy of these articles. For related work on reflections in *complex* manifolds, see [51, 52].

Next we would like to classify the *reducible* Riemannian symmetric spaces admitting a mirror (or more interestingly, admitting a transitive group of mirrors). However, since σ -models taking values in a reducible Riemannian symmetric space are of lesser interest for physical applications, we leave this classification for the mathematicians. But it is not difficult to show that a transitive group of mirrors can exist only if M is a sphere, a product of spheres, or the quotient of such a space by a discrete group.²⁵

4 Numerical Study of Embedding Algorithms for the $O(4)$ Model

In Section 2 we conjectured that the idealized embedding algorithm can perform well (i.e. have $z \ll 2$) *only* if it is based on a involutive isometry T whose fixed-point manifold has codimension 1. In order to test this conjecture, we have studied the two-dimensional N -vector model for $N = 4$ using the embedding algorithm based on a codimension-2 reflection [i.e. (3.1) with $r = 2$]. For comparison, we have also generated additional data (extending [4]) on this same model using the codimension-1 reflection.

²⁵One amusing application involves a σ -model taking values in the space $S^1 \times S^1$ (i.e. two uncoupled XY models): in addition to the standard Wolff algorithm based on the codimension-1 reflections $\theta \rightarrow -\theta$ and $\phi \rightarrow -\phi$, there is another algorithm based on the codimension-1 reflections $\theta \leftrightarrow \phi$ and $\theta \leftrightarrow -\phi$. Physically, this algorithm takes chunks from one system and pastes them into the other system (possibly reflected). We conjecture that this algorithm will also have $z \approx 0$.

4.1 Quantities to be Measured

For any observable A , define the unnormalized autocorrelation function

$$C_{AA}(t) = \langle A_s A_{s+t} \rangle - \langle A \rangle^2, \quad (4.1)$$

where expectations are taken *in equilibrium*. The corresponding normalized autocorrelation function is

$$\rho_{AA}(t) = C_{AA}(t)/C_{AA}(0). \quad (4.2)$$

We then define the *integrated autocorrelation time*

$$\begin{aligned} \tau_{int,A} &= \frac{1}{2} \sum_{t=-\infty}^{\infty} \rho_{AA}(t) \\ &= \frac{1}{2} + \sum_{t=1}^{\infty} \rho_{AA}(t) \end{aligned} \quad (4.3)$$

[The factor of $\frac{1}{2}$ is purely a matter of convention; it is inserted so that $\tau_{int,A} \approx \tau$ if $\rho_{AA}(t) \approx e^{-|t|/\tau}$ with $\tau \gg 1$.] The integrated autocorrelation time controls the statistical error in Monte Carlo measurements of $\langle A \rangle$. More precisely, the sample mean

$$\bar{A} \equiv \frac{1}{n} \sum_{t=1}^n A_t \quad (4.4)$$

has variance

$$\begin{aligned} \text{var}(\bar{A}) &= \frac{1}{n^2} \sum_{r,s=1}^n C_{AA}(r-s) \\ &= \frac{1}{n} \sum_{t=-(n-1)}^{n-1} \left(1 - \frac{|t|}{n}\right) C_{AA}(t) \end{aligned} \quad (4.5)$$

$$\approx \frac{1}{n} (2\tau_{int,A}) C_{AA}(0) \quad \text{for } n \gg \tau \quad (4.6)$$

Thus, the variance of \bar{A} is a factor $2\tau_{int,A}$ larger than it would be if the $\{A_t\}$ were statistically independent. Stated differently, the number of “effectively independent samples” in a run of length n is roughly $n/2\tau_{int,A}$. The autocorrelation time $\tau_{int,A}$ (for interesting observables A) is therefore a “figure of (de)merit” of a Monte Carlo algorithm.

We shall measure static quantities (expectations) and dynamic quantities (autocorrelation times) for the following observables:

$$\mathcal{M}^2 = \left(\sum_x \sigma_x \right)^2 \quad (4.7)$$

$$\mathcal{F} = \frac{1}{2} \left[\left| \sum_x e^{2\pi i x_1/L} \sigma_x \right|^2 + \left| \sum_x e^{2\pi i x_2/L} \sigma_x \right|^2 \right] \quad (4.8)$$

$$\mathcal{E} = \sum_{\langle xx' \rangle} \sigma_x \cdot \sigma_{x'} \quad (4.9)$$

The mean values of these observables give information on different aspects of the 2-point function

$$G(x) = \langle \boldsymbol{\sigma}_0 \cdot \boldsymbol{\sigma}_x \rangle \quad (4.10a)$$

$$\tilde{G}(p) = \sum_x e^{ip \cdot x} \langle \boldsymbol{\sigma}_0 \cdot \boldsymbol{\sigma}_x \rangle \quad (4.10b)$$

In particular, we are interested in the *susceptibility*

$$\chi = \tilde{G}(0) = V^{-1} \langle \mathcal{M}^2 \rangle \quad (4.11)$$

and the analogous quantity at the smallest nonzero momentum

$$F = \tilde{G}(p)|_{|p|=2\pi/L} = V^{-1} \langle \mathcal{F} \rangle. \quad (4.12)$$

By combining these we can obtain the (*second-moment*) *correlation length*

$$\xi = \left(\frac{(\chi/F) - 1}{4 \sin^2(\pi/L)} \right)^{1/2} \quad (4.13)$$

(see the Remark below). Finally, we have the (negative) *energy*

$$E = 2G(x)|_{|x|=1} = V^{-1} \langle \mathcal{E} \rangle. \quad (4.14)$$

Here $V = L^2$ is the number of sites in the lattice.

Remark. The definition (4.13) is sometimes summarized [4] by saying that we are fitting $\tilde{G}(p)$ to the Ansatz

$$\tilde{G}(p) = Z \left[\xi^{-2} + 4 \sum_{i=1}^d \sin^2(p_i/2) \right]^{-1} \quad (4.15)$$

at $p = 0$ and $|p| = 2\pi/L$. This is of course true; but it is important to emphasize that we are *not* assuming that $\tilde{G}(p)$ really has the free-field form (4.15) at general p (of course it doesn't). Rather, we simply use this form to motivate *one* reasonable definition of the second-moment correlation length ξ on a finite lattice. Another definition — slightly different but equally reasonable — would be

$$\begin{aligned} \xi' &= \left(\frac{1}{2d} \frac{\sum_x \left(\sum_{i=1}^d (L/\pi)^2 \sin^2(\pi x_i/L) \right) G(x)}{\sum_x G(x)} \right)^{1/2} \\ &= \frac{L^2}{4\pi^2} \left(1 - \frac{F}{\chi} \right). \end{aligned} \quad (4.16)$$

The two definitions coincide in the infinite-volume limit $L \rightarrow \infty$. Finally, let us emphasize that *neither* of these quantities is equal to the exponential correlation length (= 1/mass gap)

$$\xi_{exp} = \lim_{|x| \rightarrow \infty} \frac{-|x|}{\log G(x)}. \quad (4.17)$$

However, ξ (or ξ') and ξ_{exp} are believed to scale in the same way as $\beta \rightarrow \infty$.

The integrated autocorrelation time $\tau_{int,A}$ can be estimated by standard procedures of statistical time-series analysis [53, 54]. These procedures also give statistically valid *error bars* on $\langle A \rangle$ and $\tau_{int,A}$. For more details, see [55, Appendix C]. In this paper we have used in all cases a self-consistent truncation window of width $6\tau_{int,A}$. In setting error bars on ξ we have used the triangle inequality; such error bars are overly conservative, but we did not feel it was worth the trouble to measure the cross-correlations between \mathcal{M}^2 and \mathcal{F} .

4.2 Numerical Results

In Table 1 we present results using the codimension-1 embedding algorithm (i.e. the usual Wolff embedding); the induced Ising model is simulated by N_{hit} hits of the standard SW algorithm. Additional data on larger lattices (but only for $N_{hit} = 1$) can be found in [4]. In Tables 2 and 3 we present the analogous results for the codimension-2 algorithm; here the induced Ising model is simulated by N_{hit} hits of the standard SW algorithm generalized in the obvious way to a mixed ferromagnetic/antiferromagnetic Ising model.²⁶

In Table 4 we summarize, for the convenience of the reader, our best estimates of the static quantities χ , ξ and E on lattices of size $L = 32, 64$. These estimates come from merging all the data in Tables 1–3 together with the data from our earlier work on the codimension-1 algorithm [4] and from a separate work using the multi-grid Monte Carlo algorithm [19].²⁷ We use these merged data in our finite-size-scaling analyses whenever ξ is required. (An analogous table for $L = 128, 256$ can be found in [19].)

In the codimension-1 algorithm, the induced Ising model is ferromagnetic, and 10 SW hits are already enough to produce an “almost independent” sample from the induced Ising model. As a result, the autocorrelation times for $N_{hit} = 10, 20$ are equal within error bars, and their average can be taken to represent the idealized ($N_{hit} = \infty$) algorithm, as shown in Table 1.

In the codimension-2 algorithm, by contrast, the induced Ising model is highly frustrated (see Table 5), and all known algorithms for updating this model are extremely inefficient. Both the standard SW algorithm (as generalized to mixed ferromagnetic/antiferromagnetic Ising models) and the single-site Metropolis algorithm have *very slow* convergence to equilibrium, which gets worse as β and L are increased.

²⁶The data points at $\beta = 2.20$, $N_{hit} = 1$ for $L = 32, 64$ may be unreliable, because the data discarded at the beginning of the run may have been insufficient to ensure equilibrium. (Indeed, the values for χ , ξ and E seem systematically low.) Unfortunately, the raw data files for these runs were lost, so we are unable to reanalyze them with a larger discard interval. We include these data points in Tables 2 and 3 simply to show the order of magnitude of $\tau_{int, \mathcal{M}^2}$ and $\tau_{int, \mathcal{E}}$. We do *not* include them in the table of merged static data (Table 4).

²⁷The $\beta = 2.20$, $N_{hit} = 1$ points from Tables 2 and 3 are *not* included in these means. In all other cases, χ , ξ and E from the different algorithms agree within error bars; this is strong evidence that all the programs are correct!

Codimension = 1									
L	β	N_{hit}	Sweeps	χ	ξ	E	$\tau_{int, \mathcal{M}^2}$	$\tau_{int, \mathcal{E}}$	
32	1.70	1	100000	27.4 (0.2)	3.54 (0.01)	0.98438 (0.00037)	4.53 (0.16)	11.39 (0.61)	
32	1.70	10	50000	28.0 (0.2)	3.71 (0.02)	0.98400 (0.00037)	3.61 (0.15)	5.80 (0.31)	
32	1.70	20	50000	27.4 (0.2)	3.58 (0.02)	0.98399 (0.00039)	3.76 (0.16)	6.11 (0.33)	
32	1.70	∞					3.68 (0.11)	5.96 (0.23)	
32	1.80	1	50000	41.4 (0.4)	4.70 (0.03)	1.04361 (0.00057)	5.77 (0.31)	13.57 (1.11)	
32	1.80	10	50000	40.9 (0.3)	4.61 (0.03)	1.04445 (0.00039)	4.04 (0.18)	6.34 (0.36)	
32	1.80	20	50000	41.2 (0.3)	4.65 (0.03)	1.04422 (0.00039)	4.44 (0.21)	6.76 (0.39)	
32	1.80	∞					4.24 (0.14)	6.55 (0.27)	
32	1.90	1	50000	62.8 (0.6)	6.03 (0.04)	1.10225 (0.00054)	6.80 (0.40)	13.00 (1.05)	
32	1.90	10	50000	61.6 (0.5)	5.92 (0.03)	1.10092 (0.00037)	4.37 (0.21)	6.35 (0.36)	
32	1.90	20	50000	63.3 (0.5)	6.08 (0.04)	1.10168 (0.00037)	4.83 (0.23)	6.21 (0.34)	
32	1.90	∞					4.60 (0.16)	6.28 (0.25)	
32	2.00	1	50000	94.4 (0.8)	7.76 (0.05)	1.15555 (0.00053)	7.77 (0.48)	13.46 (1.10)	
32	2.00	10	52000	93.4 (0.7)	7.64 (0.04)	1.15518 (0.00039)	5.59 (0.29)	7.60 (0.46)	
32	2.00	20	50000	94.0 (0.7)	7.71 (0.04)	1.15491 (0.00038)	5.53 (0.29)	7.16 (0.42)	
32	2.00	∞					5.56 (0.21)	7.38 (0.31)	
32	2.10	1	60000	134.9 (1.0)	9.64 (0.06)	1.20484 (0.00045)	9.51 (0.60)	13.57 (1.01)	
32	2.10	10	50000	136.3 (0.8)	9.78 (0.05)	1.20390 (0.00035)	5.92 (0.32)	6.89 (0.40)	
32	2.10	20	50000	134.1 (0.9)	9.58 (0.05)	1.20396 (0.00036)	6.18 (0.34)	6.90 (0.40)	
32	2.10	∞					6.05 (0.23)	6.89 (0.28)	
32	2.20	1	60000	178.2 (1.1)	11.59 (0.07)	1.24760 (0.00047)	10.61 (0.70)	15.73 (1.27)	
32	2.20	10	52000	177.4 (0.9)	11.52 (0.06)	1.24765 (0.00033)	6.23 (0.34)	7.02 (0.41)	
32	2.20	20	50000	180.1 (0.9)	11.64 (0.06)	1.24872 (0.00035)	6.39 (0.36)	7.42 (0.45)	
32	2.20	∞					6.31 (0.25)	7.22 (0.30)	
64	2.00	1	60000	98.6 (0.8)	7.72 (0.05)	1.15384 (0.00023)	4.76 (0.21)	12.39 (0.89)	
64	2.00	10	50000	99.7 (0.8)	7.87 (0.05)	1.15400 (0.00018)	3.79 (0.17)	6.48 (0.37)	
64	2.00	20	50000	99.4 (0.8)	7.91 (0.05)	1.15353 (0.00019)	3.94 (0.17)	6.92 (0.40)	
64	2.00	∞					3.87 (0.12)	6.70 (0.27)	
64	2.10	1	60000	160.2 (1.4)	10.38 (0.06)	1.20229 (0.00023)	6.24 (0.32)	13.73 (1.03)	
64	2.10	10	50000	163.1 (1.4)	10.61 (0.06)	1.20145 (0.00018)	4.76 (0.23)	7.23 (0.43)	
64	2.10	20	50000	159.1 (1.3)	10.28 (0.06)	1.20191 (0.00018)	4.31 (0.20)	6.90 (0.40)	
64	2.10	∞					4.54 (0.15)	7.07 (0.29)	
64	2.20	1	60000	256.4 (2.2)	13.70 (0.08)	1.24507 (0.00022)	7.49 (0.42)	14.17 (1.08)	
64	2.20	10	50000	258.2 (1.9)	13.75 (0.08)	1.24552 (0.00017)	4.86 (0.24)	7.24 (0.44)	
64	2.20	20	50000	257.1 (2.0)	13.70 (0.08)	1.24535 (0.00017)	5.32 (0.27)	6.90 (0.40)	
64	2.20	∞					5.09 (0.18)	7.07 (0.30)	
64	2.30	1	60000	393.4 (2.8)	17.75 (0.10)	1.28437 (0.00021)	8.06 (0.47)	13.75 (1.03)	
64	2.30	10	50000	397.7 (2.7)	17.88 (0.10)	1.28444 (0.00016)	6.04 (0.33)	7.38 (0.45)	
64	2.30	20	50000	395.1 (2.6)	17.82 (0.10)	1.28444 (0.00017)	5.74 (0.31)	7.22 (0.43)	
64	2.30	∞					5.89 (0.23)	7.30 (0.31)	
64	2.40	1	60000	549.6 (3.3)	21.76 (0.12)	1.31948 (0.00020)	8.93 (0.54)	13.87 (1.05)	
64	2.40	10	50000	554.5 (3.0)	22.04 (0.12)	1.31945 (0.00016)	6.54 (0.37)	7.66 (0.47)	
64	2.40	20	50000	556.8 (3.1)	22.09 (0.12)	1.31952 (0.00016)	6.67 (0.39)	7.57 (0.47)	
64	2.40	∞					6.61 (0.27)	7.62 (0.33)	
64	2.50	1	60000	701.1 (3.4)	25.54 (0.13)	1.35087 (0.00019)	9.56 (0.60)	14.43 (1.11)	
64	2.50	10	50000	708.8 (3.0)	25.85 (0.12)	1.35091 (0.00014)	6.18 (0.34)	7.11 (0.42)	
64	2.50	20	50250	708.1 (3.0)	25.91 (0.12)	1.35080 (0.00015)	6.22 (0.34)	7.14 (0.42)	
64	2.50	∞					6.20 (0.24)	7.12 (0.30)	

Table 1: Results at $L = 32$ and $L = 64$ from the codimension-1 algorithm. The runs were either started from an equilibrium configuration or else had 1000 sweeps discarded for equilibration. Rows labelled $N_{hit} = \infty$ are averages of the $N_{hit} = 10, 20$ values. Standard error is shown in parentheses.

Codimension = 2									
L	β	N_{hit}	Sweeps	χ	ξ	E	$\tau_{int, \mathcal{M}^2}$	$\tau_{int, \mathcal{E}}$	
32	1.70	1	100000	28.0 (0.2)	3.68 (0.02)	0.98453 (0.00042)	8.92 (0.42)	14.06 (0.82)	
32	1.70	5	100000	27.8 (0.2)	3.68 (0.01)	0.98398 (0.00028)	3.57 (0.11)	6.75 (0.28)	
32	1.70	10	50000	28.3 (0.2)	3.75 (0.02)	0.98460 (0.00036)	2.80 (0.10)	5.63 (0.30)	
32	1.70	20	50000	28.0 (0.2)	3.69 (0.02)	0.98465 (0.00037)	2.51 (0.09)	5.72 (0.31)	
32	1.70	40	50000	27.6 (0.2)	3.57 (0.02)	0.98422 (0.00037)	2.30 (0.08)	5.86 (0.32)	
32	1.70	80	80000	27.7 (0.1)	3.65 (0.01)	0.98350 (0.00028)	2.24 (0.06)	5.45 (0.22)	
32	1.70	160	100000	28.0 (0.1)	3.70 (0.01)	0.98440 (0.00026)	2.23 (0.05)	5.76 (0.22)	
32	1.80	1	200000	42.5 (0.4)	4.83 (0.03)	1.04459 (0.00031)	20.63 (1.03)	16.62 (0.75)	
32	1.80	5	300000	41.1 (0.2)	4.63 (0.01)	1.04460 (0.00018)	7.33 (0.18)	8.06 (0.21)	
32	1.80	10	250000	41.3 (0.2)	4.67 (0.01)	1.04479 (0.00018)	5.25 (0.12)	7.25 (0.19)	
32	1.80	20	250000	41.3 (0.1)	4.68 (0.01)	1.04447 (0.00018)	4.17 (0.09)	6.72 (0.17)	
32	1.80	40	250000	41.4 (0.1)	4.68 (0.01)	1.04477 (0.00018)	3.69 (0.07)	6.95 (0.18)	
32	1.80	80	100000	41.1 (0.2)	4.65 (0.02)	1.04444 (0.00028)	3.37 (0.10)	6.76 (0.28)	
32	1.80	160	80000	41.6 (0.2)	4.71 (0.02)	1.04429 (0.00031)	3.15 (0.10)	6.61 (0.30)	
32	1.80	320	100000	41.5 (0.2)	4.69 (0.02)	1.04440 (0.00027)	3.19 (0.09)	6.38 (0.25)	
32	1.90	1	200000	61.7 (0.7)	5.93 (0.05)	1.10152 (0.00033)	43.76 (3.18)	20.17 (1.00)	
32	1.90	5	300000	62.0 (0.4)	5.94 (0.02)	1.10167 (0.00019)	14.80 (0.51)	9.74 (0.27)	
32	1.90	10	300000	62.5 (0.3)	6.00 (0.02)	1.10175 (0.00018)	10.79 (0.32)	8.65 (0.23)	
32	1.90	20	250000	62.2 (0.3)	5.98 (0.02)	1.10143 (0.00019)	8.58 (0.25)	7.97 (0.22)	
32	1.90	40	250000	61.8 (0.3)	5.93 (0.02)	1.10167 (0.00019)	6.95 (0.18)	7.98 (0.22)	
32	1.90	80	100000	62.0 (0.4)	5.97 (0.03)	1.10147 (0.00030)	6.24 (0.25)	8.30 (0.37)	
32	1.90	160	100000	62.3 (0.4)	5.96 (0.03)	1.10212 (0.00029)	5.54 (0.21)	7.69 (0.34)	
32	1.90	320	100000	61.9 (0.4)	5.95 (0.02)	1.10156 (0.00029)	5.39 (0.20)	7.80 (0.34)	
32	1.90	640	50000	61.7 (0.5)	5.92 (0.03)	1.10120 (0.00040)	4.95 (0.24)	7.33 (0.44)	
32	2.00	1	200000	93.2 (1.4)	7.63 (0.09)	1.15507 (0.00037)	92.52 (9.76)	26.83 (1.52)	
32	2.00	5	300000	93.8 (0.7)	7.67 (0.04)	1.15510 (0.00020)	29.77 (1.46)	12.41 (0.39)	
32	2.00	10	300000	92.7 (0.6)	7.61 (0.03)	1.15493 (0.00018)	22.17 (0.94)	10.20 (0.29)	
32	2.00	20	250000	94.3 (0.5)	7.74 (0.03)	1.15522 (0.00019)	16.42 (0.66)	9.58 (0.29)	
32	2.00	40	250000	93.4 (0.5)	7.64 (0.03)	1.15517 (0.00020)	12.52 (0.44)	9.45 (0.29)	
32	2.00	80	100000	94.8 (0.7)	7.76 (0.04)	1.15542 (0.00030)	10.85 (0.56)	9.17 (0.44)	
32	2.00	160	100000	94.5 (0.7)	7.73 (0.04)	1.15532 (0.00031)	10.16 (0.50)	9.64 (0.47)	
32	2.00	320	100000	93.4 (0.7)	7.64 (0.04)	1.15552 (0.00032)	9.64 (0.47)	9.97 (0.49)	
32	2.00	640	100000	94.5 (0.6)	7.76 (0.04)	1.15494 (0.00032)	9.24 (0.44)	9.73 (0.47)	
32	2.10	5	105000	137.4 (1.6)	9.90 (0.10)	1.20400 (0.00034)	45.50 (4.68)	13.66 (0.77)	
32	2.10	10	300000	134.5 (0.8)	9.60 (0.10)	1.20388 (0.00020)	35.91 (1.93)	12.78 (0.41)	
32	2.10	20	300000	134.5 (0.7)	9.61 (0.04)	1.20391 (0.00019)	26.97 (1.26)	11.74 (0.36)	
32	2.10	40	300000	134.4 (0.7)	9.62 (0.04)	1.20394 (0.00018)	21.30 (0.88)	10.76 (0.32)	
32	2.10	80	400000	134.3 (0.5)	9.60 (0.03)	1.20391 (0.00016)	17.66 (0.58)	10.80 (0.28)	
32	2.10	160	400000	134.8 (0.4)	9.66 (0.03)	1.20386 (0.00016)	14.88 (0.45)	10.77 (0.28)	
32	2.10	320	105000	135.4 (0.9)	9.70 (0.10)	1.20409 (0.00031)	14.76 (0.87)	11.17 (0.57)	
32	2.10	640	100000	134.1 (0.9)	9.59 (0.05)	1.20390 (0.00031)	13.16 (0.74)	10.28 (0.51)	
32	2.20	1	250000	172.4 (2.2)	11.13 (0.14)	1.24682 (0.00033)	177.34 (23.39)	34.40 (2.00)	
32	2.20	5	301000	180.0 (1.1)	11.68 (0.07)	1.24783 (0.00020)	55.67 (3.72)	15.41 (0.54)	
32	2.20	10	300000	178.7 (1.0)	11.59 (0.06)	1.24791 (0.00019)	44.06 (2.62)	13.19 (0.43)	
32	2.20	20	300000	179.7 (0.9)	11.68 (0.06)	1.24783 (0.00018)	34.04 (1.78)	12.42 (0.39)	
32	2.20	40	100000	179.7 (1.3)	11.64 (0.08)	1.24786 (0.00032)	28.45 (2.36)	12.74 (0.71)	
32	2.20	80	100000	179.0 (1.2)	11.59 (0.08)	1.24791 (0.00031)	23.63 (1.78)	11.38 (0.60)	
32	2.20	160	100100	178.8 (1.2)	11.59 (0.08)	1.24801 (0.00031)	21.67 (1.56)	12.14 (0.66)	
32	2.20	320	100000	179.7 (1.1)	11.66 (0.07)	1.24805 (0.00031)	19.23 (1.31)	11.61 (0.62)	

Table 2: Results at $L = 32$ from the codimension-2 algorithm. All runs were started in equilibrium, except for $\beta = 2.20$, $N_{hit} = 1$, where 5000 sweeps (probably not enough) were discarded for equilibration. Standard error is shown in parentheses.

Codimension = 2									
L	β	N_{hit}	Sweeps	χ	ξ	E	$\tau_{int, \mathcal{M}^2}$	$\tau_{int, \mathcal{E}}$	
64	2.00	1	200000	99.7 (1.9)	7.86 (0.10)	1.15404 (0.00017)	89.48 (9.28)	24.59 (1.34)	
64	2.00	5	300500	98.8 (0.9)	7.79 (0.05)	1.15368 (0.00010)	31.71 (1.60)	11.73 (0.36)	
64	2.00	10	250000	100.3 (0.8)	7.93 (0.05)	1.15382 (0.00010)	21.06 (0.95)	9.98 (0.31)	
64	2.00	20	200000	98.6 (0.8)	7.80 (0.04)	1.15368 (0.00011)	15.99 (0.70)	9.56 (0.33)	
64	2.00	40	100200	100.1 (1.0)	7.88 (0.06)	1.15392 (0.00015)	12.32 (0.67)	9.19 (0.44)	
64	2.00	80	100000	100.3 (0.9)	7.97 (0.05)	1.15371 (0.00015)	9.59 (0.46)	9.06 (0.43)	
64	2.00	160	100000	98.9 (0.8)	7.75 (0.04)	1.15374 (0.00014)	7.43 (0.32)	8.40 (0.38)	
64	2.00	320	100000	99.1 (0.7)	7.80 (0.04)	1.15381 (0.00014)	6.53 (0.26)	8.61 (0.39)	
64	2.10	1	50000	152.8 (9.9)	10.00 (0.40)	1.20202 (0.00036)	292.77 (110.90)	30.05 (3.66)	
64	2.10	5	950000	159.9 (1.3)	10.36 (0.05)	1.20184 (0.00006)	81.32 (3.70)	13.58 (0.25)	
64	2.10	10	700000	158.9 (1.2)	10.26 (0.05)	1.20180 (0.00006)	56.19 (2.47)	12.06 (0.25)	
64	2.10	20	750000	159.7 (1.0)	10.35 (0.04)	1.20189 (0.00005)	40.65 (1.48)	11.16 (0.21)	
64	2.10	40	400000	161.7 (1.2)	10.51 (0.05)	1.20181 (0.00008)	29.75 (1.26)	10.37 (0.26)	
64	2.10	80	400000	161.1 (1.1)	10.47 (0.05)	1.20179 (0.00008)	24.17 (0.92)	10.19 (0.26)	
64	2.10	160	100000	159.0 (2.0)	10.29 (0.09)	1.20197 (0.00015)	20.22 (1.42)	10.26 (0.52)	
64	2.10	320	100250	162.2 (1.8)	10.50 (0.10)	1.20184 (0.00015)	16.39 (1.04)	10.55 (0.54)	
64	2.10	640	25000	162.5 (3.3)	10.48 (0.15)	1.20178 (0.00028)	13.96 (1.62)	9.06 (0.85)	
64	2.20	1	200000	244.3 (10.3)	12.88 (0.39)	1.24504 (0.00020)	540.92 (141.41)	36.60 (2.49)	
64	2.20	5	1000000	256.5 (2.5)	13.69 (0.10)	1.24521 (0.00006)	165.44 (10.43)	15.61 (0.30)	
64	2.20	10	1000000	258.1 (2.0)	13.75 (0.08)	1.24532 (0.00005)	109.43 (5.61)	13.98 (0.26)	
64	2.20	20	800000	261.9 (2.0)	14.01 (0.08)	1.24540 (0.00006)	84.23 (4.24)	12.99 (0.26)	
64	2.20	40	600000	257.0 (1.9)	13.71 (0.08)	1.24534 (0.00006)	60.90 (3.01)	12.15 (0.27)	
64	2.20	80	400100	260.0 (2.2)	13.94 (0.08)	1.24541 (0.00008)	50.95 (2.82)	11.79 (0.32)	
64	2.20	160	400000	255.6 (2.0)	13.65 (0.08)	1.24536 (0.00008)	45.13 (2.35)	11.50 (0.30)	
64	2.20	320	200199	254.3 (2.5)	13.54 (0.10)	1.24527 (0.00011)	35.28 (2.30)	11.26 (0.42)	
64	2.20	640	102840	251.1 (3.2)	13.36 (0.12)	1.24524 (0.00015)	29.52 (2.46)	11.74 (0.62)	

Table 3: Results at $L = 64$ from the codimension-2 algorithm. All runs were started in equilibrium, except for $\beta = 2.20$, $N_{hit} = 1$, where 10000 sweeps (probably not enough) were discarded for equilibration. Standard error is shown in parentheses.

Merged $O(4)$ -Model Static Data				
L	β	χ	ξ	E
32	1.62	21.0 (0.1)	3.09 (0.02)	0.93417 (0.00054)
32	1.70	27.8 (0.0)	3.65 (0.01)	0.98418 (0.00011)
32	1.80	41.3 (0.0)	4.67 (0.01)	1.04456 (0.00007)
32	1.90	62.1 (0.1)	5.96 (0.01)	1.10161 (0.00007)
32	2.00	93.7 (0.1)	7.68 (0.01)	1.15509 (0.00004)
32	2.10	134.6 (0.2)	9.63 (0.01)	1.20398 (0.00004)
32	2.20	178.8 (0.2)	11.60 (0.02)	1.24787 (0.00004)
32	2.30	221.1 (0.3)	13.42 (0.02)	1.28685 (0.00004)
32	2.40	258.5 (0.3)	14.94 (0.03)	1.32155 (0.00007)
64	1.70	27.9 (0.2)	3.65 (0.02)	
64	1.80	41.2 (0.3)	4.60 (0.10)	
64	1.90	64.1 (0.5)	6.10 (0.10)	
64	2.00	99.4 (0.2)	7.83 (0.01)	1.15378 (0.00004)
64	2.10	160.5 (0.3)	10.40 (0.01)	1.20184 (0.00002)
64	2.15	202.9 (0.7)	11.93 (0.03)	1.22410 (0.00003)
64	2.20	257.9 (0.4)	13.77 (0.02)	1.24532 (0.00001)
64	2.22	283.3 (1.0)	14.58 (0.04)	1.25349 (0.00003)
64	2.24	309.5 (1.0)	15.38 (0.04)	1.26149 (0.00003)
64	2.26	337.4 (1.1)	16.20 (0.04)	1.26932 (0.00003)
64	2.28	364.7 (1.2)	16.93 (0.04)	1.27692 (0.00003)
64	2.30	395.0 (0.7)	17.81 (0.03)	1.28442 (0.00001)
64	2.35	471.5 (1.3)	19.87 (0.05)	1.30244 (0.00003)
64	2.40	551.6 (0.8)	21.92 (0.03)	1.31950 (0.00001)
64	2.43	601.5 (1.3)	23.22 (0.05)	1.32931 (0.00002)
64	2.45	632.5 (1.2)	23.97 (0.05)	1.33563 (0.00002)
64	2.50	706.7 (0.9)	25.77 (0.04)	1.35092 (0.00001)
64	2.55	779.0 (1.1)	27.49 (0.05)	1.36545 (0.00002)
64	2.60	847.9 (1.0)	29.06 (0.04)	1.37928 (0.00002)

Table 4: Best estimates of susceptibility, correlation length and energy for the $O(4)$ model on 32×32 and 64×64 lattices, from Tables 1–3 and [4, 19]. Standard error is shown in parentheses.

Codimension = 2		
L	β	Frustration
32	1.70	0.2571 (0.0001)
32	1.80	0.2452 (0.0001)
32	1.90	0.2329 (0.0001)
32	2.00	0.2205 (0.0001)
32	2.10	0.2086 (0.0001)
32	2.20	0.1973 (0.0001)
64	2.00	0.2209 (0.0001)
64	2.10	0.2092 (0.0001)
64	2.20	0.1980 (0.0001)

Table 5: Average fraction of frustrated plaquettes in the induced Ising model arising from the codimension-2 algorithm. Standard error is shown in parentheses.

A combination of SW and Metropolis appears to be no better (in rate of convergence per unit CPU time) than SW alone. Therefore, we had no choice but to simulate the induced Ising model with the best algorithm available to us — namely, standard SW — and to use an *enormous* number of hits in an effort to approximate the behavior of the idealized embedding algorithm.

(After our runs were completed, Kandel, Ben-Av and Domany [56] reported very encouraging results for simulating a frustrated Ising model using an ingenious new algorithm of Swendsen-Wang type. Their algorithm is apparently successful in cases of *full* frustration, but not in cases of partial frustration. In the codimension-2 $O(4)$ application at the β and L values studied here, the induced Ising model has approximately 20–25% of the plaquettes frustrated. We therefore do not expect the Kandel *et al.* algorithm to work miracles, but even a factor-of-2 speedup over standard SW would be highly desirable. We have not yet had an opportunity to try the Kandel *et al.* algorithm in our induced Ising model, but we hope to do so in the near future.)

From Tables 2 and 3, we see that even at $N_{hit} = 640$, the autocorrelation time $\tau_{int, \mathcal{M}^2}$ for the codimension-2 algorithm has not stabilized (except for $L = 32$ and $\beta \lesssim 1.8$). Therefore, we are obliged to attempt an *extrapolation* of our data to $N_{hit} = \infty$. This turns out to be a very tricky business, as the behavior of $\tau_{int, \mathcal{M}^2}$ as a function of N_{hit} is extremely complicated (and we have no *theoretical* understanding of it). We tried empirical fits of the form

$$\tau_{int, \mathcal{M}^2}(N_{hit}) = a + \frac{b}{N_{hit}^\Delta} \quad (4.18)$$

where $a \equiv \tau_{int, \mathcal{M}^2}(N_{hit} = \infty)$ and b are variable, and Δ is some fixed exponent. (We also tried fits with Δ variable, but these fits were quite unstable, and the error bars on Δ were large.) Reasonable fits can be obtained provided that one discards the

$\beta \setminus \Delta$	0.4	0.5	0.6	0.7	0.8	0.9	1.0	1.1	1.2
1.70	1.93(0.08)	2.01(0.07)	2.07(0.06)	2.11(0.05)	2.14(0.05)	2.16(0.04)	2.18(0.04)	2.19(0.04)	2.20(0.04)
[3 DF]	2.71	2.05	1.50	1.06	0.73	0.50	0.36	0.32	0.34
1.80	2.32(0.10)	2.57(0.08)	2.74(0.07)	2.87(0.06)	2.96(0.06)	3.04(0.06)	3.10(0.05)	3.16(0.05)	3.20(0.05)
[4 DF]	19.17	12.80	7.86	4.34	2.16	1.20	1.31	2.30	4.03
1.90	3.45(0.19)	4.04(0.16)	4.44(0.14)	4.73(0.13)	4.95(0.12)	5.12(0.12)	5.26(0.11)	5.38(0.11)	5.48(0.10)
[5 DF]	11.00	5.48	2.25	1.22	2.16	4.81	8.86	14.01	19.94
2.00	5.91(0.43)	6.98(0.36)	7.70(0.32)	8.22(0.29)	8.62(0.27)	8.94(0.26)	9.20(0.25)	9.42(0.24)	9.60(0.24)
[5 DF]	22.16	14.70	8.78	4.51	1.87	0.77	1.04	2.50	4.93
2.10	7.10(0.70)	9.23(0.57)	10.69(0.49)	11.77(0.43)	12.59(0.39)	13.23(0.36)	13.75(0.34)	14.17(0.33)	14.51(0.32)
[5 DF]	11.16	5.92	2.88	1.94	2.88	5.42	9.25	14.08	19.60
2.20	10.99(1.60)	13.96(1.34)	15.92(1.18)	17.31(1.08)	18.33(1.01)	19.12(0.96)	19.74(0.92)	20.24(0.89)	20.66(0.87)
[4 DF]	1.10	0.43	0.20	0.38	0.93	1.82	2.99	4.39	5.98
2.00	1.52(0.40)	3.23(0.32)	4.36(0.27)	5.15(0.24)	5.73(0.22)	6.16(0.21)	6.50(0.20)	6.76(0.20)	6.97(0.19)
[4 DF]	2.80	1.09	1.65	4.32	8.85	14.92	22.21	30.40	39.19
2.10	3.67(1.16)	7.98(0.97)	10.90(0.85)	13.03(0.76)	14.65(0.70)	15.93(0.66)	16.97(0.63)	17.82(0.61)	18.53(0.59)
[5 DF]	6.03	2.11	0.99	2.48	6.28	12.01	19.30	27.76	37.05
2.20	12.01(2.34)	19.84(1.94)	25.09(1.70)	28.85(1.54)	31.66(1.44)	33.84(1.36)	35.56(1.30)	36.95(1.26)	38.08(1.23)
[5 DF]	4.43	3.48	4.58	7.53	12.07	17.88	24.63	32.03	39.79

Table 6: Extrapolated values of $\tau_{int, \mathcal{M}^2}(N_{hit} = \infty)$ for $L = 32$ (upper half of table) and $L = 64$ (lower half), based on a least-squares fit to (4.18) using the data for $N_{hit} \geq 10$; error bars are one standard deviation, *statistical error only*. The second line is the value of χ^2 ; number of degrees of freedom is indicated in the first column. Our subjective selection of the “best” fit is marked in boldface.

data from the lowest values of N_{hit} (namely, $N_{hit} = 1, 5$); but the optimal exponent Δ is not well determined, and it moreover shows a clear (and more-or-less but not quite monotonic) variation with β and L . Of course, we have no explanation whatsoever for these empirical observations. (That is, we have no *theoretical* understanding of the dynamic behavior of the SW algorithm on a highly frustrated Ising model.) Therefore, the best we can do is to report the results of our extrapolations — allowing for a wide range of values of Δ — and let the reader judge their reasonableness. In Figures 2, 3 and 4 we plot $\tau_{int, \mathcal{M}^2}$ versus $1/N_{hit}^\Delta$ for a few selected values of Δ . In Table 6 we show the extrapolated values of $\tau_{int, \mathcal{M}^2}(N_{hit} = \infty)$ as a function of the exponent Δ , based on a least-squares fit to the data with $N_{hit} \geq 10$. Our subjective selection of the “best” fit is marked in boldface. The Δ values in a range ± 0.1 around this “best” value yield also reasonable fits; we take these three extrapolants as a 68% subjective confidence interval on $\tau_{int, \mathcal{M}^2}(N_{hit} = \infty)$. Clearly there is a very wide range of “reasonable” extrapolants, especially for $L = 64$ at the higher values of β . Our final results will therefore have a very large systematic uncertainty.

For the autocorrelation time $\tau_{int, \mathcal{E}}$, the extrapolation to $N_{hit} = \infty$ is fortunately less problematic: in most cases $\tau_{int, \mathcal{E}}$ is constant within error bars for $N_{hit} \gtrsim 40$, or at worst it shows in this region a very slow decrease as a function of N_{hit} . In Table 7 we show the extrapolated values of $\tau_{int, \mathcal{E}}(N_{hit} = \infty)$ as a function of the exponent

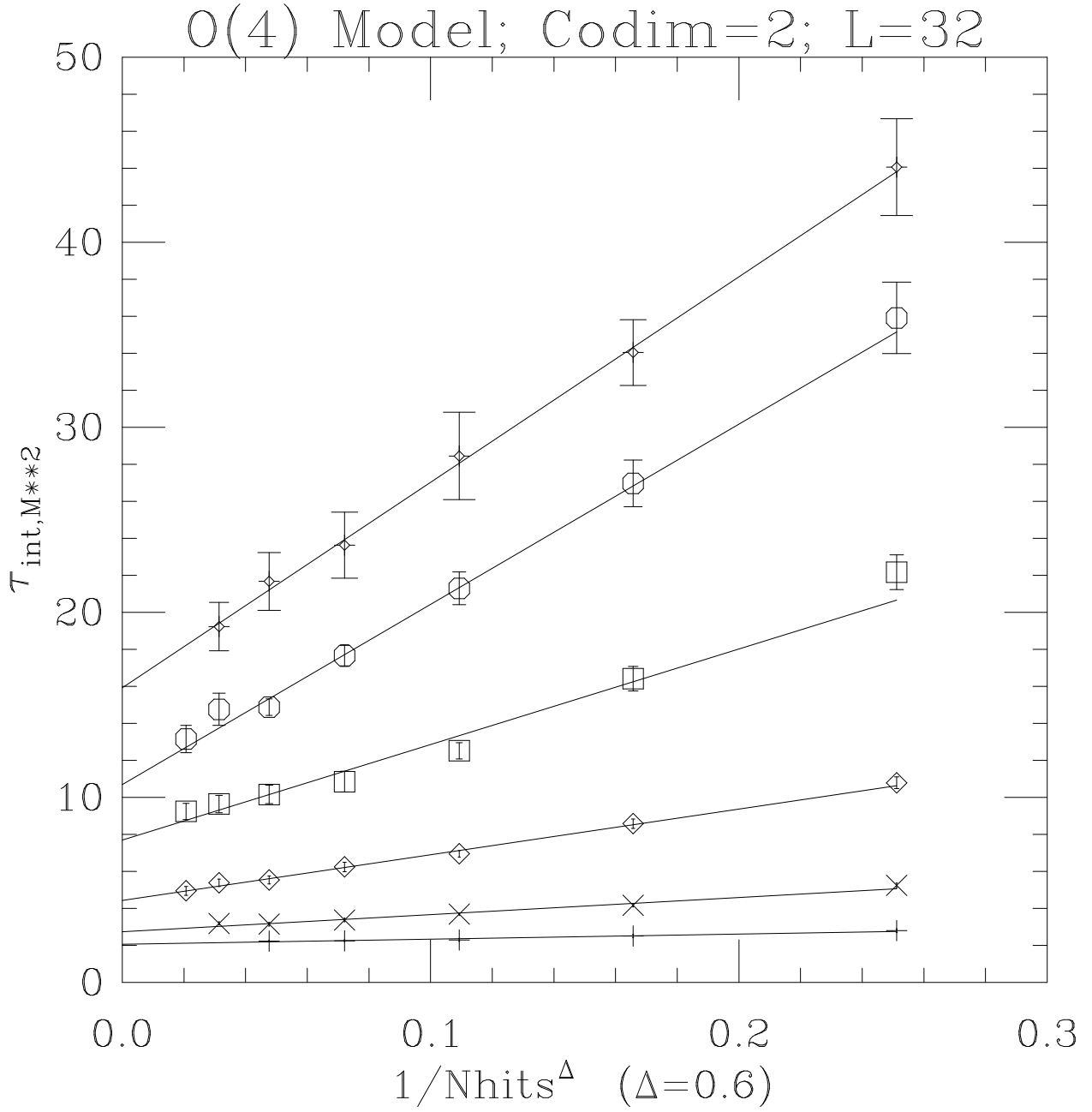


Figure 2: τ_{int, M^2} versus $1/N_{hit}^\Delta$ with $\Delta = 0.6$, for $L = 32$ and $\beta = 1.7$ (+), 1.8 (\times), 1.9 (\diamond), 2.0 (\square), 2.1 (\circ), 2.2 (\circ).

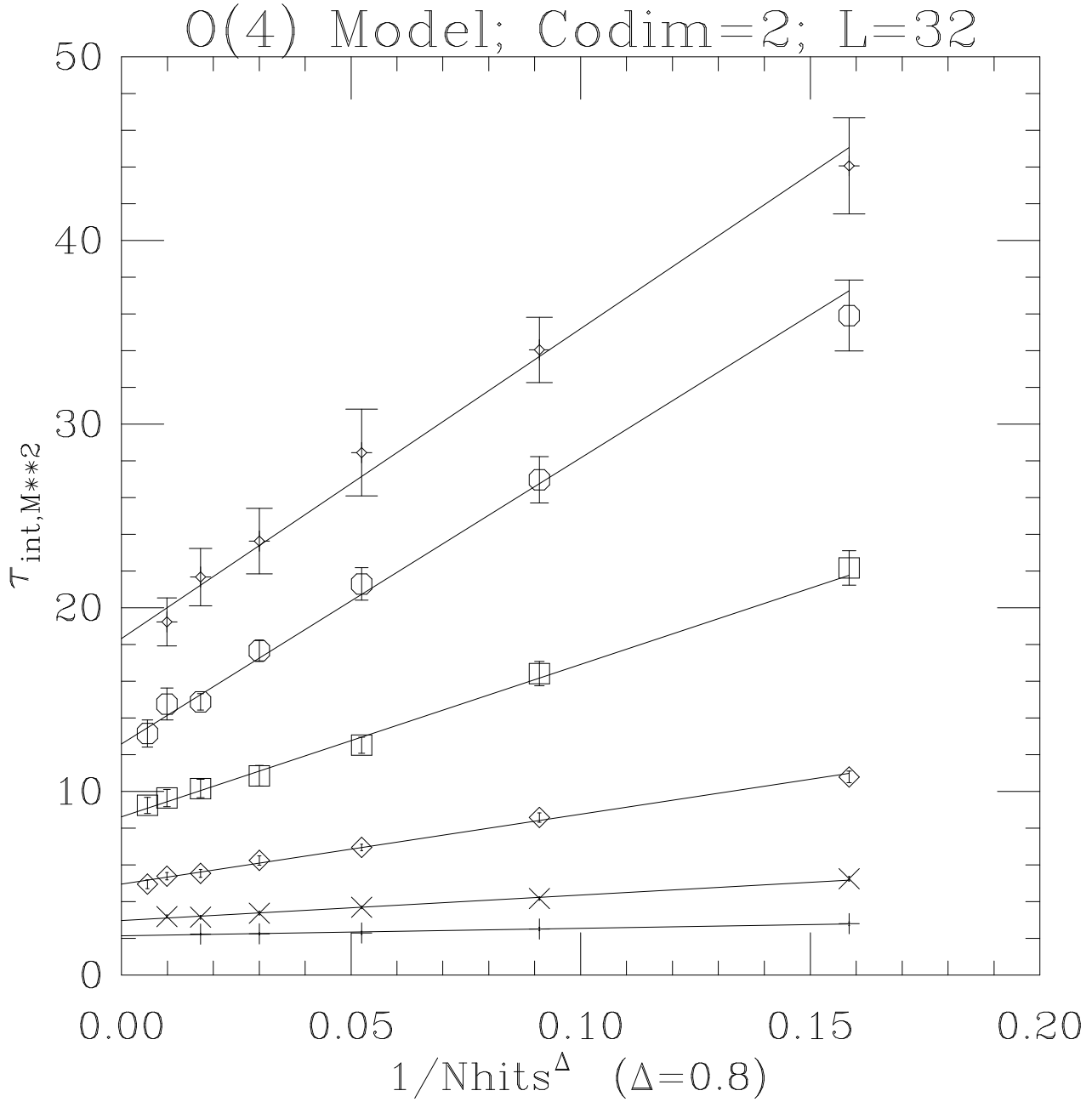


Figure 3: τ_{int, M^2} versus $1/N_{hit}^\Delta$ with $\Delta = 0.8$, for $L = 32$ and $\beta = 1.7$ (+), 1.8 (\times), 1.9 (\diamond), 2.0 (\square), 2.1 (\circ), 2.2 (\circ).

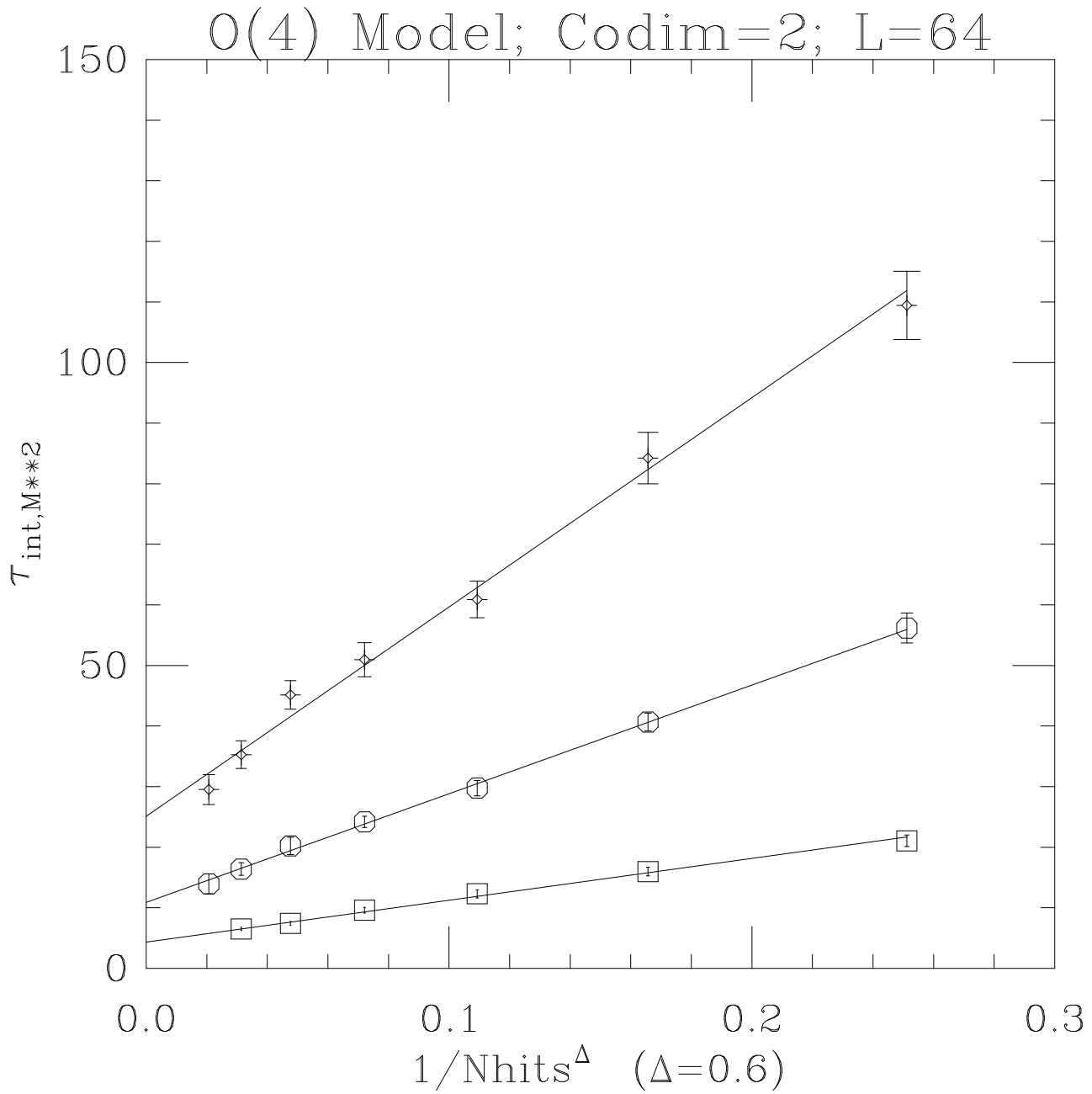


Figure 4: $\tau_{int, \mathcal{M}^2}$ versus $1/N_{hit}^{\Delta}$ with $\Delta = 0.6$, for $L = 64$ and $\beta = 2.0$ (\square), 2.1 (\circ), 2.2 (\diamond).

$\beta \setminus \Delta$	0.4	0.5	0.6	0.7	0.8	0.9	1.0	1.1	1.2
1.70	5.65(0.30)	5.65(0.25)	5.65(0.22)	5.65(0.20)	5.66(0.18)	5.66(0.17)	5.66(0.16)	5.66(0.16)	5.66(0.15)
[3 DF]	1.55	1.55	1.55	1.55	1.55	1.56	1.56	1.56	1.56
1.80	6.28(0.24)	6.37(0.20)	6.44(0.18)	6.49(0.16)	6.52(0.15)	6.55(0.14)	6.57(0.14)	6.59(0.13)	6.61(0.13)
[4 DF]	3.21	3.23	3.25	3.29	3.32	3.36	3.40	3.43	3.47
1.90	7.36(0.27)	7.48(0.23)	7.55(0.21)	7.61(0.19)	7.65(0.18)	7.68(0.17)	7.71(0.16)	7.73(0.16)	7.75(0.15)
[5 DF]	3.76	3.65	3.56	3.49	3.43	3.39	3.35	3.33	3.31
2.00	9.33(0.34)	9.37(0.29)	9.39(0.26)	9.41(0.24)	9.42(0.23)	9.43(0.22)	9.44(0.21)	9.45(0.20)	9.46(0.19)
[5 DF]	4.31	4.07	3.83	3.60	3.39	3.19	3.01	2.85	2.70
2.10	9.77(0.32)	10.02(0.27)	10.19(0.24)	10.31(0.22)	10.40(0.20)	10.47(0.19)	10.52(0.18)	10.57(0.17)	10.61(0.17)
[5 DF]	5.59	4.79	4.12	3.57	3.13	2.79	2.56	2.40	2.32
2.20	11.06(0.57)	11.28(0.49)	11.42(0.44)	11.52(0.40)	11.60(0.38)	11.66(0.36)	11.71(0.34)	11.75(0.33)	11.78(0.32)
[4 DF]	2.06	1.98	1.93	1.90	1.89	1.90	1.92	1.96	2.00

2.00	8.00(0.37)	8.22(0.31)	8.36(0.28)	8.46(0.26)	8.54(0.24)	8.60(0.23)	8.65(0.22)	8.69(0.22)	8.72(0.21)
[4 DF]	0.77	0.84	0.97	1.13	1.32	1.53	1.76	2.00	2.24
2.10	8.96(0.34)	9.29(0.29)	9.51(0.25)	9.67(0.23)	9.80(0.21)	9.90(0.20)	9.98(0.19)	10.04(0.18)	10.10(0.17)
[5 DF]	4.81	4.06	3.52	3.15	2.94	2.86	2.89	3.02	3.23
2.20	10.34(0.30)	10.70(0.25)	10.95(0.22)	11.13(0.21)	11.26(0.19)	11.37(0.18)	11.45(0.17)	11.52(0.17)	11.58(0.16)
[5 DF]	2.31	1.49	1.01	0.84	0.92	1.20	1.65	2.22	2.88

Table 7: Extrapolated values of $\tau_{int,\mathcal{E}}(N_{hit} = \infty)$ for $L = 32$ (upper half of table) and $L = 64$ (lower half), based on a least-squares fit to (4.18) using the data for $N_{hit} \geq 10$; error bars are one standard deviation, *statistical error only*. The second line is the value of χ^2 ; number of degrees of freedom is indicated in the first column. Our subjective selection of the “best” fit is marked in boldface.

Δ , based on a least-squares fit to the data with $N_{hit} \geq 10$. Here the extrapolation is in most cases insensitive to the choice of Δ , and there is no discernible systematic preference for one or another value of Δ . Therefore we have chosen (rather arbitrarily) $\Delta = 1$ as the “best” extrapolant, and the range $0.8 \leq \Delta \leq 1.2$ as defining a 68% subjective confidence interval on $\tau_{int,\mathcal{E}}(N_{hit} = \infty)$.

We can now make a finite-size-scaling analysis of the dynamic critical behavior, using the Ansatz

$$\tau_{int,A}(\beta, L) \sim \xi(\beta, L)^{z_{int,A}} g_A(\xi(\beta, L)/L) \quad (4.19)$$

for $A = \mathcal{M}^2, \mathcal{E}$. Here g_A is an unknown scaling function, and $g_A(0) = \lim_{x \downarrow 0} g_A(x)$ is supposed to be finite and nonzero.²⁸ We emphasize that the dynamic critical exponent $z_{int,A}$ is in general *different* from the exponent z_{exp} associated with the exponential autocorrelation time τ_{exp} [57, 58, 59].

²⁸ It is of course equivalent to use the Ansatz

$$\tau_{int,A}(\beta, L) \sim L^{z_{int,A}} h_A(\xi(\beta, L)/L),$$

and indeed the two Ansätze are related by $h_A(x) = x^{z_{int,A}} g_A(x)$. However, to determine whether $\lim_{x \downarrow 0} g_A(x) = \lim_{x \downarrow 0} x^{-z_{int,A}} h_A(x)$ is nonzero, it is more convenient to inspect a graph of g_A than one of h_A .

For the codimension-1 idealized algorithm ($N_{hit} = \infty$), the dynamic critical exponents are very close to zero: we estimate $z_{int,\mathcal{E}} = 0.1 \pm 0.1$ and $z_{int,\mathcal{M}^2} = 0.0 \pm 0.1$ (subjective 68% confidence intervals). Finite-size-scaling plots of $\tau_{int,A}\xi^{-z_{int,A}}$ versus ξ/L are shown in Figures 5 and 6. These estimates are of course in agreement with our previous results [4] showing that even for $N_{hit} = 1$ we have z very close to zero.

For the codimension-2 idealized algorithm, a similar analysis using the extrapolated data from Tables 6 and 7 yields the estimates $z_{int,\mathcal{M}^2} = 1.5 \pm 0.5$ and $z_{int,\mathcal{E}} = 0.5 \pm 0.2$ (subjective 68% confidence intervals). The finite-size-scaling plots corresponding to these values of z are shown in Figures 7 and 8. Clearly the estimate for z_{int,\mathcal{M}^2} is *very* imprecise, as a result of the large systematic error bars in the extrapolation of τ_{int,\mathcal{M}^2} for $L = 64$. All we can say with much certainty is that z_{int,\mathcal{M}^2} is far from zero; it is consistent with our data, but not at all guaranteed, that $z_{int,\mathcal{M}^2} \approx 2$.

It is interesting to note the relative sizes of τ_{int,\mathcal{M}^2} as compared to $\tau_{int,\mathcal{E}}$ (and also of z_{int,\mathcal{M}^2} as compared to $z_{int,\mathcal{E}}$). For the traditional local algorithms (e.g. single-site heat-bath), \mathcal{M}^2 is a much slower mode than \mathcal{E} , because it is much more strongly coupled to the long-wavelength spin waves that evolve slowly in the local dynamics.²⁹ For the codimension-1 idealized Wolff algorithm, by contrast, the two observables have roughly equal autocorrelation times (and in fact \mathcal{E} is a little slower): the Wolff collective moves are apparently equally effective at equilibrating fluctuations on all length scales. For the codimension-2 idealized algorithm, however, \mathcal{M}^2 is again much slower than \mathcal{E} : this confirms our view that the codimension-2 reflection is ineffective at equilibrating long-wavelength spin waves, and that its effect is “primarily local”.

We wish to emphasize once again the importance of studying the *idealized* embedding algorithm, and the misleading conclusions that can be caused by the failure to do so. Indeed, suppose that we had studied the codimension-2 algorithm only for $N_{hit} = 1$. Then, by the usual dynamic finite-size-scaling analysis, we would have concluded that $z_{int,\mathcal{M}^2} \approx 3$ and $z_{int,\mathcal{E}} \approx 0.75$ (*very* roughly), i.e. that the codimension-2 embedding algorithm is disastrously bad. Now, this conclusion happens to be true, but not for the reason claimed! In fact, the enormous autocorrelation times τ_{int,\mathcal{M}^2} in the $N_{hit} = 1$ algorithm reflect primarily the inability of the SW algorithm to update efficiently the highly frustrated induced Ising model (as one can verify by comparing to larger values of N_{hit}), and *not* any intrinsic defect of the codimension-2 embedding. The intrinsic properties of the embedding are found *only* by considering $N_{hit} \rightarrow \infty$.

The CPU time for this program is approximately $5.35 \times N_{hit}L^2 \mu\text{s}/\text{sweep}$ on a Cray Y-MP 8/432. Thus, the total CPU time for the the runs reported here is approximately 4000 Cray hours.³⁰

²⁹ See e.g. [19] for some quantitative measurements.

³⁰ This is only an “equivalent” figure, as the runs were actually performed on a variety of supercomputers and RISC workstations: see the Acknowledgments.

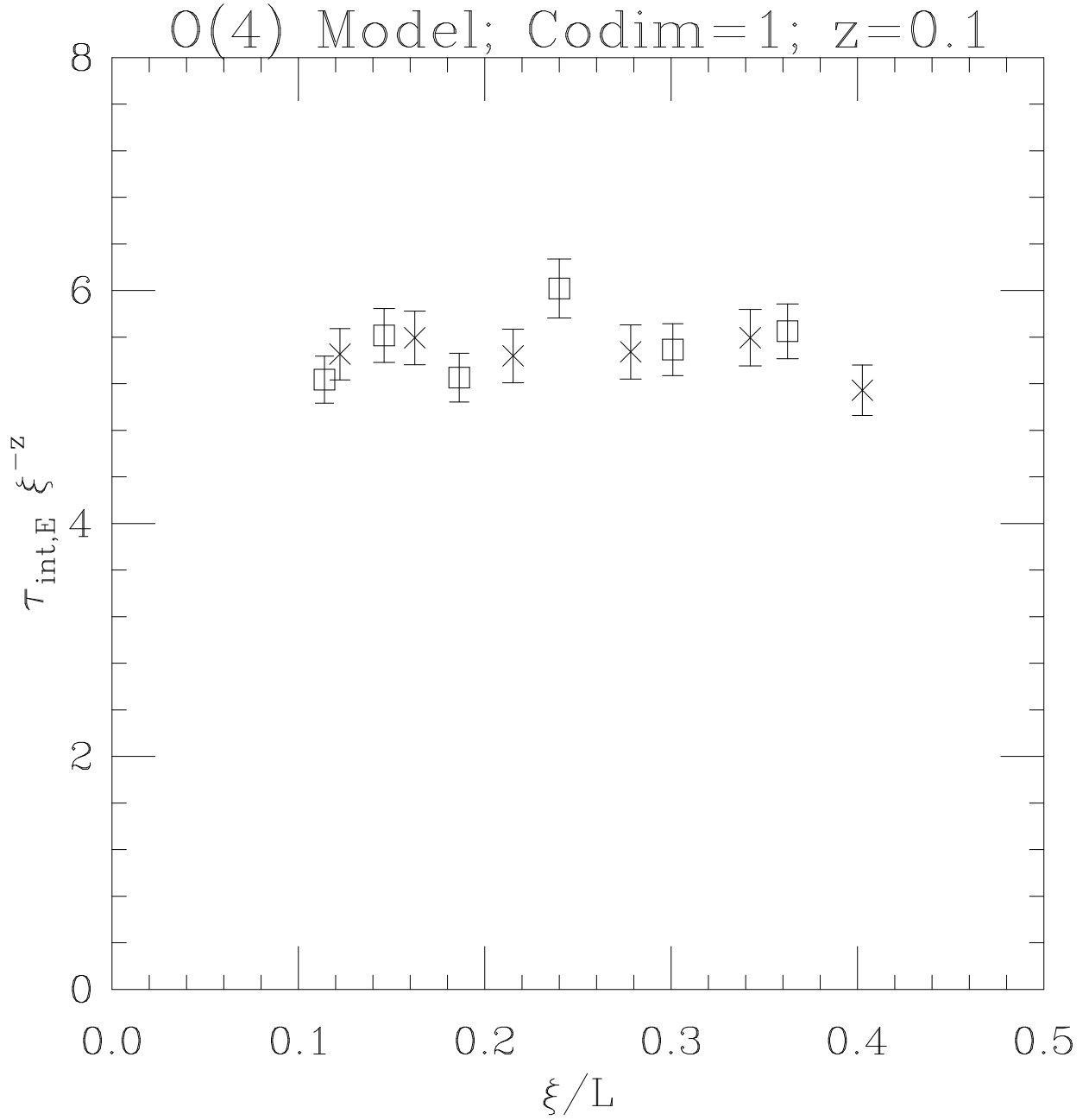


Figure 5: Dynamic finite-size-scaling plot of $\tau_{int,E} \xi^{-z_{int,E}}$ versus ξ/L for $z_{int,E} = 0.1$, for the idealized ($N_{hit} = \infty$) codimension-1 algorithm on $L = 32$ (\square) and $L = 64$ (\times).

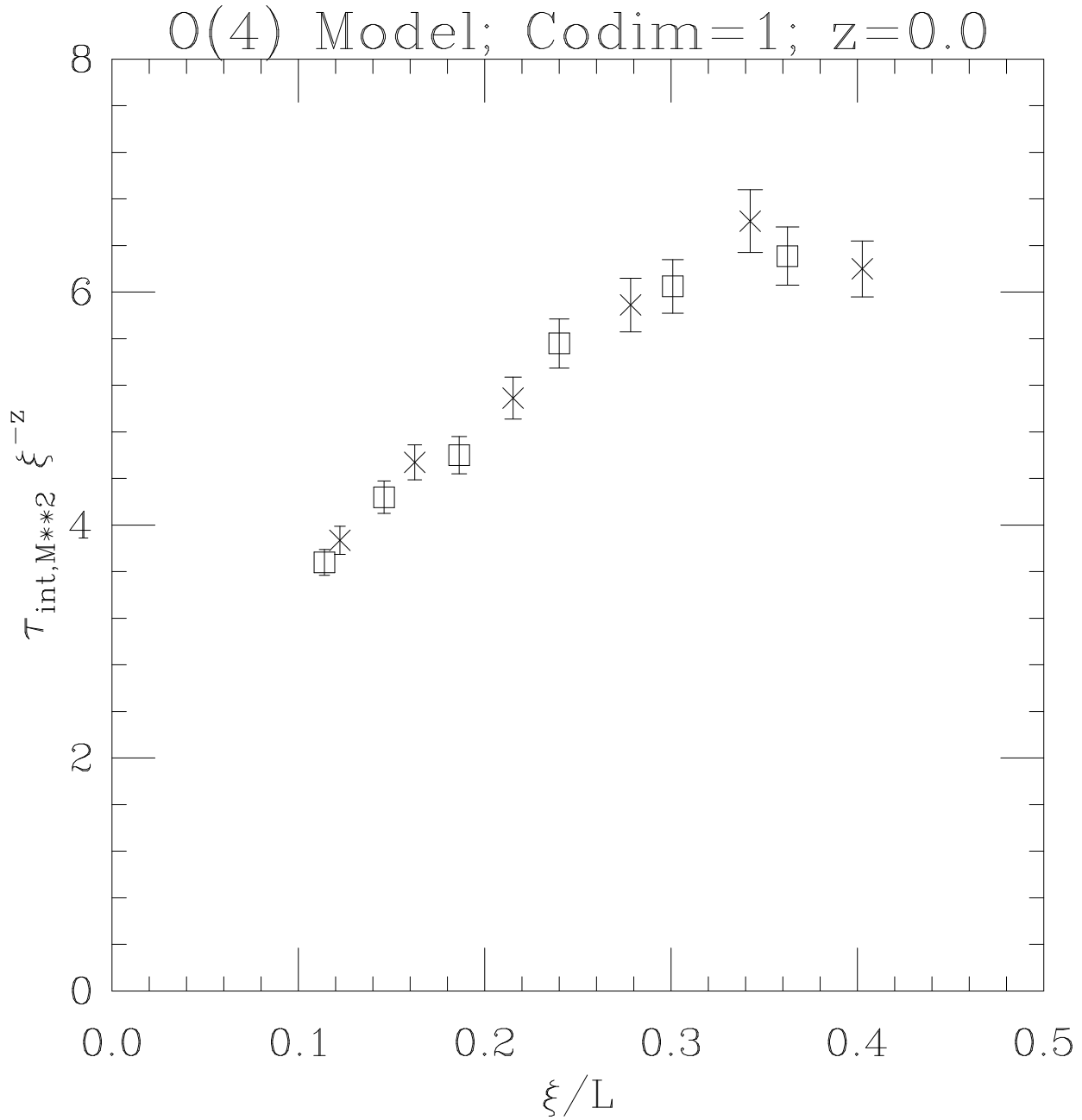


Figure 6: Dynamic finite-size-scaling plot of $\tau_{int, \mathcal{M}^2} \xi^{-z_{int, \mathcal{M}^2}}$ versus ξ/L for $z_{int, \mathcal{M}^2} = 0$, for the idealized ($N_{hit} = \infty$) codimension-1 algorithm on $L = 32$ (\square) and $L = 64$ (\times).

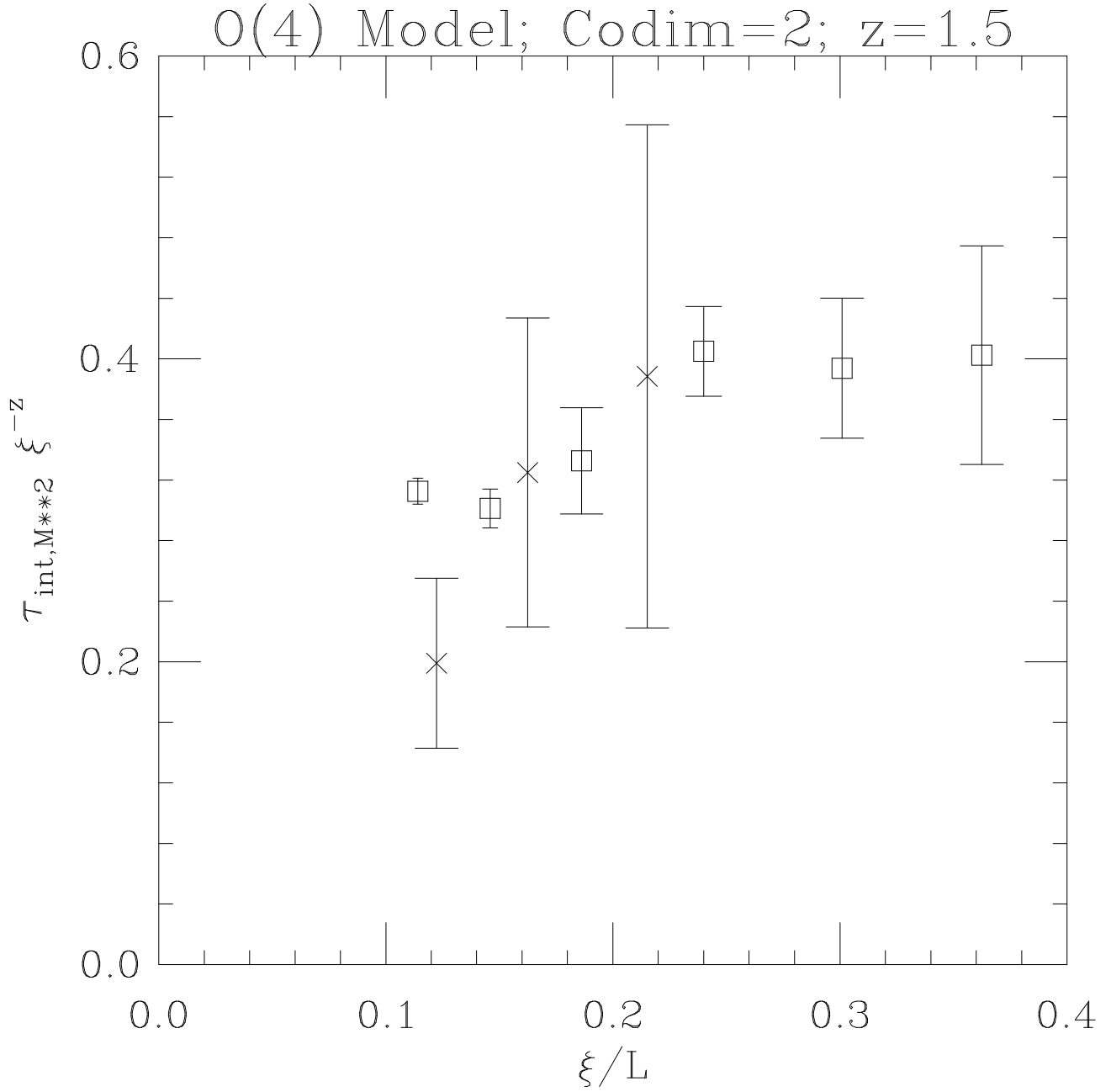


Figure 7: Dynamic finite-size-scaling plot of $\tau_{int, \mathcal{M}^2} \xi^{-z_{int, \mathcal{M}^2}}$ versus ξ/L for $z_{int, \mathcal{M}^2} = 1.5$, for the idealized ($N_{hit} = \infty$) codimension-2 algorithm. Data points are from the extrapolations in Table 6 with $L = 32$ (\square) and $L = 64$ (\times).

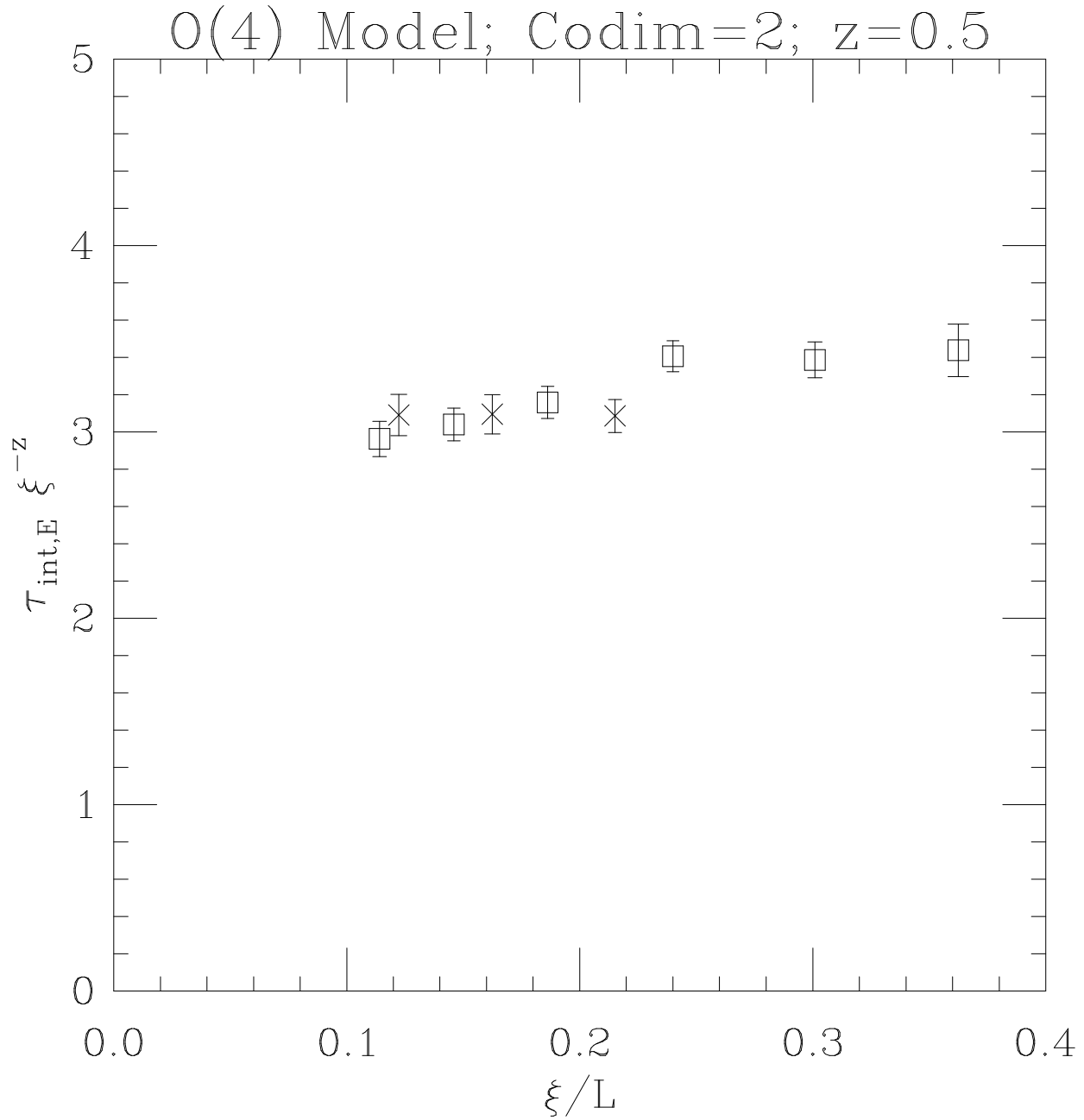


Figure 8: Dynamic finite-size-scaling plot of $\tau_{int,\varepsilon} \xi^{-z_{int,\varepsilon}}$ versus ξ/L for $z_{int,\varepsilon} = 0.5$, for the idealized ($N_{hit} = \infty$) codimension-2 algorithm. Data points are from the extrapolations in Table 7 with $L = 32$ (\square) and $L = 64$ (\times).

5 Discussion

Let us now place our analysis of Wolff-type embedding algorithms into the more general context of *arbitrary* embedding algorithms. The general idea [59] is to “foliate” the configuration space of the original model into “leaves” isomorphic to the configuration space of some “embedded” model. One then moves around the current leaf, using any legitimate Monte Carlo algorithm for simulating the conditional probability distribution restricted to that leaf (i.e. the induced Hamiltonian for the embedded model). Of course, one must combine this move with other moves, or with a different foliation, in order to make the algorithm ergodic. (This same structure arises also in multi-grid Monte Carlo, where it is termed “partial resampling” [57, 17, 14].)

As noted in the Introduction, the performance of an embedding algorithm is determined by the combined effect of two *completely distinct* issues:

- i) How well the embedding captures the important large-scale collective modes of the original model. The point is that these modes must be realizable by motions *within* a leaf.
- ii) How well some particular algorithm (e.g. standard SW or single-cluster SW) succeeds in updating the embedded model.

It is crucial to employ a test procedure that *disentangles* these two issues, if one wants to obtain *physical insight* into why a particular embedding algorithm does or does not work well.

In all of the recently-invented embedding algorithms — Wolff-type algorithms for nonlinear σ -models and $N_t = 1$ $SU(2)$ gauge theories [60], spin-flip algorithms for one-component scalar-field models [61], and reflection algorithms for solid-on-solid (SOS) and anharmonic-crystal models [62] — the embedded model happens to be an Ising model. But the principle is much more general: for example, one might consider embeddings of $U(1)$ spins in a higher σ -model, $U(1)$ or Z_N spins in an $SU(N)$ gauge theory, etc. Of course, the nontrivial problem is to find an embedding that captures at least some of the important collective modes of the original model, and once this has been done, to find an efficient algorithm for updating the embedded model.

In Section 2 we explained why an idealized embedding algorithm will do a good job of handling long-wavelength spin waves *if*, in the induced Hamiltonian for the embedded model, x -space is divided into large disconnected regions which are almost decoupled from each other. We furthermore conjectured that in a Wolff-type embedding of Ising spins into a nonlinear σ -model, this is the *only* mechanism by which long-wavelength spin waves can be handled well; and our numerical results in Section 4 gave modest support for this conjecture in at least one case. However, we wish to point out that whatever the status of this conjecture for embeddings of *Ising* spins, it certainly *cannot* be true as a general proposition about embedding algorithms. To see this, consider the extreme case in which there is only one leaf (namely, the whole configuration space): then the *idealized* embedding algorithm performs perfectly (it is just independent sampling from the Gibbs measure of the original model), but the induced Hamiltonian for the embedded model does not decouple anywhere (it is just

the original Hamiltonian). This rather trivial extreme example shows that decoupling cannot be the *only* mechanism by which an *idealized* embedding algorithm can work well. More generally, consider any two foliations \mathcal{F}_1 and \mathcal{F}_2 of the same configuration space, such that \mathcal{F}_1 is a refinement of \mathcal{F}_2 (i.e. the leaves of \mathcal{F}_2 are unions of leaves from \mathcal{F}_1). It is intuitively clear that the *idealized* embedding algorithm based on the foliation \mathcal{F}_2 (plus possibly other moves) will perform better than the one based on foliation \mathcal{F}_1 (plus the same other moves): in \mathcal{F}_2 there is more freedom to move around within a leaf. On the other hand, the induced Hamiltonian based on \mathcal{F}_2 will have fewer (if any) surfaces in x -space along which it decouples, compared to the induced Hamiltonian based on \mathcal{F}_1 : the larger the leaves, the more stringent the requirement of a complete decoupling. So “performance” and “decoupling” have opposite monotonicities as a function of the “size” of the leaves. It follows that decoupling *cannot* be the general principle that explains the good or bad performance of embedding algorithms.

In particular, it is not justified to insist on the codimension-1 property when considering non-Ising embeddings — and this is fortunate, since by Theorem A.9 (see also the remarks following it), *only* Ising embeddings can have the codimension-1 property!

There are many possibilities for embedding algorithms: each such algorithm can be interpreted as “reducing” one simulation problem to another (hopefully simpler) one. For example, consider a (possibly frustrated) $SU(N)$ principal chiral model defined by the Hamiltonian

$$H(\{U\}) = - \sum_{\langle xy \rangle} \text{Re tr}(A_{xy} U_x^\dagger U_y) , \quad (5.1)$$

where the A_{xy} are $N \times N$ complex matrices. Then one can embed $U(1)$ ($= XY$) spins as follows: let $T = \text{diag}(i, -i, 0, \dots, 0) \in \mathfrak{su}(N)$, let R be a random element of $SU(N)$, and embed the field $\{\theta_x\}$ of XY spins according to the rule

$$U_x^{new} = R \exp(\theta_x T) R^{-1} U_x^{old} . \quad (5.2)$$

It is easy to see that the induced XY Hamiltonian is of the form

$$H(\{\theta\}) = - \sum_{\langle xy \rangle} [\alpha_{xy} \cos(\theta_x - \theta_y) + \beta_{xy} \sin(\theta_x - \theta_y)] , \quad (5.3)$$

i.e. it is a nearest-neighbor XY model, with couplings that are in general *frustrated* (even if the original $SU(N)$ model is ferromagnetic). We conjecture that the *idealized* embedding algorithm corresponding to this embedding has dynamic critical exponent $z \approx 0$, at least if the $SU(N)$ model is ferromagnetic: the idea is that the spin waves in $SU(N)$, which are approximately Gaussian, can be obtained by superposing spin waves in the various $U(1)$ subgroups generated by the RTR^{-1} . If this is the case, then the problem of simulating an $SU(N)$ principal chiral model (possibly even a frustrated one) has been reduced to the problem of simulating a frustrated XY model.

Unfortunately, we have no idea how to carry out efficiently the latter simulation.³¹ But if, some day in the future, the latter problem should be solved, then it is useful to know that the former problem would also be solved.

It is also interesting to note that the Wolff and multi-grid algorithms can be understood from a unified perspective. In both cases one exploits an exact symmetry of the model (global reflection in the case of Wolff, global rotation in the case of multi-grid) and applies it in an inhomogeneous way (constant on clusters in the case of Wolff, constant on cubical blocks in the case of multi-grid). In both cases the energy cost is a surface term. This perspective may be useful in suggesting generalizations of the Wolff and/or multi-grid algorithms to broader classes of models, especially lattice gauge theories.

For example, consider a $U(1)$ gauge theory with Hamiltonian

$$H = - \sum_P \beta_P \cos \left(\sum_{\ell \in P} \theta_\ell \right), \quad (5.4)$$

where $\theta_\ell \in [0, 2\pi]$ is a gauge potential on the oriented link ℓ , $\sum_{\ell \in P} \theta_\ell$ is a properly oriented sum over the links bounding the plaquette P , and $\beta_P \geq 0$ for all P . (Usually all β_P will be equal.) Next let $\{\theta_\ell^\circ\}$ be an arbitrary curvature-free gauge field, i.e. a ground state for the Hamiltonian H .³² Now it is easy to see that a global reflection of $\{\theta_\ell\}$ around $\{\theta_\ell^\circ\}$ is a symmetry of H . Let us therefore consider applying this reflection in an inhomogeneous way, i.e. let us consider [63] the embedding of Ising spins $\{\varepsilon_\ell\}$ defined by

$$\theta_\ell \longrightarrow \theta_\ell^{new} \equiv \theta_\ell^\circ + \varepsilon_\ell(\theta_\ell - \theta_\ell^\circ). \quad (5.5)$$

Under this updating, the energy changes only on those plaquettes P for which the ε_ℓ ($\ell \in P$) are not all equal; heuristically, the energy cost is a “surface term”. Therefore, we conjecture that the *idealized* embedding algorithm based on (5.5) — with, say, a random choice of $\{\theta_\ell^\circ\}$ — has dynamic critical exponent $z \approx 0$. Now, the induced Ising Hamiltonian corresponding to (5.5) is of the form

$$H(\{\varepsilon_\ell\}) = - \sum_P \beta_P [A_P \varepsilon_{\ell_1} \varepsilon_{\ell_2} \varepsilon_{\ell_3} \varepsilon_{\ell_4} + (B_{P, \ell_1 \ell_2} \varepsilon_{\ell_1} \varepsilon_{\ell_2} + 5 \text{ similar terms})] + \text{const} \quad (5.6)$$

³¹ The multi-grid method [14, 18] is applicable to the latter problem, and its performance might not be totally disastrous. But the multi-grid method is also applicable to the original $SU(N)$ model [14, 19], and it is easy to see that multi-grid updates on the induced XY model are simply a subset of the multi-grid updates on the $SU(N)$ model. Thus, at least for the idealized two-grid cycle and presumably also for the other cycles, nothing is gained by first embedding $U(1)$ variables. An embedding is useful only if there exists an efficient algorithm for simulating the embedded model that for some reason does *not* generalize to the original model.

³² In free boundary conditions, such a field $\{\theta_\ell^\circ\}$ would be a gauge transform of the identity. However, in periodic boundary conditions (i.e. on the torus T^d) there are d additional linearly independent possibilities for $\{\theta_\ell^\circ\}$, which give arbitrary values to the d independent Polyakov loops. [In fancy language, these solutions are representatives of a basis for the first cohomology group $H^1(T^d; \mathbb{R}/\mathbb{Z}) \simeq (\mathbb{R}/\mathbb{Z})^d$.]

where $P = \{\ell_1, \ell_2, \ell_3, \ell_4\}$ and

$$A_P = \sin(\theta_{\ell_1} - \theta_{\ell_1}^\circ) \sin(\theta_{\ell_2} - \theta_{\ell_2}^\circ) \sin(\theta_{\ell_3} - \theta_{\ell_3}^\circ) \sin(\theta_{\ell_4} - \theta_{\ell_4}^\circ) \quad (5.7a)$$

$$B_{P, \ell_1 \ell_2} = -\sin(\theta_{\ell_1} - \theta_{\ell_1}^\circ) \sin(\theta_{\ell_2} - \theta_{\ell_2}^\circ) \cos(\theta_{\ell_3} - \theta_{\ell_3}^\circ) \cos(\theta_{\ell_4} - \theta_{\ell_4}^\circ) \quad (5.7b)$$

etc.

This is *not* a Z_2 gauge model; rather, it is a Z_2 spin model with a curious mixture of 2-spin and 4-spin couplings. Unfortunately, we have no idea how to simulate efficiently such a model.³³ But it would be worth investigating our conjecture that the idealized embedding algorithm works well; and if this conjecture is found to be true, then it would be worth investigating algorithms for simulating (5.6).

One might try generalizing this algorithm to an $SU(2)$ gauge theory, using the codimension-1 reflection

$$U_\ell \longrightarrow -U_\ell^\circ U_\ell^\dagger U_\ell^\circ, \quad (5.8)$$

where $\{U_\ell^\circ\}$ is a random curvature-free gauge field (see Example 4 of Section 3.1). Unfortunately, a global application of (5.8) is *not* a symmetry of the Wilson Hamiltonian, because

$$\text{Re tr}(U_1 U_2 U_3 U_4) \neq \text{Re tr}(U_1^\dagger U_2^\dagger U_3^\dagger U_4^\dagger) \quad (5.9)$$

for a non-Abelian group. Therefore, the induced Ising Hamiltonian would contain magnetic-field terms that contribute a *bulk* energy, and the idealized embedding algorithm would probably *not* work well. On the other hand, equality in (5.9) *almost* holds if the fields U_1, U_2, U_3, U_4 are close to the identity. Therefore, one might hope that for $\beta \gg 1$ (i.e. near the continuum limit), the idealized embedding algorithm corresponding to (5.8) would work well *in Landau gauge* with the choice $U_\ell^\circ \equiv I$. Of course, to implement this idea in practice one would have to find an efficient algorithm for Landau gauge-fixing — a nontrivial problem [64, 65, 66] for which the conventional algorithms also suffer from critical slowing-down. But the situation may not be completely hopeless. (We remark that other collective-mode algorithms, such as Fourier acceleration and multi-grid, may also need Landau gauge-fixing in order to perform well in the non-Abelian case [67].)

Let us conclude by mentioning several recent studies of Wolff-type embedding algorithms [6, 7, 68, 69] which complement our own. Hasenbusch and Meyer [6] studied the three-dimensional XY model at $\beta \leq \beta_c$ using the codimension-1 Wolff embedding with standard SW updates ($N_{hit} = 1$); they found $z_{int, \mathcal{E}} \approx 0.46$ and $z_{int, \mathcal{M}^2} \approx 0.31$. Janke [7] studied the same model using single-cluster SW updates, and found $z_{int, \mathcal{E}, CPU} \approx 0.25$ and $z_{int, \mathcal{M}^2, CPU} \approx 0$. However, it should be noted that these exponents may well be due to critical slowing-down in the inner SW or 1CSW subroutine; indeed, they are roughly of the same order of magnitude as the dynamic

³³ It is worth noting that the 4-spin couplings $A_{P \varepsilon_{\ell_1} \varepsilon_{\ell_2} \varepsilon_{\ell_3} \varepsilon_{\ell_4}}$ can be eliminated in favor of 2-spin couplings, by introducing a new spin ε_P at the center of each plaquette and coupling this spin individually to $\varepsilon_{\ell_1}, \varepsilon_{\ell_2}, \varepsilon_{\ell_3}, \varepsilon_{\ell_4}$ (analogously to the well-known “star-triangle transformation”). The problem is then to find an efficient simulation algorithm for the resulting pair-interacting Ising model, which is in general *frustrated*.

critical exponents of the SW and 1CSW algorithms for the ordinary three-dimensional Ising model [9, 11, 12, 25, 26].³⁴ Therefore, it remains possible that the *idealized* Wolff algorithm for the three-dimensional XY model could have $z \approx 0$. In the near future we hope to study the idealized algorithm for this model. (Since in this case the SW algorithm simulates the induced Ising model reasonably well, albeit not perfectly, it will probably not be necessary to go beyond $N_{hit} \approx 50$.)

Jansen and Wiese [68] have very recently studied the two-dimensional CP^3 and CP^4 models, using the codimension-2 embedding $z \rightarrow I_1 z$ (see Example 3 in Section 3.1 above) and single-cluster SW updates. They also studied, for purposes of comparison, a single-site Metropolis algorithm. They found that $z_{exp, \mathcal{M}^2} \approx 2$ for both algorithms. Unfortunately, this fact alone does *not* constitute evidence for our conjecture regarding the codimension-1 property: the slowing-down observed by Jansen and Wiese may well be due to the inability of the 1CSW algorithm to update efficiently the frustrated Ising model that is induced by the codimension-2 embedding. It would be necessary to study the *idealized* embedding algorithm to draw a definitive conclusion regarding the merit of this embedding.

Finally, a recent review talk of Wolff [69] contains many interesting ideas, and gives some preliminary (negative) results on embedding algorithms for the two-dimensional $SU(3)$ principal chiral model. In particular, Wolff's results are consistent with our thesis that the codimension-1 and isometry properties must hold if the algorithm is to work well. However, as in the work by Jansen and Wiese, no definitive conclusion can be drawn except from a study of the *idealized* embedding algorithm.

Acknowledgments

We wish to thank Richard Brower, Ferenc Niedermayer, Claudio Parrinello and Ulli Wolff for helpful discussions about embedding algorithms, and Oliver Attie, Sylvain Cappell and Fabio Podestà for helpful discussions about topology and geometry. The computations reported here were carried out on a loosely coupled MIMD parallel computer (with local memory and message-passing communication via Internet/Bitnet/Decnet and four neural networks) consisting of the following processors: the Cray X-MP at CRTN-ENEL (Pisa); the Cray Y-MP at CINECA (Bologna); the Cray Y-MP at the Pittsburgh Supercomputing Center; the Cyber 205 at the John von Neumann Supercomputer Center†; and the ETA-10G, ETA-10Q, Cray Y-MP, Silicon Graphics 4D/240GTX and numerous DECstation 5000, IBM RS-6000/320 and IBM RS-6000/530 workstations at SCRI (Tallahassee). We thank all these organizations for their generous contribution to this research. The authors' research was supported in part by the Istituto Nazionale di Fisica Nucleare (S.C. and A.P.), U.S. Department of Energy contract DE-FC05-85ER250000 (R.G.E.), U.S. Department

³⁴ Since the induced Ising model in the codimension-1 Wolff algorithm is ferromagnetic and short-range (though slightly disordered), one might expect it to have a dynamic critical exponent under the SW or 1CSW algorithm that is approximately (though probably not exactly) equal to that of the ordinary ferromagnetic nearest-neighbor Ising model. We say “not exactly” because the disorder — which has long-range correlations — probably does change the dynamic universality class.

of Energy contract DE-FG02-90ER40581 (A.D.S.), U.S. National Science Foundation grants DMS-8705599 and DMS-8911273 (A.D.S.), and NATO Collaborative Research Grant CRG 910251 (S.C. and A.D.S.).

A Some Topology and Geometry

A.1 Submanifolds and connectedness

Let X be a connected finite-dimensional metrizable³⁵ C^∞ manifold, and let S be a subset of X (usually a submanifold or union of submanifolds). We wish to know whether or not $X \setminus S$ is connected.

Our first theorem asserts that a manifold cannot be disconnected by deleting a subset of codimension ≥ 2 . To make this statement meaningful, we first have to define what we mean by “dimension” of an arbitrary subset $S \subset X$. The appropriate notion is provided by a branch of topology called *dimension theory* [75, 76], which assigns to each separable metric space S a dimension $\dim S$ ($= -1, 0, 1, 2, \dots$ or ∞) having the following properties:

- (a) Dimension is a topological invariant, i.e. $\dim S_1 = \dim S_2$ if S_1 and S_2 are homeomorphic.
- (b) The empty set has dimension -1 .
- (c) A nonempty open subset of an n -dimensional manifold ($n \geq 0$) has dimension n .
- (d) If $S_1 \subset S_2$, then $\dim S_1 \leq \dim S_2$.
- (e) If S is the union of countably many *closed* subsets S_i , then $\dim S = \sup_i \dim S_i$.
(It is crucial here that the sets S_i be closed. Indeed, it can be proven that any n -dimensional space can be decomposed as the union of $n + 1$ zero-dimensional subsets.)

We then have the following fundamental result:

Theorem A.1 *Let X be a connected finite-dimensional metrizable C^0 manifold, and let S be a subset of X satisfying $\dim S \leq \dim X - 2$. (In particular, this holds if S is the union of countably many closed submanifolds S_i of codimension ≥ 2 .) Then $X \setminus S$ is connected.*

³⁵ For a connected finite-dimensional C^∞ manifold X , the following conditions are equivalent: X is metrizable; X is separable and metrizable; X is second countable; X is Lindelöf; X is paracompact; there exists a Riemannian metric on X . (For a proof, see [36, vol. I, p. 271] and [70, Theorem VIII.6.5]. See also [71, p. 207].) The purpose of imposing this condition is to exclude pathological examples such as the “long line” [72, Example 45], which are locally Euclidean [73, Problem 3.12.18(b)] and even admit a C^ω differential structure [74, p. 15], but are globally “too big”.

PROOF. See [75, p. 48, Corollary 1] or [76, p. 80, Theorem 1.8.19]. ■

This can be rephrased as: if $X \setminus S$ is disconnected, then S must have codimension 0 or 1. In particular, if $X \setminus \bigcup_i S_i$ is disconnected and the S_i are closed, then at least one of the S_i must have codimension 0 or 1.

Next we wish to study theorems going in the opposite direction, i.e. asserting that $X \setminus S$ is disconnected. The naive converse of Theorem A.1 is false:

Example 1. Let X be the torus T^N , and let S be the “slice” $T^{N-1} \times \{a\}$ for some $a \in T^1$. Then S has codimension 1, but $X \setminus S$ is connected.

Example 2. Let X be the real projective space $RP^{N-1} \equiv S^{N-1}/Z_2$, and let S be the equator in X . Then S has codimension 1, but $X \setminus S$ is connected.

The key fact in both of these examples is that the manifold X is not simply connected. Indeed, if we assume that X is simply connected, then we can prove a converse to Theorem A.1:

Theorem A.2 *Let X be a simply connected finite-dimensional metrizable C^∞ manifold, and let S be a closed codimension-1 submanifold (without boundary) of X . Then $X \setminus S$ is disconnected.*

PROOF (explained to us by Sylvain Cappell). Fix a point $p \in S$, and let U be a small open neighborhood of p . Let $\gamma: [0, 1] \rightarrow U$ be a smooth curve that intersects S exactly once, doing so transversally at p . Then $q_0 \equiv \gamma(0)$ and $q_1 \equiv \gamma(1)$ are points in $U \setminus S$ “on opposite sides of S ”. Now, if $X \setminus S$ is connected (and hence path-connected), then there exists a smooth curve $\tilde{\gamma}$ in $X \setminus S$ running from q_1 to q_0 . In that case $\alpha \equiv \gamma \circ \tilde{\gamma}$ is a loop in X , which intersects S exactly once. By a slight modification near q_0 and q_1 , we can assume that α is smooth.

Now recall the basic ideas of *intersection theory mod 2* [79, Section 2.4]: Let M and X be finite-dimensional metrizable C^∞ manifolds, with M compact, and let S be a closed submanifold of X satisfying $\dim M + \dim S = \dim X$. If $f: M \rightarrow X$ is a smooth map that is transversal to S (see Section A.2 for the precise definition), we define $I_2(f, S)$ to be the cardinality of $f^{-1}[S]$ mod 2. A fundamental theorem states that if f_0, f_1 are homotopic and are both transversal to S , then $I_2(f_0, S) = I_2(f_1, S)$.

To apply this theory, we let $M = S^1$ and $f = \alpha$. By construction $I_2(\alpha, S) = 1$. On the other hand, since X is simply connected, α is homotopic to a constant map $\beta: S^1 \rightarrow X$, where the constant can be chosen to be $\notin S$; so $I_2(\beta, S) = 0$. But this is a contradiction. ■

Remarks. 1. For S compact and connected, this proof can be found in [74, Theorem 4.4.6].

2. A fancier way of phrasing this proof is to use the language of homology theory. There is a natural bilinear map $H_1(X; Z_2) \times H_{n-1}(X; Z_2) \rightarrow Z_2$ (where $n = \dim X$), called the “Poincaré duality” or “intersection pairing” [77, Theorem 65.1]: if α is a loop and S is an $(n - 1)$ -dimensional submanifold, then $[\alpha] \otimes [S]$ counts (mod 2) the number of times that α intersects S . For our loop α , this intersection number is 1,

so $[\alpha]$ is a nontrivial element of $H_1(X; Z_2)$. But this yields a contradiction if the first homology group of X mod 2 is trivial [i.e. $H_1(X; Z_2) = 0$]. Now, since $H_1(X; \mathbb{Z})$ is the quotient of the first homotopy group $\pi_1(X)$ by its commutator, simple connectedness implies the triviality of $H_1(X; \mathbb{Z})$ and hence of $H_1(X; Z_2)$; but the latter condition is weaker. For example, the lens spaces $L(n, k)$ are 3-dimensional manifolds having $H_1(X; \mathbb{Z}) = Z_n$ [77, pp. 238–243]; so for n odd, we have $H_1(X; Z_2) = 0$ but $\pi_1(X) \neq 0$. For an even more extreme example, let G be an arbitrary finite simple group, and let X be a compact polyhedron such that $\pi_1(X) = G$ [78, Theorem 6.4.6]; then $H_1(X; \mathbb{Z}) = H_1(X; Z_2) = 0$.

If X has nontrivial first homology mod 2, then removing a single codimension-1 submanifold may not disconnect X , as the two preceding examples show. Nevertheless, by removing *several* codimension-1 submanifolds we can disconnect X . For simplicity, we restrict attention to the case where X is compact.

Theorem A.3 *Let X be a compact connected n -dimensional metrizable C^∞ manifold, and let $k = \text{rank } H_1(X; Z_2)$. Let S_1, \dots, S_l be disjoint closed codimension-1 submanifolds (without boundary) of X . Then $X \setminus \bigcup_{i=1}^l S_i$ has at least $l - k + 1$ connected components. In particular, if $l \geq k + 1$, then $X \setminus \bigcup_{i=1}^l S_i$ is disconnected.*

PROOF. We imitate the proof of the Alexander duality theorem [77, Theorem 71.1]. Set $A = \bigcup_{i=1}^l S_i$, and let $l' \geq l$ be the number of connected components of A . Then, by the Poincaré duality theorem [77, Theorem 65.1], the $(n - 1)^{\text{st}}$ cohomology group mod 2 of A has rank l' , i.e. $H^{n-1}(A; Z_2) \simeq H_0(A; Z_2) \simeq Z_2^{l'}$. On the other hand, by Poincaré duality we have $H^{n-1}(X; Z_2) \simeq H_1(X; Z_2) \simeq Z_2^k$. Now there is an exact sequence

$$H^n(X; Z_2) \xleftarrow{j^*} H^n(X, A; Z_2) \xleftarrow{\delta^*} H^{n-1}(A; Z_2) \xleftarrow{i^*} H^{n-1}(X; Z_2) \quad (\text{A.1})$$

where $i: A \rightarrow X$ and $j: (X, \emptyset) \rightarrow (X, A)$ are inclusions, and δ^* is the cohomology coboundary homomorphism [77, Theorem 43.1, compare Theorem 23.3]. So δ^* induces an isomorphism

$$\ker j^* \simeq H^{n-1}(A; Z_2)/i^*[H^{n-1}(X; Z_2)] \simeq Z_2^m \quad (\text{A.2})$$

where $m \geq l' - k \geq l - k$.

Now let $\Gamma_{(2)}$ be the unique nonzero element of $H^n(X; Z_2) \simeq Z_2$ (also called an “orientation class for X over Z_2 ”); then $j_*\Gamma_{(2)}$ is a nonzero element of $H^n(X, A; Z_2)$. Let $k: X \setminus A \rightarrow X$ be inclusion. Then by Poincaré duality [77, Theorems 67.1 and 67.2] and Lefschetz duality [77, Theorem 70.6] we have the diagram

$$\begin{array}{ccc} H^n(X, A; Z_2) & \xrightarrow{j^*} & H^n(X; Z_2) \\ \downarrow \phi_* & \searrow \cap j_*\Gamma_{(2)} & \downarrow \cap \Gamma_{(2)} \\ H_0(X \setminus A; Z_2) & \xrightarrow{k_*} & H_0(X; Z_2) \end{array} \quad (\text{A.3})$$

where ϕ_* is the Lefschetz duality isomorphism, $\cap\Gamma_{(2)}$ is the Poincaré duality isomorphism, and the diagram commutes up to sign. Therefore,

$$\ker j^* \simeq \ker k_* . \tag{A.4}$$

On the other hand, by exactness of the sequence

$$0 \longrightarrow \widetilde{H}_0(X \setminus A) \longrightarrow H_0(X \setminus A) \xrightarrow{k_*} H_0(X) \longrightarrow 0 \tag{A.5}$$

[77, exercise 71.1], we have

$$\ker k_* \simeq \widetilde{H}_0(X \setminus A) . \tag{A.6}$$

Combining these isomorphisms, we conclude that

$$\widetilde{H}_0(X \setminus A) \simeq Z_2^m , \tag{A.7}$$

i.e. $X \setminus A$ has $m + 1 \geq l - k + 1$ connected components. ■

Remarks. 1. In the foregoing proof it is not necessary that S_1, \dots, S_l be disjoint; it suffices that they be “linearly independent mod 2”, in the sense that $\text{rank } H^{n-1}(\bigcup_{i=1}^l S_i; Z_2) \geq l$.

2. Is the bound $l \geq k + 1$ best possible? We suspect that it *is* best possible under the hypothesis $\text{rank } H^{n-1}(\bigcup_{i=1}^l S_i; Z_2) \geq l$, but that it is *not* best possible under the stronger hypothesis that S_1, \dots, S_l are disjoint. Indeed, if X is an orientable surface (= 2-dimensional manifold) of genus g , then $k = \text{rank } H_1(X; Z_2) = 2g$; and while $2g + 1$ *independent* circles (= codimension-1 submanifolds) may be needed to disconnect X , only $g + 1$ *disjoint* circles are needed to disconnect X [74, Exercise 9.3.17 and Theorem 9.3.6].

3. If X is a connected manifold and S is a *connected* closed codimension-1 submanifold, then $X \setminus S$ is either connected or else has exactly two connected components [74, Lemma 4.4.4]. Thus, each disjoint “cut” creates *at most one* new connected component.

A.2 Transversality and genericity

Let X and Y be finite-dimensional metrizable C^r manifolds ($1 \leq r \leq \infty$), let $f: X \rightarrow Y$ be a C^r map, and let Z be a codimension- k C^r submanifold of Y . We wish to show that “generically” the set $f^{-1}[Z] \equiv \{x: f(x) \in Z\}$ is a submanifold of codimension k in X . The appropriate tool is a branch of differential topology called *transversality theory* [74, 79, 80]. We say that f is *transversal to* Z (denoted $f \pitchfork Z$) if, for every $x \in X$, either

- (a) $f(x) \notin Z$; or
- (b) $(D_x f)(T_x X) + T_{f(x)} Z = T_{f(x)} Y$, i.e. the image of the tangent space $T_x X$ under the linear map $D_x f$ contains a subspace of $T_{f(x)} Y$ that is complementary to $T_{f(x)} Z$.

(For a nice intuitive discussion, with pictures, see [79, pp. 27 ff.] Transversality is just the right condition we need to control the inverse image $f^{-1}[Z]$:

Theorem A.4 *Let X, Y be finite-dimensional C^r manifolds ($1 \leq r \leq \infty$), let Z be a codimension- k C^r submanifold of Y , and let $f: X \rightarrow Y$ be a C^r map that is transversal to Z . Then $f^{-1}[Z]$ is either empty or else a C^r submanifold (not necessarily connected) of codimension k . Moreover, if X is Lindelöf (resp. compact) and Z is closed, then $f^{-1}[Z]$ has only countably many (resp. finitely many) connected components.*

PROOF. See [74, Theorem 1.3.3], [79, p. 28], [81, p. 24] or [80, pp. 45–46]. ■

Now the point is that *transversality is generic*:

Theorem A.5 *Let X, Y be finite-dimensional metrizable C^r manifolds ($1 \leq r \leq \infty$), and let Z be a C^r submanifold of Y . Then the set of maps*

$$\mathcal{A}_Z \equiv \{f \in C^r(X, Y): f \text{ is transversal to } Z\} \quad (\text{A.8})$$

contains a dense G_δ subset of $C^r(X, Y)$ in the C^r compact-open topology (also called the “weak topology”). In fact, if X is compact and Z is closed, then \mathcal{A}_Z is a dense open subset of $C^r(X, Y)$.

PROOF. See [74, Theorem 3.2.1]; other references are [81, pp. 25–26] and [80, pp. 46–50]. ■

Putting together Theorems A.4 and A.5, we conclude that for “almost all” maps f , the inverse image $f^{-1}[Z]$ is either empty or else a submanifold of codimension k .

We cannot exclude the possibility that $f^{-1}[Z]$ is empty: indeed, it is perfectly possible for the image $f[X]$ to avoid completely the submanifold Z . However, the point is that in physical applications there will be a *nonzero probability* for $f[X]$ to intersect Z . We could go on to formalize this idea: we would assume that a compact Lie group G acts transitively on Y , and we would seek to prove that under appropriate conditions the set

$$\{f \in C^r(X, Y): \mu_{Haar}(\{g \in G: (g \circ f)^{-1}[Z] \neq \emptyset\}) > 0\} \quad (\text{A.9})$$

contains a dense G_δ subset of $C^r(X, Y)$. But we are physicists, not mathematicians, and enough is enough.

Let us summarize the upshot of all this topology for our physical application. Consider a σ -model with x -space X and target space M , and let Z be a closed codimension-1 submanifold of M . We reason as follows:

(a) If M is simply connected, then Theorem A.2 implies that $M \setminus Z$ is disconnected. With “high probability” one expects the field σ to intersect more than one connected component of $M \setminus Z$. In this case the set $X \setminus \sigma^{-1}[Z]$ is disconnected.

(b) For arbitrary M , Theorems A.4 and A.5 and the subsequent remarks imply that with “high probability” $\sigma^{-1}[Z]$ is a nonempty closed codimension-1 submanifold of X . If X is simply connected, Theorem A.2 then implies that the set $X \setminus \sigma^{-1}[Z]$ is disconnected.

(c) If neither M nor X is simply connected, then one uses Theorem A.3 in place of Theorem A.2. One expects the probability of the desired event to be smaller, but still nonzero (uniformly for $1 \ll \xi \lesssim L$).

A.3 Fixed points of isometries

Next we discuss the fixed-point set for isometries of a Riemannian manifold.

Theorem A.6 *Let M be a finite-dimensional Riemannian manifold, and let \mathcal{S} be any set of isometries of M . Let F be the set of points of M which are left fixed by all elements of \mathcal{S} . Then:*

- (a) F is a closed set.
- (b) Each connected component F_i of F is a closed totally geodesic³⁶ submanifold of M .
- (c) For each F_i , there exists an open set $U_i \supset F_i$ that intersects none of the other connected components of F .
- (d) If M is Lindelöf (resp. compact), there are at most countably many (resp. finitely many) F_i .

PROOF. (a) is trivial, since an isometry is necessarily continuous. (b) is [82, p. 59, Theorem II.5.1], and (c) is implicit in the proof given there. To prove (d), consider the open cover of M consisting of the $\{U_i\}$ together with $V \equiv M \setminus F$. Since M is Lindelöf (resp. compact), there exists a countable (resp. finite) subcover; but by definition of U_i , this subcover must include all of the $\{U_i\}$, since otherwise it couldn't cover all of F . ■

Some partial converses to Theorem A.6(b) are mentioned in Further Remarks 1 and 2 at the end of this section.

The following lemma shows that isometries are completely determined locally (it is analogous to analytic continuation of holomorphic functions, but even stronger):

Lemma A.7 [42, p. 62, Lemma I.11.2] *Let M be a connected finite-dimensional Riemannian manifold, and let φ and ψ be isometries of M . Suppose that there exists a point $p \in M$ for which $\varphi(p) = \psi(p)$ and $(D\varphi)_p = (D\psi)_p$. Then $\varphi = \psi$.*

³⁶ A submanifold $N \subset M$ is called *totally geodesic at a point* $x \in N$ if each M -geodesic which is tangent to N at x lies in N . The submanifold N is called *totally geodesic* if it is totally geodesic at each of its points.

It follows immediately that a fixed-point manifold of codimension 0 can occur only in the case of the identity map:

Theorem A.8 *Let M be a connected finite-dimensional Riemannian manifold, and let φ be an isometry of M . If the set of fixed points of φ contains a nonempty open set (i.e. a submanifold of codimension 0), then φ is the identity map (and hence the fixed-point set is all of M).*

By a slightly more subtle argument, we can show that if the fixed-point manifold has codimension 1, then the map must be involutive:

Theorem A.9 *Let M be a connected finite-dimensional Riemannian manifold, and let φ be an isometry of M . If the set of fixed points of φ contains a submanifold of codimension 1, then φ is involutive (i.e. φ^2 is the identity map).*

PROOF. Let $N \subset \text{Fix}(\varphi)$ be a submanifold of M of codimension 1, and let $p \in N$. Then in some small neighborhood $U \ni p$ we can choose local coordinates (x_1, \dots, x_n) such that $U \cap N$ is given by $x_1 = 0$. In this basis, $(D\varphi)_p$ has the form

$$(D\varphi)_p = \left(\begin{array}{c|ccc} v_1 & v_2 & \cdots & v_n \\ \hline 0 & & & I \end{array} \right). \quad (\text{A.10})$$

Since $(D\varphi)_p$ leaves invariant the metric tensor G_p [i.e. $(D\varphi)_p^T G_p (D\varphi)_p = G_p$] and G_p is nondegenerate, it follows that $\det(D\varphi)_p = \pm 1$, i.e. $v_1 = \pm 1$. We now claim that $(D\varphi)_p^2 = I$:

(a) If $v_1 = +1$, then we must have $v_2 = \dots = v_n = 0$, because a matrix that leaves invariant a positive-definite quadratic form must be diagonalizable (over \mathbb{C}), i.e. it must not have a nontrivial Jordan block. Then $(D\varphi)_p = I$.

(b) If $v_1 = -1$, then

$$(D\varphi)_p^2 = \left(\begin{array}{c|ccc} v_1^2 & (v_1 + 1)v_2 & \cdots & (v_1 + 1)v_n \\ \hline 0 & & & I \end{array} \right) = I. \quad (\text{A.11})$$

(Alternatively, we can argue that there exists a change of basis setting $v_2 = \dots = v_n = 0$.)

Thus, in either case, φ^2 is an isometry satisfying $\varphi^2(p) = p$ and $(D\varphi^2)_p = (D\varphi)_p^2 = I$. Lemma A.7 then implies that φ^2 is the identity map. [In case (a), φ is itself the identity map, while in case (b) it is not.] ■

Remark. This theorem seems to be well known to differential geometers, but we have been unable to find a published reference. Some vaguely related theorems, which may conceivably be of interest in future generalizations of the embedding method, are:

a) Let \mathcal{S} be a *one-parameter group* of isometries (or more generally, a *connected abelian* Lie group of isometries) of a finite-dimensional Riemannian manifold M . Then each connected component of $\text{Fix}(\mathcal{S})$ has *even* codimension [83] [82, p. 60, Theorem II.5.3].

b) Let $T: M \rightarrow M$ be a smooth map which is periodic of *odd* period p (here $p \equiv \min\{q: T^q = \text{identity}\}$). Then each connected component of $\text{Fix}(\mathcal{S})$ has *even* codimension [84]. Note that T need not be an isometry; this theorem is purely algebraic and topological. For related material, see also [85].

Further Remarks. 1. Vanhecke and collaborators [86, 87, 88, 89, 90, 91] have recently investigated reflections in Riemannian manifolds from a point of view opposite (but complementary) to ours. We start from an involutive isometry and seek to study its fixed-point manifold. They start, by contrast, from a submanifold $N \subset M$, and define the local reflection φ_N about N ; this local reflection is automatically involutive, and they ask under what conditions it is a local isometry. In view of Theorem A.6(b) [or more precisely its local analogue], a necessary condition for φ_N to be a local isometry is that N be totally geodesic. It is natural to ask whether this condition is sufficient. Vanhecke *et al.* prove the following interesting theorem ([86, Theorem 5.7] and [89, Corollaries 4(a) and 5]), which is somewhat reminiscent of Theorem 3.3: Let M be a Riemannian manifold. Then the following are equivalent:

(a) For each geodesic curve (= totally geodesic 1-dimensional submanifold) $N \subset M$, the local reflection φ_N is a local isometry.

(b) For each totally geodesic submanifold $N \subset M$, the local reflection φ_N is a local isometry.

(c) M is a space of constant curvature.

2. Another partial converse to Theorem A.6(b) is due to Chen and Nagano [92, Theorem 3.1]: In the manifold $Q_m = SO(m+2)/(SO(m) \times SO(2))$ for $m \geq 2$, a complete connected submanifold $N \subset Q_m$ is totally geodesic if *and only if* it is a connected component of the fixed-point set of some *finite* set of *involutive* isometries of Q_m . It would be interesting to know to which other symmetric spaces, if any, this result extends. Some totally geodesic submanifolds $N \subset Q_m$ of codimension m have been found by Nikić [93].

3. In Example 3 of Section 3.1, we proved that in CP^{N-1} ($N \geq 3$) there are no isometries having a fixed-point manifold of codimension 1. Wolf [94] has shown much more: in CP^{N-1} ($N \geq 3$) there are no closed totally geodesic submanifolds of codimension 1. Moreover, the same holds for quaternionic projective space QP^{N-1} . In fact, Wolf [94, Theorem 1] obtains a complete list of the totally geodesic submanifolds of S^{N-1} , RP^{N-1} , CP^{N-1} , QP^{N-1} and *Cayley* P^2 .

A.4 Codimension and frustration

Here we prove some theorems mentioned in Section 2.3, regarding the relations between codimension and frustration. Theorem A.10 and Corollary A.11 state that non-frustration implies codimension 1. Corollary A.12 shows further that in the case of an irreducible symmetric space, non-frustration occurs *only* in the codimension-1

algorithm for the N -vector model — i.e. the original Wolff algorithm.

Theorem A.10 *Let M be a finite-dimensional Riemannian manifold with metric tensor g , and let T be an involutive isometry of M . Let $E: M \times M \rightarrow \mathbb{R}$ be a function satisfying $E(\boldsymbol{\sigma}, \boldsymbol{\sigma}') = a + bd(\boldsymbol{\sigma}, \boldsymbol{\sigma}')^2 + o(d(\boldsymbol{\sigma}, \boldsymbol{\sigma}')^2)$ as $\boldsymbol{\sigma}' \rightarrow \boldsymbol{\sigma}$, where $a \in \mathbb{R}$, $b > 0$, and d is the geodesic distance on M . Define*

$$J(\boldsymbol{\sigma}, \boldsymbol{\sigma}') = E(\boldsymbol{\sigma}, T\boldsymbol{\sigma}') - E(\boldsymbol{\sigma}, \boldsymbol{\sigma}') . \quad (\text{A.12})$$

Now let $\boldsymbol{\sigma}^ \in \text{Fix}(T)$. Suppose that there exists an integer $m \geq 3$ and a neighborhood $U \ni \boldsymbol{\sigma}^*$ such that for all $\boldsymbol{\sigma}_1, \dots, \boldsymbol{\sigma}_m, \boldsymbol{\sigma}_{m+1} \equiv \boldsymbol{\sigma}_1 \in U$ we have*

$$\prod_{j=1}^m J(\boldsymbol{\sigma}_j, \boldsymbol{\sigma}_{j+1}) \geq 0 . \quad (\text{A.13})$$

Then the connected component of $\text{Fix}(T)$ containing $\boldsymbol{\sigma}^$ has codimension 1.*

PROOF. Use a chart on U such that $\boldsymbol{\sigma}^* = 0$ (by abuse of language we identify a point in U with its coordinates given by the chart) and $g_{\mu\nu}(\boldsymbol{\sigma}^*) = \delta_{\mu\nu}$. Then the linear map $(DT)_{\boldsymbol{\sigma}^*}$ is represented in these coordinates by an orthogonal matrix \mathbf{T} satisfying $\mathbf{T}^2 = I$. Thus, \mathbf{T} is symmetric with eigenvalues ± 1 , and the number of negative eigenvalues equals the codimension of the connected component of $\text{Fix}(T)$ containing $\boldsymbol{\sigma}^*$. Finally, J is given in these coordinates by

$$J(\boldsymbol{\sigma}, \boldsymbol{\sigma}') = b \left[d(\boldsymbol{\sigma}, T\boldsymbol{\sigma}')^2 - d(\boldsymbol{\sigma}, \boldsymbol{\sigma}')^2 \right] + o(d(\boldsymbol{\sigma}, \boldsymbol{\sigma}')^2, d(\boldsymbol{\sigma}, T\boldsymbol{\sigma}')^2) \quad (\text{A.14a})$$

$$= b \left[(\boldsymbol{\sigma} - \mathbf{T}\boldsymbol{\sigma}')^2 - (\boldsymbol{\sigma} - \boldsymbol{\sigma}')^2 \right] + o(\boldsymbol{\sigma}^2, \boldsymbol{\sigma}'^2) \quad (\text{A.14b})$$

$$= 2b\boldsymbol{\sigma} \cdot (I - \mathbf{T})\boldsymbol{\sigma}' + o(\boldsymbol{\sigma}^2, \boldsymbol{\sigma}'^2) \quad (\text{A.14c})$$

Now, if $\text{rank}(I - \mathbf{T}) \geq 2$ and $m \geq 3$, it is easy to choose $\boldsymbol{\sigma}_1, \dots, \boldsymbol{\sigma}_m$ with arbitrarily small magnitudes such that $\boldsymbol{\sigma}_i \cdot (I - \mathbf{T})\boldsymbol{\sigma}_{i+1} > 0$ for $i = 1, \dots, m - 1$ and $\boldsymbol{\sigma}_m \cdot (I - \mathbf{T})\boldsymbol{\sigma}_1 < 0$. [Using polar coordinates in some fixed two-dimensional subspace of $\text{Ran}(I - \mathbf{T})$, let $\boldsymbol{\sigma}_j$ point at angle $\theta_j = (j - 1)\Theta/(m - 1)$ for $j = 1, \dots, m$, where $\pi < \Theta < 3\pi/2$.] This proves the theorem. ■

Corollary A.11 *Let M , T , E and J be as in Theorem A.10. Suppose that for each $\boldsymbol{\sigma}^* \in \text{Fix}(T)$ there exists an integer $m_{\boldsymbol{\sigma}^*} \geq 3$ and a neighborhood $U_{\boldsymbol{\sigma}^*} \ni \boldsymbol{\sigma}^*$ such that for all $\boldsymbol{\sigma}_1, \dots, \boldsymbol{\sigma}_m, \boldsymbol{\sigma}_{m+1} \equiv \boldsymbol{\sigma}_1 \in U_{\boldsymbol{\sigma}^*}$ we have*

$$\prod_{j=1}^m J(\boldsymbol{\sigma}_j, \boldsymbol{\sigma}_{j+1}) \geq 0 . \quad (\text{A.15})$$

Then either

$$(a) \text{Fix}(T) = \emptyset$$

or else

(b) every connected component of $\text{Fix}(T)$ has codimension 1.

PROOF. Immediate. ■

Corollary A.12 *Let M, T, E and J be as in Theorem A.10, and assume further that M is an irreducible compact Riemannian symmetric space of dimension n . Suppose that for each $\sigma^* \in \text{Fix}(T)$ there exists an integer $m_{\sigma^*} \geq 3$ and a neighborhood $U_{\sigma^*} \ni \sigma^*$ such that for all $\sigma_1, \dots, \sigma_m, \sigma_{m+1} \equiv \sigma_1 \in U_{\sigma^*}$ we have*

$$\prod_{j=1}^m J(\sigma_j, \sigma_{j+1}) \geq 0. \quad (\text{A.16})$$

Then either

(a) $\text{Fix}(T) = \emptyset$

or else

(b) M is isometric to S^n , and under this isometry T is the codimension-1 reflection $\sigma \rightarrow I_1 \sigma$.

PROOF. If $\text{Fix}(T) \neq \emptyset$, then by Corollary A.11 each connected component of $\text{Fix}(T)$ must have codimension 1. By Theorem 3.3, M must be isometric to either S^n or RP^n . But in Section 3.1 (Example 2), we classified the involutive isometries of RP^n : in particular, we found that for $n \geq 2$, every involutive isometry with $\text{Fix}(T) \neq \emptyset$ has at least one connected component of $\text{Fix}(T)$ of codimension ≥ 2 . So M must be isometric to S^n , and the theorem follows from our classification of the involutive isometries of S^n (Section 3.1, Example 1). ■

B Involutive Isometries of $SU(N)$

Let G be a compact simple Lie group³⁷, with Lie algebra \mathfrak{g} . Then there is a *unique* (up to constant multiples) Riemannian metric on G that is invariant under both left and right translations; at the identity element $e \in G$ this metric is given by the negative of the Killing-Cartan form

$$B(X, Y) = \text{tr}(\text{ad}X \text{ad}Y) \quad \text{for } X, Y \in \mathfrak{g} \quad (\text{B.1})$$

³⁷ We make the usual abuse of language, and call a Lie group “simple” if its Lie *algebra* is simple (i.e. has no nontrivial ideals). Of course G need *not* be simple in the group-theoretic sense: for example, $SU(N)$ has a nontrivial (but discrete) center, isomorphic to Z_N .

(see [47, pp. 57–58, Lemme 5]). We shall always consider G to be equipped with this unique bi-invariant Riemannian metric.

For $G = SU(N)$, the Lie algebra $\mathfrak{g} = \mathfrak{su}(N)$ is the space of all traceless antihermitian $N \times N$ matrices, and the Killing-Cartan form is

$$B(X, Y) = -\text{const} \times \text{Re tr}(X^\dagger Y) \quad \text{for } X, Y \in \mathfrak{su}(N). \quad (\text{B.2})$$

The isometry group of $SU(N)$ has been determined by Cartan [95] (see also Wolf [96, secs. 2.4 and 4.1.2]):

Theorem B.1 [95] *The isometries of $SU(N)$ are the following:*

- (a) $A \longrightarrow UAV$
- (b) $A \longrightarrow UA^\dagger V$
- (c) $A \longrightarrow U\bar{A}V$
- (d) $A \longrightarrow UA^T V$

for $U, V \in SU(N)$. For $N \geq 3$, two isometries in this list are equal if and only if they belong to the same class (a), (b), (c) or (d) and in addition their determining matrices (U, V) and (U', V') satisfy $U' = CU$, $V' = C^{-1}V$ for some $C \in \mathcal{C} \equiv \text{center of } SU(N)$. For $N = 2$ the same statement holds provided that we consider only the classes (a) and (b). [For $N = 2$ the classes (c) and (d) are redundant because $\bar{A} = JA(-J)$ and $A^T = JA^\dagger(-J)$, where $J = i\tau^2 = \begin{pmatrix} 0 & 1 \\ -1 & 0 \end{pmatrix}$ and $\pm J \in SU(2)$.]

Our next task is to classify these isometries modulo conjugacy:

Theorem B.2 *Two isometries of $SU(N)$ are conjugate if and only if they belong to the same class (a), (b), (c) or (d) [for $N = 2$, (a) or (b)] and in addition their determining matrices (U, V) and (U', V') are related in one of the ways (i)–(iv) listed below:*

Class (a):

- (i) $U' = CXUX^{-1}, \quad V' = C^{-1}Y^{-1}VY$
- (ii) $U' = CXV^\dagger X^{-1}, \quad V' = C^{-1}Y^{-1}U^\dagger Y$
- (iii) $U' = CX\bar{U}X^{-1}, \quad V' = C^{-1}Y^{-1}\bar{V}Y$
- (iv) $U' = CXV^T X^{-1}, \quad V' = C^{-1}Y^{-1}U^T Y$

Class (b):

- (i) $U' = CXUY, \quad V' = C^{-1}XVY$

- (ii) $U' = CXV^\dagger Y, \quad V' = C^{-1}XU^\dagger Y$
- (iii) $U' = CX\bar{U}Y, \quad V' = C^{-1}X\bar{V}Y$
- (iv) $U' = CXV^T Y, \quad V' = C^{-1}XU^T Y$

Class (c):

- (i) $U' = CXUX^T, \quad V' = C^{-1}Y^T VY$
- (ii) $U' = CXV^\dagger X^T, \quad V' = C^{-1}Y^T U^\dagger Y$
- (iii) $U' = CX\bar{U}X^T, \quad V' = C^{-1}Y^T \bar{V}Y$
- (iv) $U' = CXV^T X^T, \quad V' = C^{-1}Y^T U^T Y$

Class (d):

- (i) $U' = CXU\bar{Y}, \quad V' = C^{-1}\bar{X}VY$
- (ii) $U' = CXV^\dagger \bar{Y}, \quad V' = C^{-1}\bar{X}U^\dagger Y$
- (iii) $U' = CX\bar{U}\bar{Y}, \quad V' = C^{-1}\bar{X}\bar{V}Y$
- (iv) $U' = CXV^T \bar{Y}, \quad V' = C^{-1}\bar{X}U^T Y$

In all cases $X, Y \in SU(N)$ and $C \in \mathcal{C} \equiv$ center of $SU(N)$.

PROOF. Consider an isometry f of class (a), say $f(A) = UAV$, and let us compute $g \circ f \circ g^{-1}$ with all possible isometries g :

- (i) $g(A) = XAY \implies (g \circ f \circ g^{-1})(A) = (XUX^{-1})A(Y^{-1}VY)$
- (ii) $g(A) = XA^\dagger Y \implies (g \circ f \circ g^{-1})(A) = (XV^\dagger X^{-1})A(Y^{-1}U^\dagger Y)$
- (iii) $g(A) = X\bar{A}Y \implies (g \circ f \circ g^{-1})(A) = (X\bar{U}X^{-1})A(Y^{-1}\bar{V}Y)$
- (iv) $g(A) = XA^T Y \implies (g \circ f \circ g^{-1})(A) = (XV^T X^{-1})A(Y^{-1}U^T Y)$

The claim then follows from Theorem B.1. Analogous computations handle the cases when f is an isometry of class (b), (c) or (d). ■

Next we determine which isometries are involutive:

Theorem B.3 *An isometry of $SU(N)$ is involutive if and only if:*

Class (a): $U^2 = V^{-2} \in \mathcal{C} \equiv$ center of $SU(N)$.

Class (b): $UV^{-1} \in \mathcal{C}$.

Class (c): Either (1) $U = U^T$ and $V = V^T$
or (2) $U = -U^T$ and $V = -V^T$ and N is even.

Class (d): Either (1) $U = \bar{V}$
or (2) $U = -\bar{V}$ and N is even.

PROOF. We compute two successive applications of the given isometry, and demand (using the last part of Theorem B.1) that it be equal to the identity map.

Class (a): $A \rightarrow UAV \rightarrow U(UAV)V$. So we need $U^2 = C$, $V^2 = C^{-1}$ with $C \in \mathcal{C}$.

Class (b): $A \rightarrow UA^\dagger V \rightarrow U(UA^\dagger V)^\dagger V = (UV^\dagger)A(U^\dagger V)$. So we need $UV^\dagger = C$, $U^\dagger V = C^{-1}$ with $C \in \mathcal{C}$. The two conditions are equivalent; they amount to $U = CV = VC$, i.e. $UV^{-1} \in \mathcal{C}$.

Class (c): $A \rightarrow U\bar{A}V \rightarrow U\overline{U\bar{A}V} = (U\bar{U})A(\bar{V}V)$. So we need $U\bar{U} = C$, $\bar{V}V = C^{-1}$ with $C \in \mathcal{C}$. Equivalently we need $U = CU^T$, $V = C^{-1}V^T$. But then $U = CU^T = C(CU^T)^T = CC^T U$; and since the central elements of $SU(N)$ are multiples of the identity matrix, we have $C = C^T$; so we need $C^2 = I$. But this means that $C = I$ if N is odd, or $C = \pm I$ if N is even.

Class (d): $A \rightarrow UA^T V \rightarrow U(UA^T V)^T V = (UV^T)A(U^T V)$. So we need $UV^T = C$, $U^T V = C^{-1}$ with $C \in \mathcal{C}$. Equivalently we need $U = C\bar{V}$, $V = C^{-1}\bar{U}$. But for a central element of $SU(N)$, $C^{-1} = \bar{C}$, so we can write the second equation as $V = \bar{C}\bar{U}$, hence $\bar{V} = CU$. But then we have $U = C^2 U$, so $C^2 = I$. It follows that $C = I$ if N is odd, or $C = \pm I$ if N is even. ■

Next we classify the involutive isometries modulo conjugacy:

Theorem B.4 *Every involutive isometry of $SU(N)$ is conjugate to one of the following:*

(a_{r,s}) $A \rightarrow I_r A I_s$ with $r + s$ even, $r \leq s$ and $r \leq N/2$.

Here $I_r = \text{diag}(\underbrace{-1, \dots, -1}_{r \text{ times}}, \underbrace{+1, \dots, +1}_{N-r \text{ times}})$.

(b1) $A \rightarrow A^\dagger$.

(b2) [Only for N even] $A \rightarrow e^{2\pi i/N} A^\dagger$.

(c1) $A \rightarrow \bar{A}$.

(c2a) [Only for N even] $A \rightarrow -J\bar{A}J$.

(c2b) [Only for $N = 4k$, k integer] $A \rightarrow e^{2\pi i/N} J\bar{A}J$.

(c2c) [Only for $N = 4k + 2$, k integer] $A \rightarrow J\bar{A}J$.

(d1) $A \rightarrow A^T$.

(d2) [Only for N even] $A \longrightarrow -A^T$.

Moreover, none of the above isometries [for $N = 2$, none of the above isometries of classes (a) and (b)] are conjugate one to another.

PROOF. *Class (a):* The map $A \longrightarrow UAV$ is involutive iff $U^2 = V^{-2} = C = e^{2\pi im/N} I$. It then follows that the eigenvalues of U (resp. V) are all $\pm e^{\pi im/N}$ (resp. $\pm e^{-\pi im/N}$), so the matrices U and V can be diagonalized as $U = X(e^{\pi im/N} I_r)X^{-1}$, $V = Y^{-1}(e^{-\pi im/N} I_s)Y$ with $X, Y \in SU(N)$ and $0 \leq r, s \leq N$. Note that m, r and s must all have the same parity modulo 2 (since $\det U = \det V = +1$), so in particular $r + s$ must be even. By Theorem B.2(a)(i) it follows that the map $A \longrightarrow UAV$ is conjugate to $A \longrightarrow (e^{\pi im/N} I_r)A(e^{-\pi im/N} I_s) = I_r A I_s$. By Theorem B.2(a)(ii) [or (iv)] we can take $r \leq s$. Trivially $I_r A I_s = I_{N-r} A I_{N-s}$, so we can take $r \leq N/2$. Finally, it follows from Theorem B.2(a) that there are no further conjugacies between members of this class.

Class (b): The map $A \longrightarrow UA^\dagger V$ is involutive iff $U = e^{2\pi im/N} V$. By Theorem B.2(b)(i) with $X = e^{-2\pi ik/N} V^{-1}$ and $Y = I$, this map $A \longrightarrow e^{2\pi im/N} V A^\dagger V$ is conjugate to $A \longrightarrow e^{2\pi i(m-2k)/N} A^\dagger$. If N is odd, the integer k can be chosen so that $m - 2k = 0 \pmod{N}$; if N is even, k can be chosen so that $m - 2k = 0$ or $1 \pmod{N}$. Finally, it follows from Theorem B.2(b) that if N is even, these two alternatives are not conjugate one to another.

Class (c1): Consider the map $A \longrightarrow U\bar{A}V$ with $U = U^T$, $V = V^T$. We can write $U = R + iS$ where R and S are real symmetric matrices. Expanding out $UU^\dagger = U^\dagger U = I$, we conclude that $RS = SR$ and $R^2 + S^2 = I$. It follows that we can simultaneously diagonalize R and S using a real rotation matrix $L \in SO(N)$:

$$R = L \operatorname{diag}(\lambda_1, \dots, \lambda_N) L^T \quad (\text{B.3a})$$

$$S = L \operatorname{diag}(\mu_1, \dots, \mu_N) L^T \quad (\text{B.3b})$$

with λ_i, μ_i real and $\lambda_i^2 + \mu_i^2 = 1$. Hence

$$\begin{aligned} U &= L \operatorname{diag}(e^{i\theta_1}, \dots, e^{i\theta_N}) L^T \\ &\equiv LDL^T \end{aligned} \quad (\text{B.4})$$

with $L \in SO(N)$ and D a diagonal matrix in $SU(N)$. Now let $E = \operatorname{diag}(\pm e^{i\theta_1/2}, e^{i\theta_2/2}, \dots, e^{i\theta_N/2})$, with the sign chosen so that $E \in SU(N)$; we have shown that $U = XX^T$ where $X \equiv LE \in SU(N)$. Similarly, $V = Y^T Y$ with $Y \in SU(N)$. It follows from Theorem B.2(c)(i) that the map $A \longrightarrow U\bar{A}V$ is conjugate to $A \longrightarrow \bar{A}$.

Class (c2): Consider the map $A \longrightarrow U\bar{A}V$ with $U = -U^T$, $V = -V^T$ and N even. We can write $U = R + iS$ where R and S are real antisymmetric matrices. Expanding out $UU^\dagger = U^\dagger U = I$, we conclude that $RS = SR$ and $R^2 + S^2 = -I$. It follows from Lemma B.5 below that R and S can be simultaneously brought into real Schur form by a real rotation matrix $L \in SO(N)$:

$$R = L \operatorname{blockdiag}(\lambda_1 \mathbf{J}, \dots, \lambda_{N/2} \mathbf{J}) L^T \quad (\text{B.5a})$$

$$S = L \operatorname{blockdiag}(\mu_1 \mathbf{J}, \dots, \mu_{N/2} \mathbf{J}) L^T \quad (\text{B.5b})$$

with $\mathbf{J} = \begin{pmatrix} 0 & 1 \\ -1 & 0 \end{pmatrix}$, λ_i, μ_i real and $\lambda_i^2 + \mu_i^2 = 1$. Hence

$$\begin{aligned} U &= L \text{ blockdiag}(e^{i\theta_1} \mathbf{J}, \dots, e^{i\theta_{N/2}} \mathbf{J}) L^T \\ &\equiv LDJL^T \end{aligned} \quad (\text{B.6})$$

with $L \in SO(N)$, $D = \text{diag}(e^{i\theta_1}, e^{i\theta_1}, \dots, e^{i\theta_{N/2}}, e^{i\theta_{N/2}}) \in SU(N)$, and $J = \text{blockdiag}(\mathbf{J}, \dots, \mathbf{J})$. Now let $E = \text{diag}(e^{i\theta_1/2}, e^{i\theta_1/2}, \dots, e^{i\theta_{N/2}/2}, e^{i\theta_{N/2}/2})$; either $E \in SU(N)$ or else $e^{-\pi i/N} E \in SU(N)$, according as $\det E = \pm 1$. We have then shown that either

$$U = XJX^T \quad \text{with} \quad X = LE \in SU(N) \quad (\text{B.7})$$

or else

$$U = e^{2\pi i/N} XJX^T \quad \text{with} \quad X = e^{-\pi i/N} LE \in SU(N). \quad (\text{B.8})$$

And obviously the same holds for V . Thus, by Theorem B.2(c)(i) we have shown that every isometry of class (c2) is conjugate to either $A \rightarrow J\bar{A}J$ or $A \rightarrow e^{2\pi i/N} J\bar{A}J$.

We now show that these two isometries are not conjugate one to the other. We firstly prove that there do not exist $X, Y \in SU(N)$ and $C = cI \in \text{center of } SU(N)$ such that $J = CXJX^T e^{2\pi i/N}$ and $J = C^{-1}YJY^T$. Indeed, if such matrices exist, then $C^{1/2} e^{\pi i/N} X$ and $C^{-1/2} Y$ are symplectic matrices and as such must have determinant $+1$ [41, pp. 347–349]. But $\det(C^{1/2} e^{\pi i/N} X) = -c^{N/2}$ and $\det(C^{-1/2} Y) = c^{-N/2} = c^{N/2}$, which is a contradiction. It easily follows, by using Theorem B.2(c), that the two isometries are not conjugate one to another.

It is convenient to make now a slightly different choice of representatives from the two conjugacy classes. Note that when when $N = 4k$ (k integer), the isometry $A \rightarrow J\bar{A}J$ is conjugate to $A \rightarrow -J\bar{A}J$ [take $X = iI$ and $Y = I$ in Theorem B.2(c)(i)], while for $N = 4k + 2$ the isometry $A \rightarrow e^{2\pi i/N} J\bar{A}J$ is conjugate to $A \rightarrow -J\bar{A}J$ [take $X = e^{2\pi i(N-2)/4N} I$, $Y = I$]. Thus, in either case we can choose $A \rightarrow -J\bar{A}J$ as one representative, while for $N = 4k$ (resp. $N = 4k + 2$) we take $A \rightarrow e^{2\pi i/N} J\bar{A}J$ (resp. $A \rightarrow J\bar{A}J$) as the other.

Finally, we prove that isometry (c1) is not conjugate to (c2a), (c2b) or (c2c). By Theorem B.2(c), such a conjugacy would imply the existence of $X \in SU(N)$ and $C \in \mathcal{C}$ such that $XJX^T = C$. But then $X' \equiv C^{-1/2} X \in U(N)$ would satisfy $X'JX'^T = I$, or equivalently $X'J = \overline{X'}$. Taking complex conjugates, we obtain $\overline{X'J} = X'$ (since J is real). Then $X'J^2 = \overline{X'J} = X'$, which implies that $J^2 = I$. But in fact $J^2 = -I$, so we have a contradiction.

Class (d): The map $A \rightarrow UA^T V$ is involutive iff $V = \pm \bar{U}$ (with the $-$ sign allowed only if N is even). By Theorem B.2(d)(i) with $X = U^{-1}$ and $Y = I$, this map $A \rightarrow \pm UA^T \bar{U}$ is conjugate to $A \rightarrow \pm A^T$. Finally, it follows from Theorem B.2(d) that if N is even, these two alternatives are not conjugate one to another [if $X\bar{Y} = C \in \mathcal{C}$, then $\bar{X}Y = \bar{C} = C^{-1} \neq -C^{-1}$]. ■

Lemma B.5 *Let A_1, \dots, A_k be commuting real antisymmetric $N \times N$ matrices. Then there exists a real rotation matrix $L \in SO(N)$ such that for each $i = 1, \dots, k$,*

$$L^T A_i L = \begin{cases} \text{blockdiag}(\lambda_{i,1}\mathbf{J}, \dots, \lambda_{i,N/2}\mathbf{J}) & \text{if } N \text{ is even} \\ \text{blockdiag}(\lambda_{i,1}\mathbf{J}, \dots, \lambda_{i,(N-1)/2}\mathbf{J}, 0) & \text{if } N \text{ is odd} \end{cases} \quad (\text{B.9})$$

where the $\lambda_{i,j}$ are real numbers.

PROOF. Since A_1, \dots, A_k are commuting anti-hermitian matrices, they have a common eigenvector $v \in \mathbb{C}^N$:

$$A_i v = i\lambda_i v \quad \text{for each } i, \quad (\text{B.10})$$

where the λ_i are real. Since the A_i are real, we have also

$$A_i \bar{v} = -i\lambda_i \bar{v} \quad \text{for each } i. \quad (\text{B.11})$$

There are now two cases:

(a) If the real and imaginary parts of v are linearly independent (i.e. v is not a multiple of a real vector), then $w_+ \equiv (v + \bar{v})/\|v + \bar{v}\|$ and $w_- \equiv (v - \bar{v})/i\|v - \bar{v}\|$ are perpendicular unit vectors in \mathbb{R}^N , and

$$A_i w_+ = -\lambda_i w_- \quad (\text{B.12a})$$

$$A_i w_- = \lambda_i w_+ \quad (\text{B.12b})$$

[If at least one of the λ_i is nonzero, then $v \perp \bar{v}$ and hence $\|v + \bar{v}\| = \|v - \bar{v}\|$, so the normalizations work out right. If all of the λ_i are zero, then (B.12) is trivial.] Moreover, the subspace of \mathbb{R}^N orthogonal to $\{w_+, w_-\}$ is invariant under each operator A_i .

(b) If v is a multiple of a real vector w (which we take to be of unit norm), then all the λ_i must be zero. Moreover, the subspace of \mathbb{R}^N orthogonal to w is invariant under each operator A_i .

We now continue the same process of reduction, working on the operators A_i restricted to $\{w_+, w_-\}^\perp$ or $\{w\}^\perp$. In this way we produce an orthonormal basis $\{w_1, \dots, w_N\} \in \mathbb{R}^N$ consisting of all the vectors w_\pm or w generated at each step; we order this basis so as to put first all pairs w_\pm , then all individual vectors w . The columns of the desired matrix L are given by this basis. (If necessary, w_1 and w_2 can be interchanged so as to guarantee $\det L = +1$.) ■

Finally we determine the fixed-point manifolds for each of the involutive isometries listed in Theorem B.4:

Theorem B.6 *The fixed-point manifolds F of the involutive isometries listed in Theorem B.4 are:*

- (a_{r,r}) $A \longrightarrow I_r A I_r$: $F =$ matrices of the form $\begin{pmatrix} B & 0 \\ 0 & C \end{pmatrix}$ with $B \in U(r)$, $C \in U(N-r)$ and $(\det B)(\det C) = 1$. This is the connected symmetric space $S(U(r) \times U(N-r))$; it is a subgroup of $SU(N)$ of codimension $2r(N-r)$.
- (a_{r,s}) $A \longrightarrow I_r A I_s$ with $r \neq s$: $F = \emptyset$.
- (b1) $A \longrightarrow A^\dagger$: F is a disjoint union of components $F_r = \{U I_r U^\dagger : U \in SU(N)\}$ for r even ($0 \leq r \leq N$). The manifold F_r is the symmetric space $SU(N)/S(U(r) \times U(N-r))$; it has codimension $r^2 + (N-r)^2 - 1$.
- (b2) [N even] $A \longrightarrow e^{2\pi i/N} A^\dagger$: F is a disjoint union of components $F_r = \{e^{\pi i/N} U I_r U^\dagger : U \in SU(N)\}$ for r odd ($0 \leq r \leq N$). The manifold F_r is isometric to the symmetric space $SU(N)/S(U(r) \times U(N-r))$; it has codimension $r^2 + (N-r)^2 - 1$.
- (c1) $A \longrightarrow \bar{A}$: F consists of real matrices $A \in SO(N)$. This is a connected symmetric space; it is a subgroup of $SU(N)$ of codimension $\frac{1}{2}(N^2 + N - 2)$.
- (c2a) [N even] $A \longrightarrow -J\bar{A}J$: $F = USp(N/2) \equiv Sp(N/2, \mathbb{C}) \cap U(N)$. This is a connected symmetric space; it is a subgroup of $SU(N)$ of codimension $\frac{1}{2}(N^2 - N - 2)$.
- (c2b) [$N = 4k$, k integer] $A \longrightarrow e^{2\pi i/N} J\bar{A}J$: $F = \emptyset$.
- (c2c) [$N = 4k + 2$, k integer] $A \longrightarrow J\bar{A}J$: $F = \emptyset$.
- (d1) $A \longrightarrow A^T$: $F = \{U U^T : U \in SU(N)\}$. The manifold F is the connected symmetric space $SU(N)/SO(N)$; it has codimension $\frac{1}{2}(N^2 + N)$.
- (d2) [N even] $A \longrightarrow -A^T$: F is a disjoint union of two components F_1 and F_2 with $F_1 = \{U J U^T : U \in SU(N)\}$ and $F_2 = \{e^{2\pi i/N} U J U^T : U \in SU(N)\}$. The manifold F_1 is the connected symmetric space $SU(N)/USp(N/2)$; it has codimension $\frac{1}{2}(N^2 - N)$. The manifold F_2 is isometric to F_1 .

PROOF. Class (a_{r,r}): This is immediate.

Class (a_{r,s}): If $A = I_r A I_s$ with A invertible, then $I_r = A I_s A^{-1}$, i.e. I_r is similar to I_s . But this is of course false if $r \neq s$.

Class (b1): If $A = A^\dagger$, then A has eigenvalues ± 1 and it can be diagonalized in the form $A = U I_r U^\dagger$ with $U \in SU(N)$; moreover, r is even because $A \in SU(N)$. Conversely, every matrix of this form is in $SU(N)$ and satisfies $A = A^\dagger$. Obviously these manifolds are disjoint, as I_r cannot be similar to I_s if $r \neq s$.

Let us now consider $U, V \in SU(N)$ such that $U I_r U^\dagger = V I_r V^\dagger$. Then $U^\dagger V I_r = I_r U^\dagger V$, i.e. $U^\dagger V$ commutes with I_r and thus belongs to $S(U(r) \times U(N-r))$. Thus $V = U K$ with $K \in S(U(r) \times U(N-r))$. Conversely, if $V = U K$ with $K \in S(U(r) \times U(N-r))$, then $U I_r U^\dagger = V I_r V^\dagger$. Therefore, the manifold F_r is in one-to-one correspondence with the cosets $SU(N)/S(U(r) \times U(N-r))$.

Class (b2): If $A = e^{2\pi i/N} A^\dagger$, then $Ae^{-\pi i/N}$ is a hermitian unitary matrix. One can then apply the same reasoning used for class (b1), but r must be odd rather than even.

Class (c1): This is immediate.

Class (c2a): For $A \in SU(N) \subset U(N)$, clearly $A = -J\bar{A}J$ iff $A^T J A = A^T \bar{A} J = J$, i.e. iff $A \in USp(N/2)$. In [41, pp. 347–349] it is proven that $USp(N/2) \subset SU(N)$ and that $USp(N/2)$ is connected.

Classes (c2b) and (c2c): If $A = cJ\bar{A}J$ and $A \in U(N)$, then $A^T J A = -cA^T \bar{A} J = -cJ$. Therefore $\sqrt{-c}A$ is a symplectic matrix, and thus [41, pp. 347–349] $\det(\sqrt{-c}A) = +1$. But for $A \in SU(N)$ with N even, this means that $(-c)^{N/2} = +1$, which is a contradiction in the two cases ($N = 4k$, $c = e^{2\pi i/N}$) and ($N = 4k + 2$, $c = 1$).

Class (d1): If $A = A^T \in SU(N)$, then [see the proof of case (c1), Theorem B.4] $A = UU^T$ with $U \in SU(N)$. Let us now consider $U, V \in SU(N)$ such that $UU^T = VV^T$. Then $U^\dagger V = \overline{U^\dagger V}$, i.e. $U^\dagger V$ is real and thus belongs to $SO(N)$. Thus $V = UK$ with $K \in SO(N)$. Conversely, if $V = UK$ with $K \in SO(N)$, then $UU^T = VV^T$. Therefore, the manifold F is in one-to-one correspondence with the cosets $SU(N)/SO(N)$.

Class (d2): If $A = -A^T$, then [see the proof of case (c2), Theorem B.4] $A = UJU^T$ or $A = e^{2\pi i/N} UJU^T$ with $U \in SU(N)$, and only one of these two cases holds for any given A .

Let us now consider $U, V \in SU(N)$ such that $UJU^T = VJV^T$. Then $U^\dagger V J (U^\dagger V)^T = J$, i.e. $U^\dagger V$ belongs to $USp(N/2)$. Thus $V = UK$ with $K \in USp(N/2)$, and the converse also holds. Therefore, the manifold F_1 is in one-to-one correspondence with the cosets $SU(N)/USp(N/2)$. Clearly F_2 is isometric to F_1 .

■

References

- [1] U. Wolff, Phys. Rev. Lett. **62**, 361 (1989).
- [2] U. Wolff, Nucl. Phys. **B322**, 759 (1989).
- [3] U. Wolff, Nucl. Phys. **B334**, 581 (1990).
- [4] R.G. Edwards and A.D. Sokal, Phys. Rev. **D40**, 1374 (1989).
- [5] M. Hasenbusch, Nucl. Phys. **B333**, 581 (1990).
- [6] M. Hasenbusch and S. Meyer, Phys. Lett. **B241**, 238 (1990).
- [7] W. Janke, Phys. Lett. **A148**, 306 (1990).
- [8] S. Caracciolo, R.G. Edwards, A. Pelissetto and A.D. Sokal, Nucl. Phys. B (Proc. Suppl.) **20**, 72 (1991).

- [9] R.H. Swendsen and J.-S. Wang, Phys. Rev. Lett. **58**, 86 (1987).
- [10] R.G. Edwards and A.D. Sokal, Phys. Rev. **D38**, 2009 (1988).
- [11] U. Wolff, Phys. Lett. **B228**, 379 (1989).
- [12] P. Tamayo, R.C. Brower and W. Klein, J. Stat. Phys. **58**, 1083 (1990).
- [13] C.F. Baillie and P.D. Coddington, Phys. Rev. **B43**, 10617 (1991).
- [14] J. Goodman and A.D. Sokal, Phys. Rev. **D40**, 2035 (1989).
- [15] R. Ben-Av, D. Kandel, E. Katznelson, P.G. Lauwers and S. Solomon, J. Stat. Phys. **58**, 125 (1990).
- [16] R.C. Brower and S. Huang, Phys. Rev. **D41**, 708 (1990).
- [17] J. Goodman and A.D. Sokal, Phys. Rev. Lett. **56**, 1015 (1986).
- [18] R.G. Edwards, J. Goodman and A.D. Sokal, Nucl. Phys. **B354**, 289 (1991).
- [19] R.G. Edwards, S.J. Ferreira, J. Goodman and A.D. Sokal, Multi-Grid Monte Carlo III. Two-Dimensional $O(4)$ -Symmetric Nonlinear σ -Model, SCRI preprint FSU-SCRI-91-181 (December 1991), to appear in Nucl. Phys. B[FS].
- [20] G. Parisi, in *Progress in Gauge Field Theory* (1983 Cargèse lectures), ed. G. 't Hooft *et al.* (Plenum, New York, 1984).
- [21] G.G. Batrouni, G.R. Katz, A.S. Kronfeld, G.P. Lepage, B. Svetitsky and K.G. Wilson, Phys. Rev. **D32**, 2736 (1985).
- [22] E. Dagotto and J.B. Kogut, Phys. Rev. Lett. **58**, 299 (1987).
- [23] E. Dagotto and J.B. Kogut, Nucl. Phys. **B290** [FS20], 451 (1987).
- [24] D.W. Heermann and A.N. Burkitt, Physica **A162**, 210 (1990).
- [25] J.-S. Wang, Physica **A164**, 240 (1990).
- [26] P.D. Coddington and C.F. Baillie, Empirical relations between static and dynamic exponents for Ising model cluster algorithms, Syracuse University preprint SCCS-141 (1991); and P.D. Coddington, private communication.
- [27] W. Klein, T. Ray and P. Tamayo, Phys. Rev. Lett. **62**, 163 (1989).
- [28] I.M. James, Bull. London Math. Soc. **3**, 257 (1971).
- [29] S. Caracciolo, R.G. Edwards, A. Pelissetto and A.D. Sokal, Dynamic critical behaviour of Wolff's algorithm for RP^N σ -models, SCRI preprint FSU-SCRI-92C-09 (January 1992), to appear in the Proceedings of the Lattice '91 conference, Nucl. Phys. B (Proc. Suppl.) —, — (1992); and paper in preparation.

- [30] G. Parisi, Phys. Rev. Lett. **43**, 1784 (1979).
- [31] M. Mézard, G. Parisi, N. Sourlas, G. Toulouse and M. A. Virasoro, Phys. Rev. Lett. **52**, 1156 (1984) and J. Physique **45**, 843 (1984).
- [32] M. Mézard, G. Parisi and M.A. Virasoro, *Spin Glass Theory and Beyond* (World Scientific, Singapore, 1988).
- [33] S. Caracciolo, G. Parisi, S. Patarnello and N. Sourlas, Europhys. Lett. **11**, 783 (1990) and J. Physique **51**, 1877 (1990).
- [34] D.A. Fisher and D.A. Huse, Phys. Rev. Lett. **56**, 1601 (1986) and Phys. Rev. **B38**, 386 (1988).
- [35] I. Morgenstern and K. Binder, Phys. Rev. **B22**, 288 (1980); A.P. Young, Phys. Rev. Lett. **50**, 917 (1983); W.L. McMillan, Phys. Rev. **B28**, 5216 (1983); A.J. Bray and M.A. Moore, J. Phys. **C17**, L463 (1984).
- [36] S. Kobayashi and K. Nomizu, *Foundations of Differential Geometry*, Volumes I and II (New York, Interscience, 1963 and 1969).
- [37] V. Bargmann, J. Math. Phys. **5**, 862 (1964).
- [38] J.A. Wolf, *Spaces of Constant Curvature*, 5th ed., (Houston, Publish or Perish, 1984).
- [39] D.S.P. Leung, J. Diff. Geom. **8**, 153 (1973).
- [40] D.S.P. Leung, Indiana Univ. Math. J. **24**, 327 (1974); **24**, 1199 (E) (1975).
- [41] W. Miller, Jr., *Symmetry Groups and Their Applications* (New York–London, Academic Press, 1972).
- [42] S. Helgason, *Differential Geometry, Lie Groups, and Symmetric Spaces* (New York–San Francisco–London, Academic Press, 1978).
- [43] R.D. Pisarski, Phys. Rev. **D20**, 3358 (1979).
- [44] E. Brézin, S. Hikami and J. Zinn-Justin, Nucl. Phys. **B165**, 528 (1980).
- [45] D.H. Friedan, Ann. Phys. **163**, 318 (1985).
- [46] J. Lott, Commun. Math. Phys. **107**, 165 (1986).
- [47] B. Doubrovine, S. Novikov and A. Fomenko, *Géométrie Contemporaine: Méthodes et Applications*, 2^{ème} partie (Moscou, MIR, 1982).
- [48] N. Iwahori, in *Proceedings of the United States – Japan Seminar on Differential Geometry* (Tokyo, Nippon Hyoronsha, 1966), pp. 57–62.

- [49] L.V. Sabinin, in *Nekotorye Kraevye Zadachi Obyknovennykh Differentsial'nykh Uravnenii* [Some Boundary Value Problems of Ordinary Differential Equations, in Russian], ed. I.S. Sargsjan (Moscow, Univ. Družby Narodov, 1970), pp. 116–126 [see Math. Reviews **50**, #4195 and **51**, #4111].
- [50] A.L. Oniščik, in *Geometricheskie Metody v Zadachak Algebry i Analiza, Vyp. 2* [Geometric Methods in Problems of Algebra and Analysis, no. 2, in Russian], ed. A.V. Černavskii (Yaroslavl', Jaroslav. Gos. Univ., 1980), pp. 64–85, 161 [see Math. Reviews **82d**:00004 and **82j**:53092].
- [51] E. Gottschling, Commun. Pure. Appl. Math. **22**, 693 (1969).
- [52] M. Meschiari, Ann. Scuola Norm. Sup. Pisa **26**, 403 (1972).
- [53] M.B. Priestley, *Spectral Analysis and Time Series*, 2 vols. (Academic, London, 1981), Chapters 5-7.
- [54] T.W. Anderson, *The Statistical Analysis of Time Series* (Wiley, New York, 1971).
- [55] N. Madras and A.D. Sokal, J. Stat. Phys. **50**, 109 (1988).
- [56] D. Kandel, R. Ben-Av and E. Domany, Phys. Rev. Lett. **65**, 941 (1990) and Phys. Rev. **B45**, 4700 (1992).
- [57] A.D. Sokal, *Monte Carlo Methods in Statistical Mechanics: Foundations and New Algorithms*, Cours de Troisième Cycle de la Physique en Suisse Romande (Lausanne, June 1989).
- [58] S. Caracciolo, A. Pelissetto and A.D. Sokal, J. Stat. Phys. **60**, 1 (1990).
- [59] A.D. Sokal, Nucl. Phys. B (Proc. Suppl.) **20**, 55 (1991).
- [60] H.G. Evertz, R. Ben-Av, M. Marcu and S. Solomon, Nucl. Phys. B (Proc. Suppl.) **20**, 85 (1991).
- [61] R.C. Brower and P. Tamayo, Phys. Rev. Lett. **62**, 1087 (1989).
- [62] H.G. Evertz, M. Hasenbusch, M. Marcu, K. Pinn and S. Solomon, Nucl. Phys. B (Proc. Suppl.) **20**, 80 (1991) and Phys. Lett. **B254**, 185 (1991).
- [63] R.C. Brower, private communication (circa 1989).
- [64] C.T.H. Davies *et al.*, Phys. Rev. **D37**, 1581 (1988).
- [65] J.E. Mandula and M. Ogilvie, Phys. Lett. **B248**, 156 (1990).
- [66] A. Hulsebos, M.L. Laursen, J. Smit and A.J. van der Sijs, Nucl. Phys. B (Proc. Suppl.) **20**, 98 (1991).
- [67] S. Duane, R. Kenway, B.J. Pendleton and D. Roweth, Phys. Lett. **B176**, 143 (1986).

- [68] K. Jansen and U.-J. Wiese, Nucl. Phys. **B370**, 762 (1992).
- [69] U. Wolff, Cluster algorithms for non-linear sigma models, CERN preprint CERN-TH 6126/91 (June 1991).
- [70] J. Dugundji, *Topology* (Boston, Allyn and Bacon, 1966).
- [71] H.L. Royden, *Real Analysis*, 3rd ed. (New York, Macmillan, 1988).
- [72] L.A. Steen and J.A. Seebach, Jr., *Counterexamples in Topology*, 2nd ed. (New York–Heidelberg–Berlin, Springer-Verlag, 1978).
- [73] R. Engelking, *General Topology* (Warsaw, PWN–Polish Scientific Publishers, 1977).
- [74] M.W. Hirsch, *Differential Topology* (New York–Heidelberg–Berlin, Springer-Verlag, 1976).
- [75] W. Hurewicz and H. Wallman, *Dimension Theory* (Princeton, N.J., Princeton University Press, 1948).
- [76] R. Engelking, *Dimension Theory* (Amsterdam–Oxford–New York, North-Holland, 1978).
- [77] J.R. Munkres, *Elements of Algebraic Topology* (Redwood City, CA, Addison-Wesley, 1984).
- [78] P.J. Hilton and S. Wylie, *Homology Theory* (Cambridge, Cambridge University Press, 1965).
- [79] V. Guillemin and A. Pollack, *Differential Topology* (Englewood Cliffs, NJ, Prentice-Hall, 1974).
- [80] R. Abraham and J. Robbin, *Transversal Mappings and Flows* (New York–Amsterdam, Benjamin, 1967).
- [81] J. Palis, Jr. and W. de Melo, *Geometric Theory of Dynamical Systems* (New York–Heidelberg–Berlin, Springer-Verlag, 1982).
- [82] S. Kobayashi, *Transformation Groups in Differential Geometry* (New York–Heidelberg–Berlin, Springer-Verlag, 1972).
- [83] S. Kobayashi, Nagoya Math. J. **13**, 63 (1958).
- [84] P.A. Smith, Ann. Math. **46**, 357 (1945).
- [85] A. Borel, Comment. Math. Helv. **29**, 27 (1955).
- [86] L. Vanhecke and T.J. Wiltmore, Math. Ann. **263**, 31 (1983).
- [87] P. Tondeur and L. Vanhecke, Geom. Dedicata **28**, 77 (1988).

- [88] B.Y. Chen and L. Vanhecke, *Bull. Austral. Math. Soc.* **38**, 377 (1988).
- [89] B.Y. Chen and L. Vanhecke, *Geom. Dedicata* **29**, 259 (1989).
- [90] P. Tondeur and L. Vanhecke, *Simon Stevin* **63**, 107 (1989).
- [91] P. Tondeur and L. Vanhecke, *Monatsh. Math.* **108**, 211 (1989).
- [92] B.-Y. Chen and T. Nagano, *Duke Math. J.* **44**, 745 (1977).
- [93] J. Nikić, *Mat. Vesnik* **4**, 323 (1980).
- [94] J.A. Wolf, *Illinois J. Math.* **7**, 447 (1963).
- [95] É. Cartan, *Ann. Mat. Pura Appl.* **4**, 209 (1927) [reprinted in É. Cartan, *Oeuvres Complètes*, Partie I (Paris, Éditions du CNRS, 1984), pp. 793–840].
- [96] J.A. Wolf, *Comment. Math. Helv.* **37**, 65 (1962).